

University of Windsor

Scholarship at UWindor

Electronic Theses and Dissertations

Theses, Dissertations, and Major Papers

1-1-1981

Component magnetization of the iron formation and deposits at the Adams Mine, Kirkland Lake, Ontario.

Arthur William Quick
University of Windsor

Follow this and additional works at: <https://scholar.uwindsor.ca/etd>

Recommended Citation

Quick, Arthur William, "Component magnetization of the iron formation and deposits at the Adams Mine, Kirkland Lake, Ontario." (1981). *Electronic Theses and Dissertations*. 6765.
<https://scholar.uwindsor.ca/etd/6765>

This online database contains the full-text of PhD dissertations and Masters' theses of University of Windsor students from 1954 forward. These documents are made available for personal study and research purposes only, in accordance with the Canadian Copyright Act and the Creative Commons license—CC BY-NC-ND (Attribution, Non-Commercial, No Derivative Works). Under this license, works must always be attributed to the copyright holder (original author), cannot be used for any commercial purposes, and may not be altered. Any other use would require the permission of the copyright holder. Students may inquire about withdrawing their dissertation and/or thesis from this database. For additional inquiries, please contact the repository administrator via email (scholarship@uwindsor.ca) or by telephone at 519-253-3000ext. 3208.

NOTE TO USERS

This reproduction is the best copy available.

UMI[®]

COMPONENT MAGNETIZATION OF THE IRON FORMATION
AND DEPOSITS AT THE ADAMS MINE
KIRKLAND LAKE, ONTARIO.

by

Arthur William Quick

A Thesis
submitted to the Faculty of Graduate Studies
through the Department of
Geology in Partial Fulfillment
of the requirements for the Degree
of Master of Applied Science at
The University of Windsor

Windsor, Ontario, Canada.
1981

UMI Number: EC54748

INFORMATION TO USERS

The quality of this reproduction is dependent upon the quality of the copy submitted. Broken or indistinct print, colored or poor quality illustrations and photographs, print bleed-through, substandard margins, and improper alignment can adversely affect reproduction.

In the unlikely event that the author did not send a complete manuscript and there are missing pages, these will be noted. Also, if unauthorized copyright material had to be removed, a note will indicate the deletion.

UMI[®]

UMI Microform EC54748
Copyright 2010 by ProQuest LLC
All rights reserved. This microform edition is protected against
unauthorized copying under Title 17, United States Code.

ProQuest LLC
789 East Eisenhower Parkway
P.O. Box 1346
Ann Arbor, MI 48106-1346

©

Arthur William Quick
All Rights Reserved

1981

758485

TABLE OF CONTENTS

ABSTRACT.....	vi
ACKNOWLEDGEMENTS.....	viii
LIST OF FIGURES.....	ix
LIST OF TABLES.....	xii
LIST OF APPENDICES.....	xiii
CHAPTER	
I. INTRODUCTION.....	1
1.1 Problem and proposal.....	1
1.2 History of the mine.....	2
II. GEOLOGY.....	5
2.1 Regional Geology.....	5
2.2 Boston Township iron range.....	8
2.2.1 Iron Formation.....	8
2.2.2 Cherty quartzite.....	9
2.2.3 Basic and intermediate volcanics.....	10
2.2.4 Intrusives.....	10
2.2.4a Lamprophyre dikes.....	10
2.2.4b Syenite stock and dikes.....	11
2.2.4c Diabase dikes.....	13
2.3 Geologic history.....	13
2.4 Structure of the Boston Township iron range.....	14
2.5 Orebodies.....	15
III. EXPERIMENTAL METHODS.....	16
3.1 Sampling.....	16
3.2 Sample preparation.....	16
3.3 Sample treatment.....	21
3.3.1 Specific gravity.....	21
3.3.2 Magnetic susceptibility.....	21
3.3.3 Anisotropy of magnetic susceptibility.....	21
3.3.4 Natural Remanent Magnetization... ..	22
3.3.5 AF demagnetization.....	22
3.3.6 Thermal cleaning.....	23
3.3.7 Chemical cleaning.....	29
3.3.8 Stability test.....	29
3.4 Computations.....	30
3.5 Magnetic model.....	31
IV. RESULTS	
4.1 Specific gravity.....	32
4.2 Magnetic susceptibility.....	32
4.3 Anisotropy of magnetic susceptibility....	36

TABLE OF CONTENTS - cont'd.

CHAPTER

4.4	Natural Remanent Magnetization.....	42
4.4.1	Host rock NRM.....	42
4.4.1a	NRM intensity.....	42
4.4.1b	Koenigsberger ratio.....	43
4.4.1c	Storage test.....	43
4.4.2	Iron formation NRM.....	43
4.4.2a	NRM intensity.....	43
4.4.2b	Koenigsberger ratio.....	43
4.4.2c	NRM to k_1 relationship..	48
4.4.2d	Storage test.....	48
4.4.2e	Shock test.....	48
4.5	Statistical analysis.....	52
4.5.1	IF statistical analysis.....	52
4.5.2	HR statistical analysis.....	54
4.6	AF demagnetization of IF.....	54
4.6.1	Pilot specimens.....	54
4.6.2	Smoothing method.....	59
4.7	Fold test - AF cleaning.....	65
4.8	Thermal cleaning of iron formation.....	72
4.8.1	Pilot specimens.....	72
4.9	Chemical cleaning of iron formation.....	76
4.9.1	Pilot specimens.....	76
4.9.2	Remaining specimens.....	80
4.10	Baked contact test.....	80
4.10.1	AF demagnetization of dike and baked contact zone.....	80
4.10.1a	Pilot specimens.....	80
4.10.2	Thermal cleaning of dike and contact zone.....	83
4.11	AF demagnetization of the host rock.....	87
4.11.1	Pilot specimens.....	87
4.11.2	Smoothing method.....	91
4.12	Thermal cleaning of host rock.....	96
4.12.1	Pilot specimens.....	96
4.13	Pole position.....	96
4.13.1	Iron formation.....	96
4.13.2	Host rock.....	99
4.14	Magnetic model.....	99
4.14.1	Infinite depth extent.....	99
V.	CONCLUSIONS AND RECOMMENDATIONS.....	107
	APPENDICES.....	110
	REFERENCES.....	115
	VITAE AUCTORIS.....	118

ABSTRACT

The magnetic characteristics and the ore genesis of the Algoman-type iron formation (IF) and host rock (HR) at the Adams Mine near Kirkland Lake were determined from a study of 171 IF blocks and 45 HR sites oriented in situ. The mean specific gravity (SG) of the IF specimens is 3.24 gm/cm^3 , i.e., mixed ore and lean IF. The low field magnetic susceptibility perpendicular to bedding (k_{\perp}) for the IF gives a lognormal mean of $4.520 \times 10^{-2} \text{ cgs/cm}^3$ which is $192k_{\text{HR}}$, such that the HR values can be neglected in the magnetic anomaly computation. The relationship $k_{\perp} = 0.0698\text{SG} - 0.179$ gives a correlation coefficient of +0.73 and gives $k_{\perp \text{IF}} = 0.0645 \text{ cgs/cm}^3$ for economic iron ore. The magnetic susceptibility in the IF bedding plane (k_{\parallel}) is $1.69k_{\perp}$ indicating strong anisotropy. Both the HR and IF natural remanent magnetization (NRM) intensities are lognormally distributed with means of 5.97×10^{-6} and $1.12 \times 10^{-2} \text{ emu/cm}^3$ respectively giving Koenigsberger ratios (Q) of 0.013 and 0.67. In computing the magnetic anomaly for the ore zone the HR NRM and induced magnetization can be neglected and the IF NRM augments the induced magnetization (J_i) by 17%. Stability tests show that NRM is not laboratory-acquired viscous remanence. Shock tests show that blasting may have reduced the NRM intensity by 40% in certain specimens close to where blasting had occurred.

After AF cleaning, thermal cleaning and chemical

cleaning, the remanence of 50% of the IF samples survive statistical screening tests. Smoothing and contouring of the remanence vectors on a stereonet isolated a stable pre-folding A remanence component of 256° , 7° , 3° , (declination, inclination) cone of 95% confidence) which indicates an age of ~ 2.7 Ga. It is thought to represent the primary remanence that the IF acquired during deposition. After smoothing and contouring, the HR shows two stable post-folding remanence directions. The B component isolated at 305° , 79° , 4° gives an age of ~ 2.15 Ga and is associated with the intrusion of the Otto syenite stock. The C component isolated at 190° , 54° , 4° gives an age of ~ 1.85 Ga and is possibly associated with the emplacement of the Abitibi dike swarm or possibly the Hudsonian orogeny. The diabase dike shows a D component of 176° , 33° , 5° which gives an age of ~ 1.83 Ga.

Using a computer model which incorporates the induced component, the anisotropy of susceptibility, the NRM component, the demagnetizing factor of 2π , and assuming an infinite depth extent for the IF. The computed peak values for the South pit aeromagnetic anomaly at the Adams Mine is in excellent agreement with the observed anomaly. Other pits give similar results. Also, if the deposits were flat-lying the anomalies would be reduced to 32% of their present peak values.

ACKNOWLEDGEMENTS

I would like to thank Dr. D.T.A. Symons and Dr. M. Stupavsky for their advice and direction throughout this project.

I would also like to thank Mr. R.A. Rouleau of DOFASCO for permission to work in the Adams Mine; Mr. K. Oliver, the Mine Geologist for geologic advice and collecting help; Messrs. J. Huschilt, D. Dunsmore, and D.D. Symons for their efforts in sample collecting and preparation; Mrs. C. Chinnick and Miss A. Stanta for technical help.

LIST OF FIGURES

Figure		Page
1.	Location of the Adams Mine.....	3
2.	Regional Geology of the Adams Mine area.....	6
3.	Geology of the Adams Mine.....	12
4a.	Outline of Peria Pit, Adams Mine.....	17
4b.	Outline of North Pit, Adams Mine.....	18
4c.	Outline of Central Pit, Adams Mine.....	19
4d.	Outline of South Pit, Adams Mine.....	20
5.	Histogram of the S.G. of 547 IF specimens.....	33
6.	Lognormal histogram of k_1 susceptibility for 524 HR specimens.....	34
7.	Lognormal histogram of k_1 susceptibility for 592 IF specimens.....	34
8.	Regression line of specific gravity versus k_1 susceptibility for 581 IF specimens.....	35
9a.	Histogram of k_{min} (k_1) directions for 592 IF specimens.....	37
9b.	Histogram of k_{max} directions for 592 IF specimens.....	38
10a.	Histogram of k_{min} (k_1) directions for 50 recut IF specimens.....	39
10b.	Histogram of k_{max} directions for 50 recut IF specimens.....	39
11.	Histogram of k_{int}/k_{min} for 592 IF specimens.....	40
12.	Histogram of k_{max}/k_{min} for 592 IF specimens.....	41
13.	Lognormal histogram of NRM intensity for 524 HR specimens.....	44
14.	Lognormal histogram of the Koenigsberger ratio (Q) for 524 HR specimens.....	44
15a.	Histogram of NRM intensity change of HR specimens over five weeks.....	45
15b.	Directional changes of NRM vectors of HR specimens over five weeks.....	45
16.	Lognormal histogram of NRM intensity for 592 IF specimens.....	46
17.	Lognormal histogram of the Koenigsberger ratio (Q) for 592 IF specimens.....	47
18.	Regression line of NRM intensity versus k_1 susceptibility for 536 IF specimens.....	49
19a.	Histogram of NRM intensity change of IF specimens over four weeks.....	51
19b.	Directional changes of NRM vectors of IF specimens over four weeks.....	51
20a.	Histogram of NRM intensity change of IF specimens after induced shock.....	53
20b.	Direction changes of NRM vectors of IF specimens after induced shock.....	53

LIST OF FIGURES - cont'd.

Figure	Page
21. IF AF demagnetization curve-paleomagnetic stability index for directional changes.....	56
22. IF AF demagnetization curve-relative intensity.....	57
23. Directional changes of AF demagnetization on equal area projection for IF pilot specimens.....	58
24. Mean directional changes during AF demagnetization steps for IF pilot specimens.....	60
25. Plot of optimum AF cleaning field for IF and HR specimens.....	61
26. Relative intensity of NRM after cleaning at optimum AF field.....	61
27. Smoothing and contouring of AF cleaned IF specimens corrected for bedding tilt (down direction).....	63
27a. Smoothing and contouring of AF cleaned IF specimens corrected for bedding tilt (up direction).....	64
28. Smoothing and contouring of homogeneous AF cleaned IF samples corrected for bedding tilt (down direction).....	66
28a. Smoothing and contouring of homogeneous AF cleaned IF samples corrected for bedding tilt (up direction).....	67
29. Smoothing and contouring of AF cleaned IF specimens not corrected for bedding tilt (down direction).....	69
30. Smoothing and contouring of homogeneous AF cleaned IF samples not corrected for bedding tilt (down direction).....	71
31. IF thermal cleaning curve-relative intensity.....	73
32. IF thermal cleaning curve-paleomagnetic stability index.....	74
33. Directional changes during thermal cleaning for IF specimens.....	75
34. Directional changes during chemical cleaning for IF specimens.....	77
35. IF chemical cleaning curve-paleomagnetic stability index.....	78
36. IF chemical cleaning curve-relative intensity.....	79
37. Sample location for diabase dike baked contact.....	81
38. Baked contact AF demagnetization curve-paleomagnetic stability index.....	82
39. Baked contact AF demagnetization curve-relative intensity.....	84
40. Dike direction and vector removed direction for the baked contact zone.....	85
41. Baked contact thermal cleaning curve-relative intensity.....	86

LIST OF FIGURES - cont'd.

Figure	Page
42. Directional changes of AF demagnetization for HR pilot specimens.....	88
43. HR AF demagnetization curve-paleomagnetic stability index.....	89
44. HR AF demagnetization curve-relative intensity.....	90
45. Smoothing and contouring of AF cleaned HR specimens uncorrected for bedding tilt (down direction).....	92
46. Smoothing and contouring of AF cleaned HR specimens corrected for bedding tilt (down direction).....	93
47. Smoothing and contouring of NRM HR specimens uncorrected for bedding tilt (down direction)....	95
48. Apparent polar wandering curve-iron formation.....	98
49. Apparent polar wandering curve-host rock.....	100
50. Computed magnetic anomaly of IF at 305 m elevation (peak total field).....	102
51. Computed magnetic anomaly of IF at 305 m elevation (total field).....	103

LIST OF TABLES

Table	Page
1. Table of lithologic units.....	7
2. Sampling and remanence data of IF sites.....	24
3. Sampling and remanence data of HR sites.....	28
4. Summary and regression fit between S.G. and k_1	33
5. Summary and regression fit between k_1 and NRM_1	50
6. Pilot specimens grouped into each AF_1 -demagnetiz- ing field.....	60
7. Fold test.....	70
8. Summary of host rock remanence direction.....	94
9. Pole positions of the Adams Mine.....	97
10a. Summary and comparison of magnetic properties of the Sherman mine, Moose Mountain mine and Adams mine iron formation.....	104
10b. Summary and comparison of magnetic properties of the host rock at the Sherman, Moose Mountain and Adams mines.....	105
11. Summary of aeromagnetic response of IF.....	106

LIST OF APPENDICES

Appendix		Page
I	Computer program for the calculation of the magnetic anomaly over a thin sheet of infinite strike and depth extent.....	110

CHAPTER I

INTRODUCTION

1.1 PROBLEM AND PROPOSAL

Airborne and ground magnetic surveys to measure the magnetic field intensity have been the primary methods used in the exploration for iron ore deposits in Ontario. The most intense anomalies are then surveyed in greater detail and sampled. These anomalies are usually found over vertically dipping beds of iron formation (IF). The magnetization of the IF depends on the nature and abundance of the magnetic minerals, the attitude of the bedding with respect to the Earth's magnetic field (EMF), the direction and intensity of the remanence, and the anisotropy of magnetic susceptibility.

The purpose of the study is twofold: 1) to define the magnetic properties of the IF at the Adams Mine with the aim of constructing a magnetic model to assist in the interpretation of aeromagnetic and magnetometer surveys; and 2) to measure the paleomagnetic properties of the IF and host rock (HR) so that the ore genesis of the deposits can be determined. These two factors will help in proposing a more meaningful and successful exploration rationale.

This study examines the Adams Mine deposit near

Kirkland Lake in Boston Township (Figure 1). The geographic co-ordinates of the mine are longitude 79.90°W , and latitude 48.01°N .

1.2 HISTORY OF THE MINE

The Adams Mine is located in the Boston Township iron range. The iron range was discovered in 1902. The earliest geologic report is attributed to Dr. G.A. Young (Ratcliffe, 1957). However, the deposit lay dormant for the next 46 years because of its low iron (Fe) content.

In 1948 the Dominion Gulf Company conducted an air-borne magnetometer survey over the area at an elevation of 150m which revealed a 17,000 γ anomaly. The strong magnetic anomalies were caused by a number of rather continuous beds of banded IF up to 180m wide. Unfortunately few beds exceeded a 20% Fe content over a width of 30m and so exploration interest diminished.

In 1954, Jones and Laughlin Steel Corporation optioned the property from Dominion Gulf and continued the exploration work in response to an increasing demand for iron.

In 1962 Jones and Laughlin announced the decision to develop the property at a production level of 1,000,000 tons of iron ore pellets per year. Over the next two and a half years, the South and Central orebodies were prepared for production while the plant was being

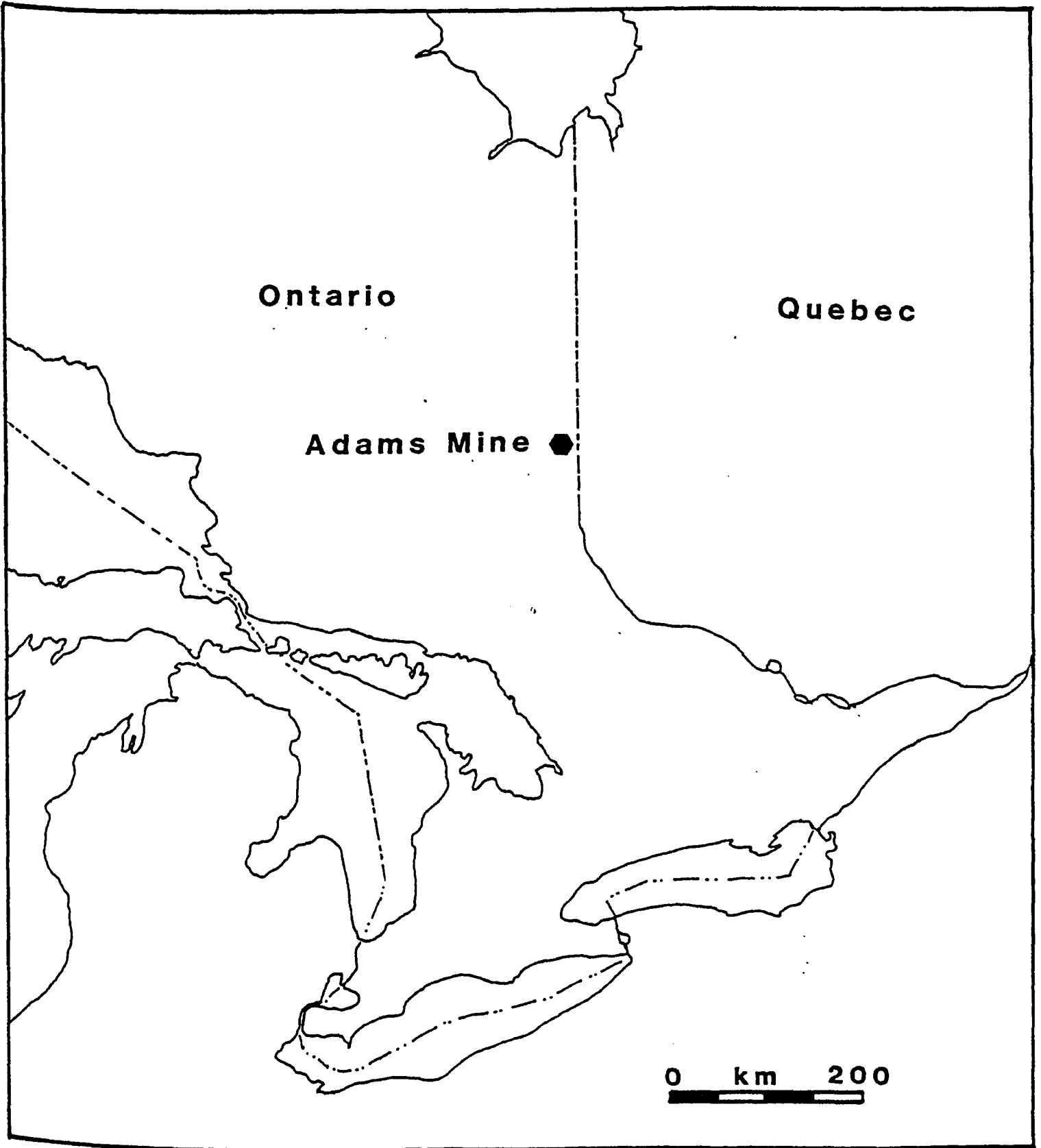


FIG. 1. Location of the Adams Mine

constructed. The first shipment of pellets was made in December 1964.

CHAPTER II

GEOLOGY

2.1 REGIONAL GEOLOGY

The geology of the mine area has been studied by Dubuc (1965) and Lawton (1957) (Figure 2). The following is a brief summary from their reports.

The rocks of the Boston Township are Precambrian in age (Table 1). They consist mainly of Archean volcanics, sediments and intrusives. The Archean rocks are intruded by Proterozoic diabase dikes.

The oldest Archean rocks in the area are a series of Keewatin-type lava flows, volcanic fragmental rocks and sedimentary rocks. The IF is an important member of this series. Unconformably overlying the Keewatin-type rocks are the Timiskaming-type clastic sediments which are dominately conglomerates and greywackes.

There are two groups of Archean basic intrusives of post-Keewatin age. The older group is composed of diorite and metadiorite and the younger group is composed of serpentinite, hornblendite, diorite and minor diorite porphyry.

These Archean rocks underwent folding and faulting which resulted in an easterly striking syncline with its south limb removed by faulting and erosion. After deformation the rocks were then intruded by Haileyburian-type diorites, serpentinites and gabbros. These were followed by Algomian-

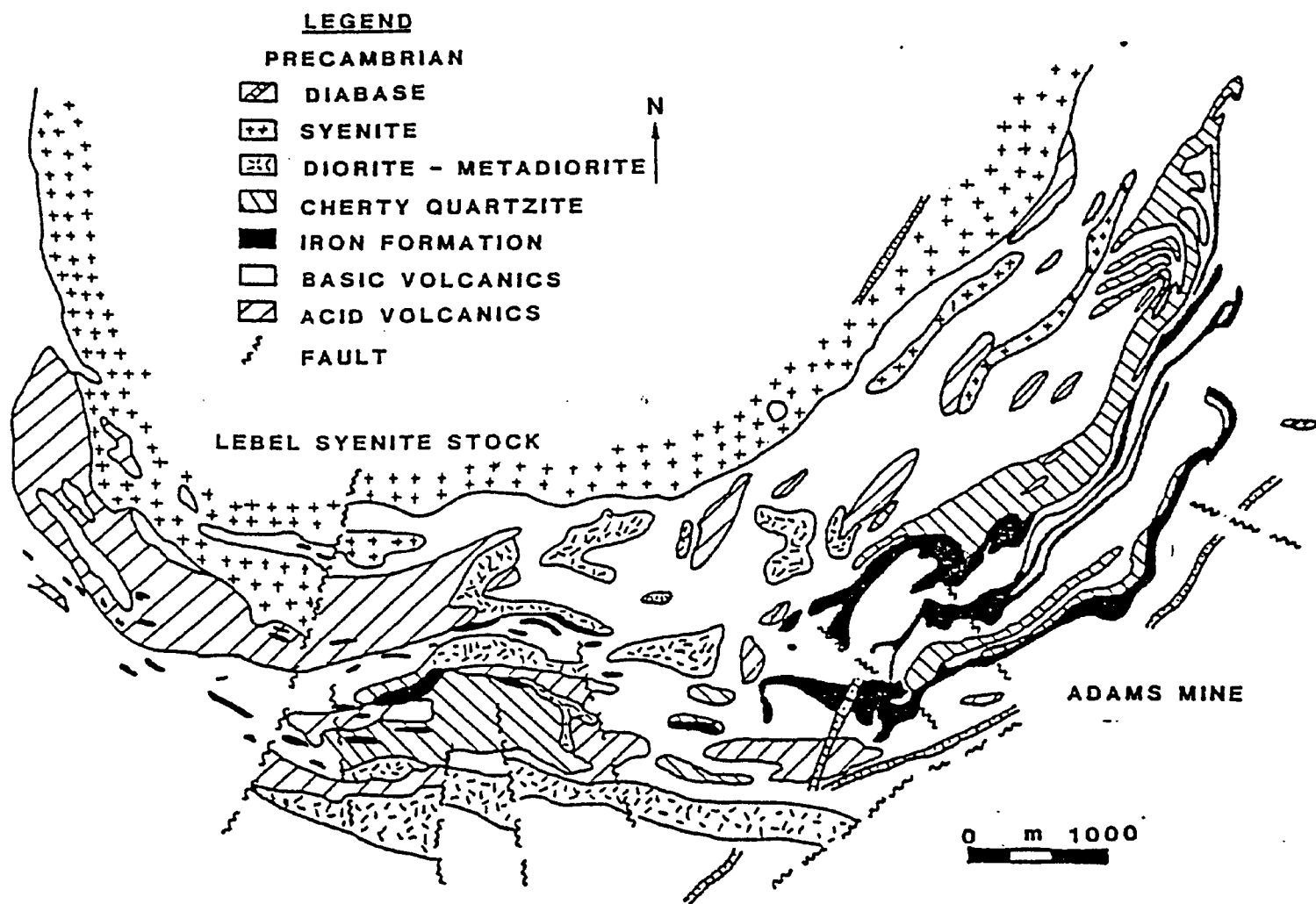


FIG. 2. Regional geology of the Adams Mine area

TABLE 1. Table of lithologic units (K.D. Lawton. 1957)

		Approx. Radiometric Age (Ma)
CENOZOIC		
Recent and Pleistocene:	Clay, sand, gravel and boulders	
-----Unconformity-----		
<u>PRECAMBRIAN</u>		
PROTEROZOIC		
Abitibi:	Diabase	2140 ⁴
-----Intrusive Contact-----		
ARCHEAN		
Algoman:	Syenite Intrusion-Lebel Syenite stock Syenite and lamprophyre dikes	2400 ³
-----Intrusive Contact-----		
Haileyburian:	Diorite; gabbro	
-----Intrusive Contact-----		
Timiskaming:	Fine grained sedimentary rocks Conglomerate	2418 ²
-----Unconformity-----		
Post-Keewatin:	Diorite and Metadiorite	
-----Intrusive Contact-----		
Keewatin:	Cherty Quartzite Iron Formation Basic and Intermediate Volcanic	2703 ¹

NOTES: 1. Nunes and Jensen (1980); 2. Fairbairn et al (1966); 3. Purdy and York (1968); 4. Hurley and Gates (1973).

type granites, syenites and finally by Abitibi-type dikes including more basic derivatives.

2.2 BOSTON TOWNSHIP IRON RANGE

The iron deposits in Boston Township are low-grade Algoman-type banded IF. They are confined to a single range which is 9.6 km long and varies in thickness from 850 to 1100 m. The range is not of economic interest throughout its entire length. The general shape of the range is an arc which is more or less conformable to the southeastern boundary of the Algoman-type Label syenite stock. The stock is a large circular intrusion of ~6.4 km diameter which is situated ~1 km northwest of the iron range.

The range is made up of several horizons of IF and cherty quartzite separated mainly by basic to intermediate lava flows of basalt and andesite composition. Minor interbeds of tuffaceous sedimentary rocks and acidic volcanic rocks are also present. Irregular intrusive bodies of Haileyburian-type diorite or metadiorite, Algoman-type syenite and lamprophyre cut the IF strata within the range.

2.2.1 Iron Formation

The IF is typical of that found in the Keewatin series of Precambrian rocks in the Superior Geologic Province (Moore and Armstrong, 1946). It is a well-banded sedimentary rock consisting essentially of alternating

layers of magnetite and chert. The magnetite beds are black with a very fine grain size of less than 1 mm. The magnetite layers have an average thickness of 1 cm and rarely exceed 2.5 cm. The chert beds vary from greyish to reddish in colour. Their grain size is generally very fine also, but occasionally a sugary texture can be detected. The chert layers occur as fine laminae or massive beds several centimetres thick.

Minor amounts of other minerals are also found in the IF. Reddish garnet occurs as isolated masses of anhedral grains. In places, the garnet is accompanied by epidote. Within the magnetite layer, hematite occurs as small irregular lenses and as thin individual beds. It is found where the chert layers are reddish in colour. Tremolite and actinolite needles are generally present within or adjacent to the magnetite layers. Chlorite is abundant and occurs as massive beds from the alteration of basic volcanic rocks. Pyrite is invariably found with the chlorite either as thin layers or as scattered cubes.

2.2.2 Cherty Quartzite

The cherty quartzite, predominately silica, is similar to the chert of the IF and likely has the same origin. The magnetic iron content rarely exceeds 5% and therefore the cherty quartzite is usually considered to be a highly siliceous facies of the IF. The magnetite occurs mostly as disseminations in the silica. Graphite

is found as a fine dissemination and generally imparts a black colour to local chert bands. Pyrite and pyrrhotite are quite common. They are found in beds up to 15 cm thick. The higher the percentage of chert, the poorer the bedding definition, and thus the cherty quartzite is not as well bedded as the IF. On the average the cherty quartzite beds are only 6 to 9 m thick, but they may reach 305 m in surface width over a length of 1.5 km.

2.2.3 Basic and Intermediate Volcanics

The Keewatin-type volcanic rocks within the iron range are basic to intermediate in composition. They are found as massive flows which vary in texture from very fine to coarse. Pillow structures, where present, have been used for stratigraphic top determinations. Fine grained, very well bedded tuffs are most abundant at the east and west ends of the range. In some places, the contact between the IF and lava flows is separated by a zone of light greenish sedimentary rock, generally 3 to 4.5 m wide, which is probably tuffaceous in origin.

2.2.4 Intrusives

2.2.4a Lamprophyre Dikes

The lamprophyre dikes are greyish green and characterized by biotite phenocrysts in a fine grained matrix. Small isolated chloritized zones are common in the dikes. These zones probably represent altered

volcanic inclusions. The lamprophyre dikes were intruded late in the Archean and may represent the last igneous activity of the terminal Algonian orogeny (Lawton, 1957).

In the South and Central orebodies (Figure 3) there are northeast trending lamprophyre dikes up to 1 m in thickness. Lamprophyre dikes up to 3 m wide also occupy a well defined east-west fracture pattern, with a few thin dikes trending northwesterly. At least two different ages of lamprophyre have been established because the east-west system is cut by the northeast trending system.

2.2.4b Syenite Stock and Dikes

The Lebel Syenite stock is located 4.6 km to the WSW of the iron range. It closely resembles the Otto syenite stock. They are probably comagmatic and may be upward protuberances of a large body of syenite or granite (Lawton, 1957).

The Lebel syenite is composed of an aggregate of coarse feldspar crystals set in a sparse groundmass of mafic minerals and fine feldspar grains. Marginal phases of the stock may be more basic than the interior of the mass owing to assimilation of country rock.

The syenite dikes are composed predominately of medium grained feldspar. In places, separate intrusions of lamprophyre and syenite dikes occur side by side. In

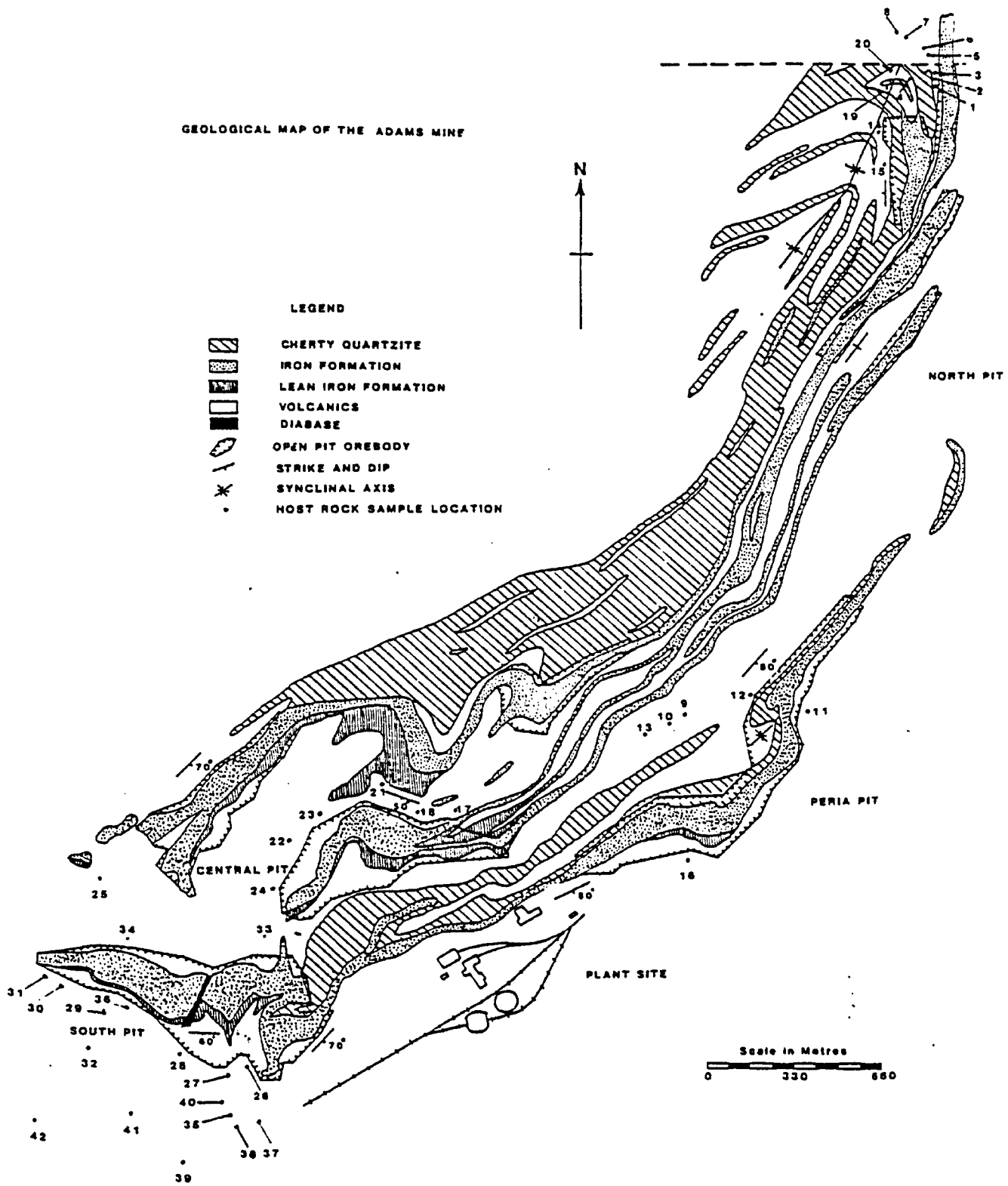


FIG. 3. Geology map of Adams Mine

other places the composition of the dike is gradational between a lamprophyre and a syenite. Presumably the parent magma has differentiated to give rise in most cases to either an acid or basic dike but in a few cases to an intrusion of some intermediate composition (Dubuc, 1965).

2.2.4c Diabase Dike

Diabase dikes of Abitibi age intrude the Archean rocks. A steeply-dipping diabase dike of 50m in surface width has intruded the South orebody at about its midpoint. The diabase consists of a typical dark greenish-grey massive diabase which weathers to a dark brown colour. It shows diabase texture with chilled margins and a coarse-grained central portion.

2.3 GEOLOGICAL HISTORY

The IF in the Boston Township is a sedimentary deposit. The main constituents of the IF are silica and iron. Their source is thought to be from the weathering and leaching of the earlier volcanic flows and tuffs (Armstrong and Moore, 1946). The silica and iron were transported, probably in the colloidal state to basins of accumulation where they were deposited as chemical sediments. The general sequence of deposition appears to be lean iron formation, followed by magnetite oxide facies IF, and finally cherty quartzite. Consolidation

and metamorphism followed during which the IF was re-crystallized to its present state.

Thick volumes of IF and pyroclastics are evidence for considerable volcanic activity during deposition of the IF. The intercalated volcanic flows appear to have invaded only part of the sedimentary basin at any one time. In the western portion of the range, where only small detached lenses of IF occur, volcanic flows likely covered the whole area.

2.4 STRUCTURE OF THE BOSTON TOWNSHIP IRON RANGE

The presence of a syncline in the northeast end is indicative of the structure of the iron range. The axis of the fold strikes $N35^{\circ}E$ and plunges steeply at $\sim 60^{\circ}SW$.

In the east and northeast portion of the range the limbs dip 50° to 90° to the south and southeast. However, at the extreme northeast end the dips change from vertical to northwest. At least two main horizons of IF in the northeastern portion are overturned and facing north-northwest as indicated by pillow structures. It would therefore appear that the IF series is the result of isoclinal folding to yield an overturned southeastern limb of a major synclinal structure. Most of the northeastern limb is truncated by the Lebel syenite stock.

Several faults, radial to the Lebel syenite stock, are found cutting the iron range. Where these faults have

cut the IF, very little displacement appears to have taken place.

2.5 OREBODIES

Enlargements of the IF horizons caused by folding and brecciation led to the development of the orebodies. A total of eight different orebodies have been outlined on the Adams Mine property of which seven are located in the eastern portion of the range.

The orebodies are essentially made up of IF which grades up to 26% magnetic Fe over widths exceeding 90m. In some places, especially along the hanging walls, there are minor amounts of lean IF grading from 12 to 18% magnetic Fe.

Structurally the individual orebodies are quite complex. Contacts are quite irregular and often reverse their position locally without the influence of faulting. Such situations are caused by severe folding and the pinching out of beds. It is also believed that considerable dislocation of the beds took place during the period of sedimentation and a certain amount of slumping must have taken place prior to induration (Dubuc, 1965).

CHAPTER III

EXPERIMENTAL METHODS

3.1 SAMPLING

In order to ensure as complete a coverage of the Adams Mine as possible 171 hand-oriented iron formation (IF) samples and 45 drilled host rock (HR) sites were collected.

The 171 IF samples were collected as uniformly as possible throughout the four pits (Figures 4 a-d). Each sample was hand oriented in situ using topographic sitings and a modified inclinometer to an accuracy of $\sim 3^\circ$.

At each of the 45 HR sites (Figure 3), 5 cores were drilled several metres apart. The cores were oriented in situ using a solar compass along with a Brunton compass and topographic sitings to an accuracy of $\sim 2^\circ$.

3.2 SAMPLE PREPARATION

The HR sites were drilled using a 2.5cm diameter barrel. Each core was cut into at least two 2.54cm long core specimens yielding a total of 529 HR specimens.

From each of the 171 hand samples, at least 4 specimens of 1cm diameter and 0.86cm length were drilled for alternating field (AF) cleaning. An additional 2 specimens were drilled from each sample where possible for

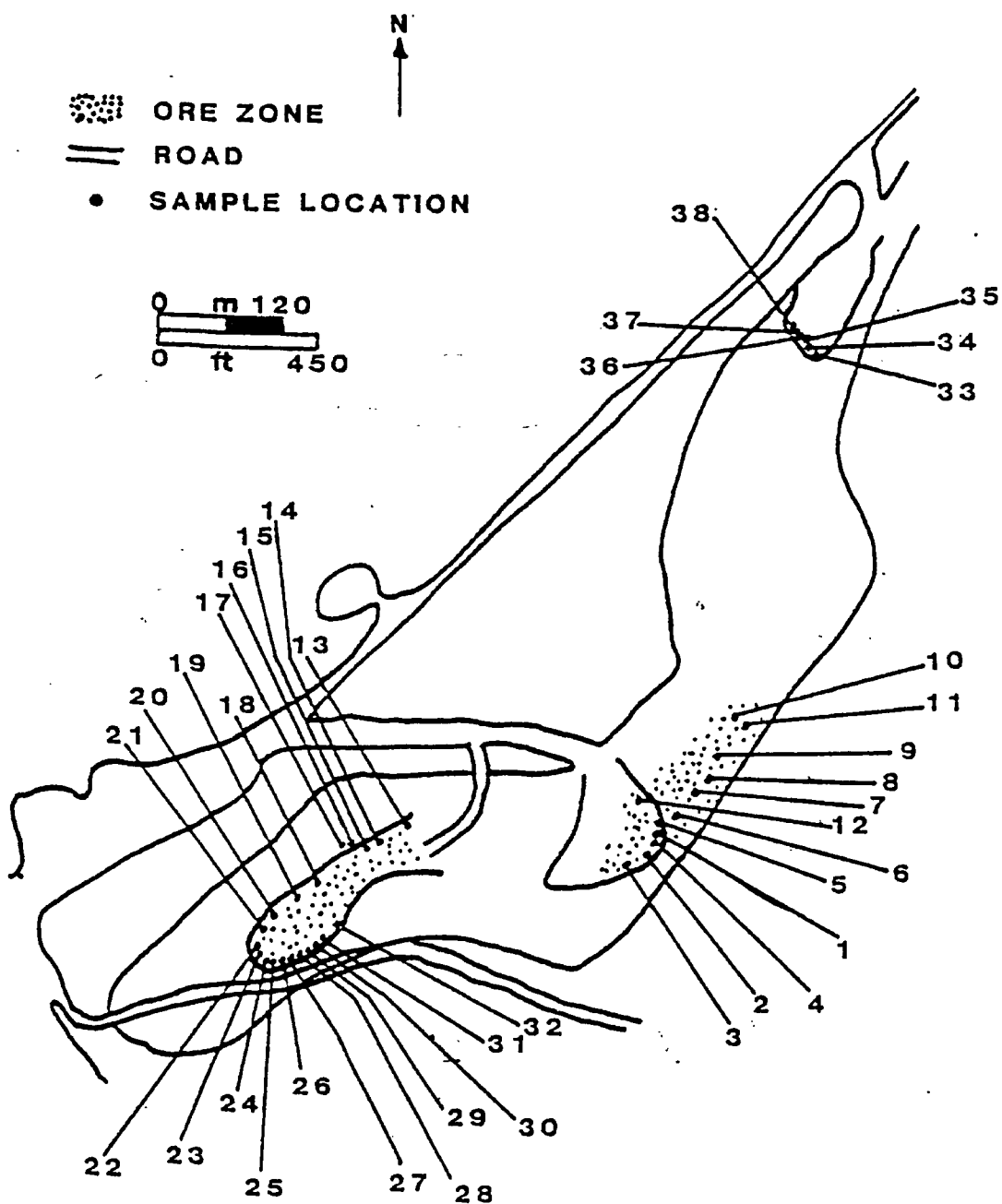


FIG. 4a. Outline of Peria Pit, Adams Mine, showing locations of block samples of iron formation.

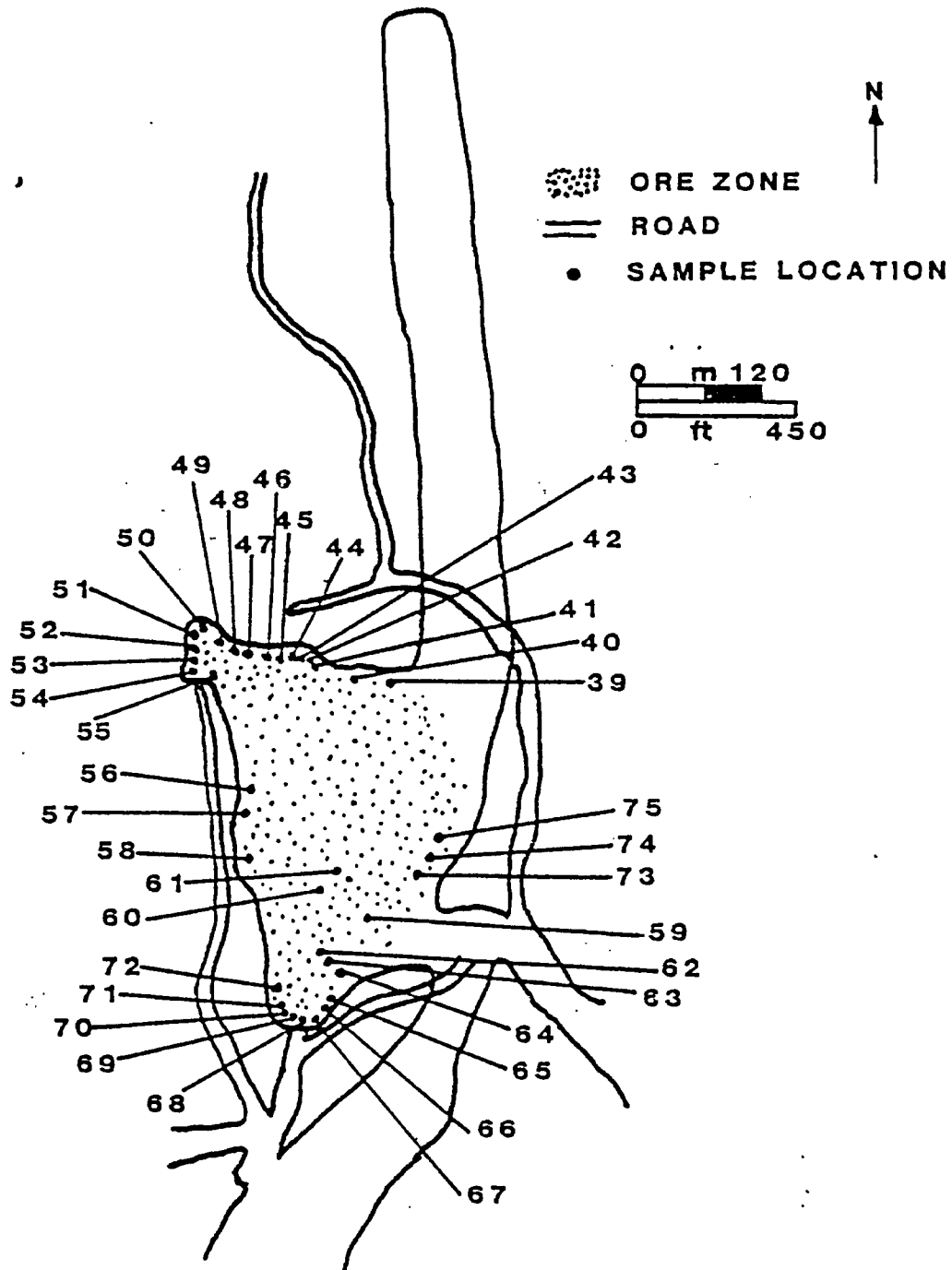


FIG. 4b. Outline of North Pit, Adams Mine, showing locations of block samples of iron formation.

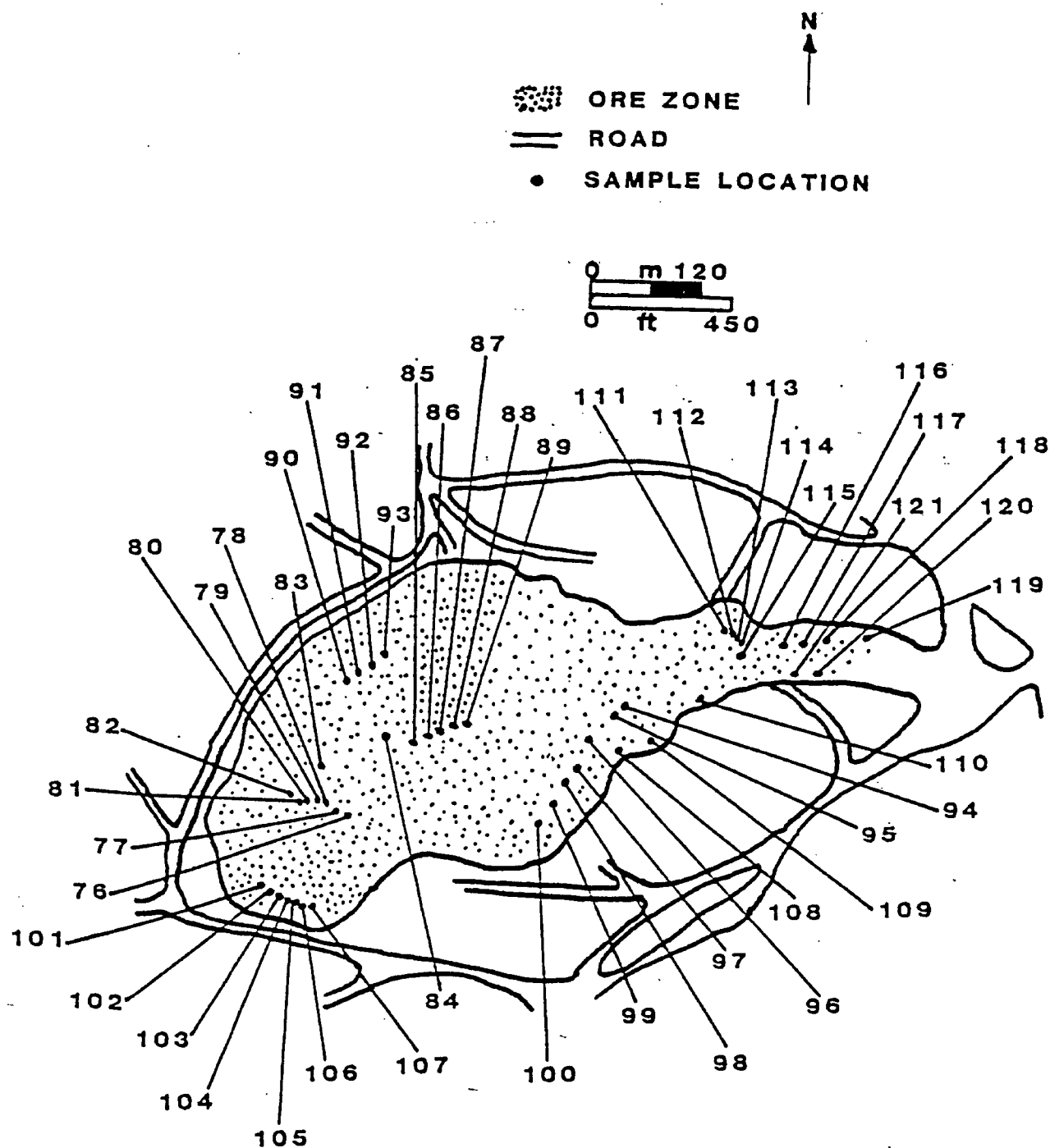


FIG. 4c. Outline of Central Pit, Adams Mine, showing locations of block samples of iron formation.

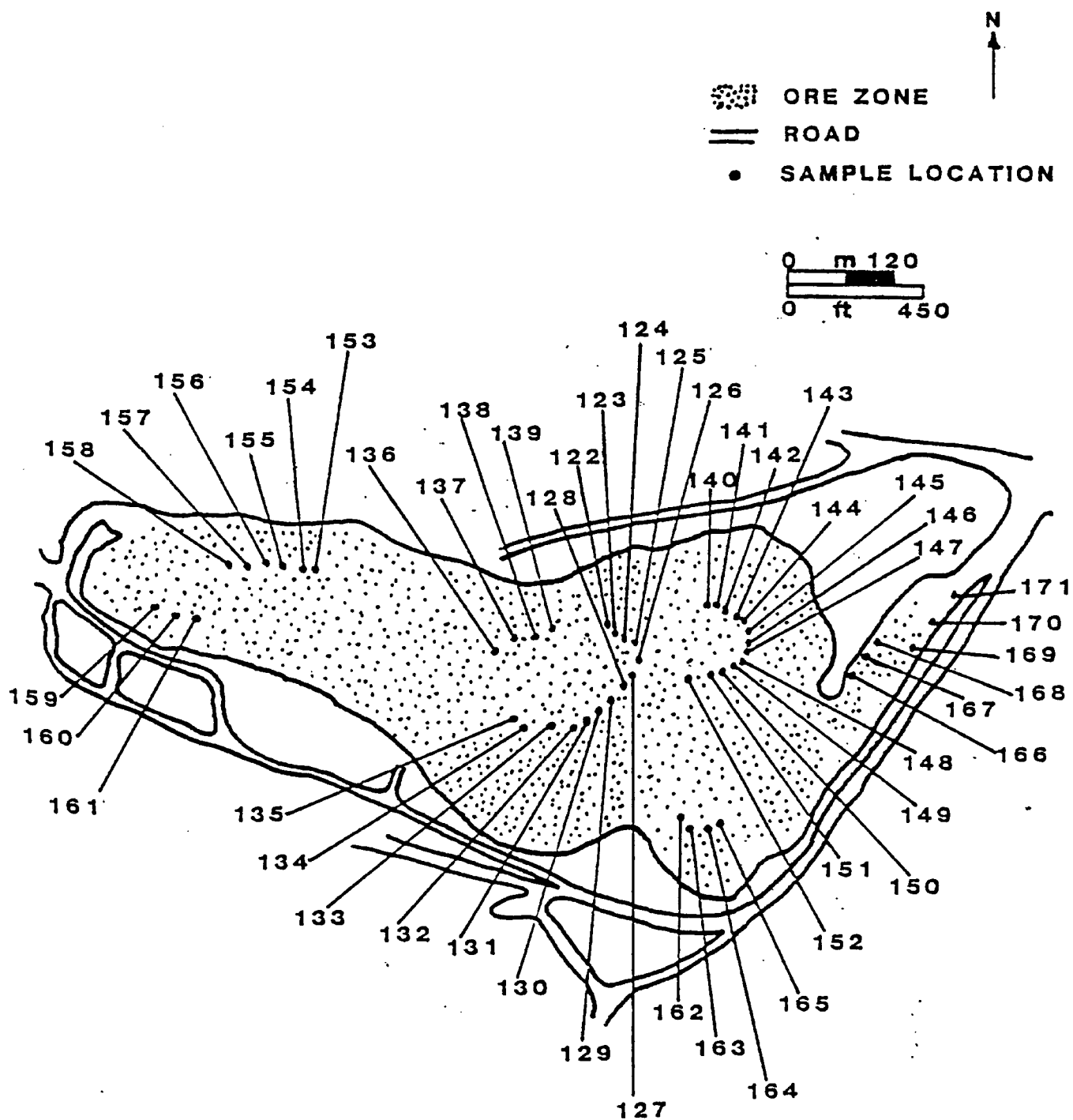


FIG. 4d. Outline of South Pit, Adams Mine, showing locations of block samples of iron formation.

thermal and chemical cleaning along with other stability tests.

Because it is possible that the small IF cores could be confined to one band of the IF and hence be unrepresentative of the IF as a whole, 15 large 2.50cm diameter specimens were drilled from some hand samples.

3.3 SAMPLE TREATMENT

3.3.1 Specific Gravity

The specific gravity was measured with a modified picnometer on 547 IF specimens to an accuracy of $\pm 0.001 \text{ gm/cm}^3$.

3.3.2 Magnetic Susceptibility

The 524 HR specimens, the 589 small IF specimens and the 15 large IF specimens were measured using a toroid bridge (Christie and Symons, 1969) to find their low-field susceptibility perpendicular to bedding (K_1).

3.3.3 Anisotropy of Magnetic Susceptibility

The low-field magnetic susceptibility of the 592 small IF specimens and the 15 large IF specimens was measured on the toroid bridge along 9 directions. The principal axial directions and magnitudes of the susceptibility ellipsoid were computed from the matrix elements. It is important for this measurement that the length to diameter ratio is 0.86.

3.3.4 Natural Remanent Magnetization

The natural remanent magnetization (NRM) of 1476 specimens was measured on a Schonstedt SSM-1A spinner magnetometer using either a 3-spin or 6-spin mode depending on the strength of their magnetic signal. The NRM intensity and direction for each specimen were computed from the measurements made along their three principle directions.

3.3.5 AF Demagnetization

A total of 70 IF pilot specimens with a homogeneous NRM direction and an average intensity were selected for cleaning by AF demagnetization. The specimens were selected to equally represent the four pits that were sampled. Each specimen was step demagnetized in AF fields of 5, 10, 15, 20, 30, 40, 50, 60, 70, 80, 90 and 100mT peak intensity using a Schonstedt GSD-1 AF demagnetizer.

One pilot specimen was selected from each HR site which had a representative NRM direction and intensity for that site. The pilot specimens were cleaned by AF step demagnetization in the same peak alternating fields as used for the IF.

Because it would be too time consuming to AF step demagnetize and measure all of the specimens, the pilot specimens were used to select the optimum AF peak intensities for demagnetizing the remaining IF and HR specimens for

each site or sample. The optimum values for AF cleaning were chosen by using the Paleomagnetic Stability Index (PSI) method of Symons and Stupavsky (1974) for directional analysis, and the intensity decay curves of the pilot specimens (Table 2 and 3).

3.3.6 Thermal Cleaning

A total of 22 IF pilot specimens with an average NRM direction and intensity were selected to equally represent each pit. The specimens were thermally demagnetized at temperatures of 100, 200, 300, 400, 500, 550, 600 and 650°C using a furnace having a non-inductive heating element. The furnace is housed in a nested series of five mu-metal shields in a shielded room. The specimens were placed in inverted directions on successive steps in order to detect the acquisition of remanence components caused by the incomplete elimination by shielding of the EMF during the cooling stage when the magnetic domains are reset. Because of high PSI values and scattered remanence directions, the remaining IF specimens weren't thermally cleaned.

Also 24 representative HR specimens were thermally demagnetized at the same temperature increments as for the IF.

TABLE 2. Sampling and remanence data of Iron Formation sites

Sample	Pit	AF intensity mT	Data screening			N	Remanent magnetization			
			a	b	c		Length R	Decl. °	Incl. A95 +down °	
1	Peria	50				4	3.845	301.52	-15.51	21.43
2	Peria	50				4	3.923	329.19	3.67	14.87
3	Peria	50	1			3	2.916	199.79	3.68	25.85
4	Peria	50	1			3	2.973	279.79	-2.38	14.40
5	Peria	70				0				
6	Peria	50				0				
7	Peria	40				4	3.867	338.71	3.06	19.77
8	Peria	40				0				
9	Peria	40				0				
10	Peria	40	1			3	2.909	109.00	46.08	26.91
11	Peria	40	1			3	2.966	144.45	-10.69	16.13
12	Peria	20				4	3.863	122.85	20.19	20.08
13	Peria	40		1		2	1.967	269.83	-8.91	46.77
14	Peria	40				0				
15	Peria	40				0				
16	Peria	30				4	3.860	238.61	15.66	20.33
17	Peria	40				0				
18	Peria	30				0				
19	Peria	30				0				
20	Peria	50				0				
21	Peria	50				0				
22	Peria	20				0				
23	Peria	50	1			3	2.923	276.85	7.44	24.72
24	Peria	30				0				
25	Peria	50	1			3	2.914	65.27	4.45	26.11
26	Peria	60	1			3	2.959	129.76	68.99	17.89
27	Peria	70				0				
28	Peria	50				0				
29	Peria	50				0				
30	Peria	50				0				
31	Peria	50	1			3	2.845	312.33	11.42	35.76
32	Peria	50				0				
33	Peria	50	1			3	2.873	5.84	-2.14	32.22
34	Peria	40				4	3.940	346.13	2.54	13.14
35	Peria	30				4	3.840	134.30	46.29	21.77
36	Peria	50	1			3	2.984	217.35	7.42	11.07
37	Peria	30	1			3	2.867	155.63	-6.64	33.02
38	Peria					0				
39	North	50				0				
40	North	50	1			3	2.888	269.69	3.20	30.01
41	North	60				4	3.852	311.29	-8.13	20.93
42	North	60				4	3.819	225.58	2.59	23.23
43	North	60				0				
44	North	70	1			3	2.980	280.18	10.84	12.47
45	North	60				0				

TABLE 2. (contd.)

Sample	Pit	AF intensity mT	Data screening			N	Remanent magnetization			
			a	b	c		Length R	Decl. °	Incl. +down °	A95 °
46	North	60	1			3	2.964	244.80	-13.13	16.74
47	North	60				0				
48	North	50	1			3	2.823	256.41	2.60	38.53
49	North	50				0				
50	North	50	1			3	2.938	271.90	22.25	21.99
51	North	50	1			3	2.850	198.26	-5.42	35.22
52	North	40				0				
53	North	60				0				
54	North	70				4	3.935	117.60	32.81	13.66
55	North	60				0				
56	North	60				0				
57	North	60				0				
58	North	60				0				
59	North	60				4	3.886	268.41	-6.18	18.29
60	North	60				0				
61	North	70				0				
62	North	60	1			3	2.930	290.99	9.21	23.59
63	North	50	1			3	2.976	279.73	3.32	13.66
64	North	50				0				
65	North	50				0				
66	North	50				0				
67	North	30				4	3.836	281.22	10.76	22.07
68	North	40				4	3.893	280.15	1.73	17.68
69	North	40				0				
70	North	50				0				
71	North	50				0				
72	North	50				4	3.787	259.71	1.21	25.37
73	North	*								
74	North	60				0				
75	North	70				3	2.859	317.10	-2.21	34.09
76	Central	60				0				
77	Central	60		1		2	1.991	217.98	34.14	24.49
78	Central	60	1			2	1.920	346.54	4.76	78.02
79	Central	60				3	2.844	191.81	19.94	35.96
80	Central	60	1			3	2.824	162.25	19.15	38.37
81	Central	60				0				
82	Central	60				0				
83	Central	60				0				
84	Central	70				0				
85	Central	70				4	3.850	13.39	8.36	21.07
86	Central	60	1			3	2.956	227.90	28.63	18.40
87	Central	40	1			3	2.895	275.78	5.40	29.10
88	Central	60				0				
89	Central	60				4	3.835	299.09	31.04	65.17
90	Central	60				0				

TABLE 2. (contd.)

Sample	Pit	AF intensity mT	Data screening			N	Remanent magnetization			
			a	b	c		Length R	Decl. °	Incl. +down °	A95 °
91	Central	70				0				
92	Central	60				4	3.898	293.87	-8.46	17.22
93	Central	60				0				
94	Central	60				0				
95	Central	40				4	3.900	189.70	-79.81	17.05
96	Central	30				4	3.785	243.18	3.69	25.49
97	Central	60				0				
98	Central	80				4	3.850	328.75	-17.72	21.07
99	Central	60				4	3.985	344.47	11.22	6.49
100	Central	*								
101	Central	50	1			3	2.919	153.41	47.10	25.38
102	Central	50				0				
103	Central	60				4	3.846	270.25	5.00	21.34
104	Central	50	1			3	2.904	254.16	20.07	27.77
105	Central	40				4	3.937	248.30	14.58	13.47
106	Central	50				4	3.816	202.27	-0.64	23.48
107	Central	60				0				
108	Central	60				0				
109	Central	60				4	3.800	263.35	14.98	24.50
110	Central	60				4	3.979	120.14	-3.50	7.73
111	Central	50	1			3	2.968	254.01	22.53	15.84
112	Central	50	1			3	2.858	298.43	-0.02	34.16
113	Central	60	1			3	2.905	277.36	28.45	27.63
114	Central	60	1			3	2.898	269.83	-12.00	28.63
115	Central	50				0				
116	Central	50				4	3.788	333.60	5.89	25.32
117	Central	30				4	3.821	240.09	7.11	23.10
118	Central	50				4	3.914	243.76	0.64	15.73
119	Central	50				4	3.766	263.70	39.72	26.70
120	Central	50				4	3.864	237.88	22.20	19.99
121	South	50				0				
122	South	60				0				
123	South	70				4	3.896	176.44	-22.10	17.41
124	South	50		1		2	1.974	204.65	-2.36	41.52
						2	1.887	71.06	-21.68	81.93
125	South	50				0				
126	South	50				0				
127	South	60				0				
128	South	60				0				
129	South	60	1			3	2.918	359.31	-3.50	25.46
130	South	50				4	3.96	225.42	-3.73	10.67
131	South	50	1			3	2.829	191.03	15.56	37.74
132	South	40				4	3.808	245.68	-4.53	24.01
133	South	50	1			3	2.922	186.32	25.54	24.91
134	South	50				0				
135	South	50				0				

TABLE 2. (contd.)

Sample	Pit	AF intensity mT	Data screening			N	Remanent magnetization			
			a	b	c		Length R	Decl. °	Incl. +down °	A95 °
136	South	40				4	3.812	305.32	-8.65	23.75
137	South	50				0				
138	South	60		1		2	1.888	253.06	-17.63	82.77
						2	1.999	109.26	-42.96	6.30
139	South	60				4	3.810	291.11	9.51	23.87
140	South	50	1			3	2.994	230.44	11.14	6.55
141	South	50	1			3	2.893	234.91	-0.68	29.29
142	South	50				0				
143	South	50				0				
144	South	50	1			3	2.870	339.79	-1.12	32.62
145	South	50	1			3	2.967	320.46	2.86	15.91
146	South	50				0				
147	South	50				0				
148	South	50				0				
149	South	50		1		2	1.970	258.49	5.95	44.57
						2	1.907	32.78	35.74	85.56
150	South	50				0				
151	South	60				0				
152	South	70				4	3.895	248.08	-1.63	17.49
153	South	70				0				
154	South	60				4	3.929	339.25	1.33	14.30
155	South	70				0				
156	South	30				4	3.819	54.60	5.33	23.23
157	South	50				0				
158	South	50				0				
159	South	30				0				
160	South	20	1			3	2.843	20.49	32.28	36.03
161	South	60				4	3.835	303.24	0.24	22.13
162	South	60				0				
163	South	70				4	3.918	286.98	11.73	15.37
164	South	20				0				
165	South	50				0				
166	South	50				0				
167	South	50				0				
168	South	60				0				
169	South	80				0				
170	South	50				0				
171	South	30				0				

NOTES: R is the length of vector resultant. A95 is the radius of the cone of 95% confidence (Fisher 1953) in degrees. * is sample where no cores were obtained. Data screening: (a) core rejected as anomalous with respect to remaining cores from the sample, (b) sample considered to contain two direction populations, (c) sample rejected as specimen directions diverge from sample mean direction by more than 20°.

TABLE 3. Sampling and remanence data of Host Rock sites

Site	Pit	AF intensity mT	Data screening			N	Remanent magnetization			
			a	b	c		Length R	Decl. °	Incl. +down °	A95 °
1	North	20	4	1		0				
2	North	20	3			2	1.966	190.51	48.31	47.89
3	North	30		1		3	2.820	212.52	-15.37	38.98
4	North	30	5			0				
5	North	30	3		2	0				
6	North	40	2		1	2	1.916	80.42	-73.32	80.33
7	North	30	4	1		0				
8	North	30	3		2	0				
9	Peria	30	5			0				
10	Peria	30	2		1	2	1.973	311.73	55.21	42.59
11	Peria	40	3			2	1.977	337.25	66.32	39.02
12	Peria	20	1		1	3	2.922	250.47	76.93	35.33
13	Peria	20	5			0				
14	North	30	5			0				
15	North	30	5			0				
16	Peria	30	4	1		0				
17	Central	30	5			0				
18	Central	40	2			3	2.922	283.21	-41.02	35.33
19	North	30	4	1		0				
20	North	30	5			0				
21	Central	30	1		2	2	1.943	45.14	50.96	64.01
22	Central	30	2		1	2	1.932	245.11	70.19	70.82
23	Central	30	5			0				
24	Central	30	5			0				
25		30	5			0				
26	South	30	4		1	0				
27	South	30	5			0				
28	South	30	5			0				
29	South	30	4		1	0				
30	South	30	2		3	0				
31	South	20	5			0				
32	South	30	4	1		0				
33	South	20	2		1	2	1.921	21.32	55.84	61.85
34	South	40	5			0				
35	South	20	1			4	3.785	297.15	69.25	25.47
36	South	30	5			0				
37	South	30	5			0				
38	South	40	3		2	0				
39	South	20			5		4.750	193.29	50.93	19.70
40	South	40	5			0				
41		30			5		4.821	188.60	45.21	15.34
42		20			2	3	2.966	336.65	82.52	16.22
43		40	3			2	1.975	338.43	76.73	17.85
44		30	4		1	0				
45		20	5			0				

NOTES: R is the length of the vector resultant. A95 is the radius of the cone of 95% confidence (Fisher 1953) in degrees. Data screening: (a) core rejected because the 2 specimen directions diverged by more than 20°, (b) core rejected as sole remaining direction to inadequately represent the site, and (c) core rejected as anomalous with respect to remaining cores from the site.

3.3.7 Chemical Cleaning

A total of 18 representative IF pilot specimens were selected for chemical cleaning. The specimens were immersed in fresh 12N HCl and stored in a mu-metal shielding can between measurements. The specimens were washed in water and allowed to dry before their remanence was remeasured. The specimens were measured after 21, 87, 180, 271, 385, 525, 668, 830, 1017, 1161 and 1641 hours.

An additional 79 IF specimens were selected for chemical cleaning and measured after 600, 985 and 1465 hours of immersion.

3.3.8 Stability Tests

Storage tests were done to assess the degree of stability of the remanence caused by the acquisition of viscous remanence (VRM) components by IF.

First, the NRM of 18 IF and 18 HR specimens were measured. Then the specimens were taken out of the shielded room and exposed to the Earth's magnetic field (EMF). Half of the specimens were placed perpendicular to the EMF and the other half were placed parallel to the EMF. The specimens were remeasured after storage periods of 12, 23 and 37 days.

A shock test was performed on 26 IF specimens to assess how dynamite blasting used in mining the rock

could affect the NRM response. After measuring the NRM of the specimens, they were hit 20 times on an aluminum plate and their remanence remeasured. The test was performed first with the specimens oriented parallel to the EMF and then repeated perpendicular to the EMF.

3.4 COMPUTATIONS

In order to handle the ~20 quantitative variables for the 1476 specimens, it is mandatory to use a computer for the computations and data analysis. Existing laboratory computer programs, stored on disk in the computer library, were used for this purpose. Input data included specimen identification, longitude and latitude, k_1 susceptibility and specific gravity. These programs calculate and plot: 1) the declination, inclination and intensity of the remanence; and 2) the declination, inclination and magnitudes of the axes of the anisotropy of susceptibility ellipsoids. Additional statistical programs were used to calculate the means and confidence limits.

BMDP5D programs (BMDP-77) were used to plot the output in histogram form for analysis. The program has been adapted to calculate the means and confidence limits using both normal and lognormal statistics for the various output parameters.

The BMDP6D program was used to correlate between

two data sets, plot the data and do regression fits with correlation statistics. These statistical tests help define the limits of each of the parameters that are required for the magnetic model to be proposed.

3.5 MAGNETIC MODEL

The magnetic model program was compiled and tested in studies of the Sherman Mine by Symons and Stupavsky (1979) and the Moose Mountain Mine by Symons, Walley and Stupavsky (1980). The program (Walley, 1980) incorporates all the important factors for interpreting magnetic anomalies over a magnetic sheet. Most magnetic model computer programs used to calculate the induced magnetic components of a sheet include a variety of thicknesses, magnetite contents, and strike and dips relative to the Earth's varying geomagnetic field. Some programs also incorporate the remanence and/or the demagnetizing factor. No previous programs incorporate all of these plus the effect of magnetic anisotropy.

The magnetic model used in this study follows the standard theoretical equations for the induced component. The demagnetizing factor and the anisotropy of susceptibility equations follow Gay (1963) and the remanence equations follow Strangway (1965). See Appendix 1 for the model computations.

CHAPTER IV

RESULTS

4.1 SPECIFIC GRAVITY

The specific gravity (S.G.) of 547 IF specimens have a mean value of 3.24 gm/cm^3 (Standard Deviation (s.d.) = 0.51) (Figure 5). This value is lower than the expected ore value because the pit sampling includes low grade and barren wall-rock samples. The mean SG for the individual pits range from 3.06 to 3.44 (Table 4). The calculated SG of the economic ore at Adams Mine, with a 22% magnetic Fe content is 3.49.

4.2 MAGNETIC SUSCEPTIBILITY.

A total of 524 HR specimens show a lognormal distribution for $k_{\underline{1}}$, with a lognormal mean of $2.35 \times 10^{-4} \text{ cgs/cm}^3$ (Figure 6).

A total of 592 IF specimens show a lognormal distribution for $k_{\underline{1}}$ with a lognormal mean of $4.52 \times 10^{-2} \text{ cgs/cm}^3$ (Figure 7). The mean values range from 3.57 to $6.09 \times 10^{-2} \text{ cgs/cm}^3$ for the individual pits (Table 4).

Because $k_{\underline{1}\text{IF}} = 192 k_{\underline{1}\text{HR}}$, it is reasonable to neglect the $k_{\underline{1}\text{HR}}$ in calculating the IF magnetic anomaly.

A total of 592 IF specimens show a good regression fit between the SG and $k_{\underline{1}\text{IF}}$ with a correlation coefficient of +0.73 (Figure 8) and give the relationship:

$$k_{\underline{1}\text{IF}} = 0.0698\text{SG} - 0.179$$

TABLE 4. Summary of regression fit between S.G. and k_1

Pit	Number of Specimens N	S.G. gm/cm ³	Mag. susc. cgs/ccx10 ⁻²	Regression Fit: $k_1 = mS.G. + c$		
				m	c	r
Peria	129	3.14	3.76	0.0540	-0.1321	0.613
North	112	3.16	4.14	0.0637	-0.1597	0.728
Central	158	3.06	3.57	0.0476	-0.1097	0.562
South	180	3.44	6.09	0.1073	-0.3081	0.887

NOTES: Regression fit calculated by BMDP6D program.
r is the correlation coefficient.

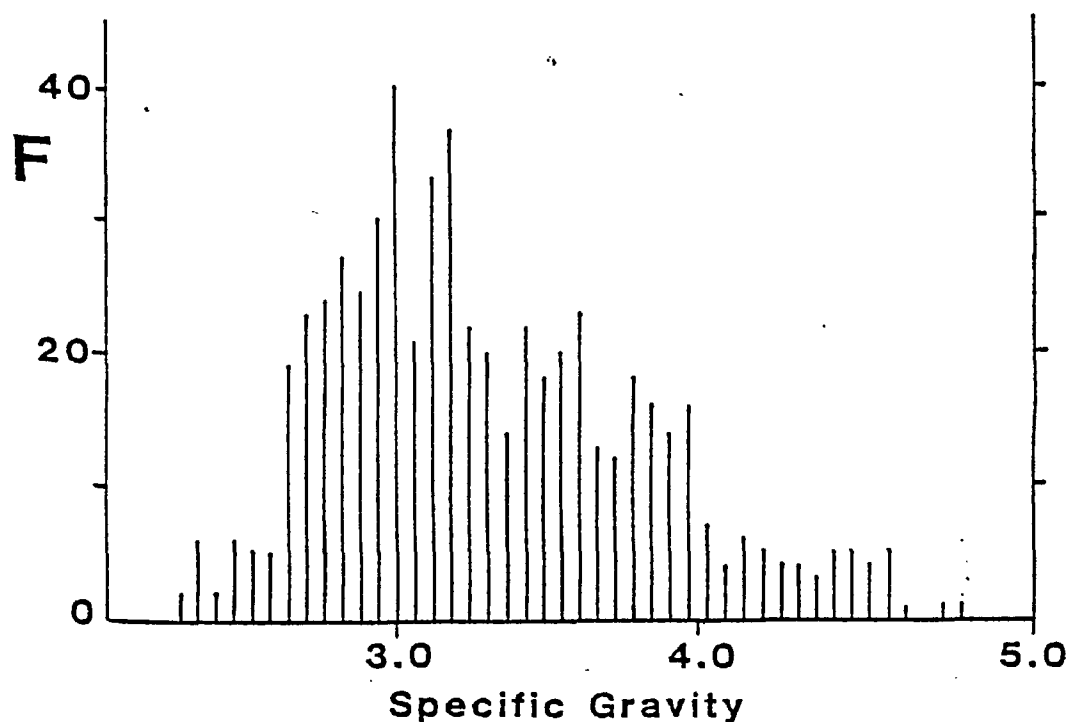


FIG. 5. Histogram of the specific gravities of 547 iron formation specimens.

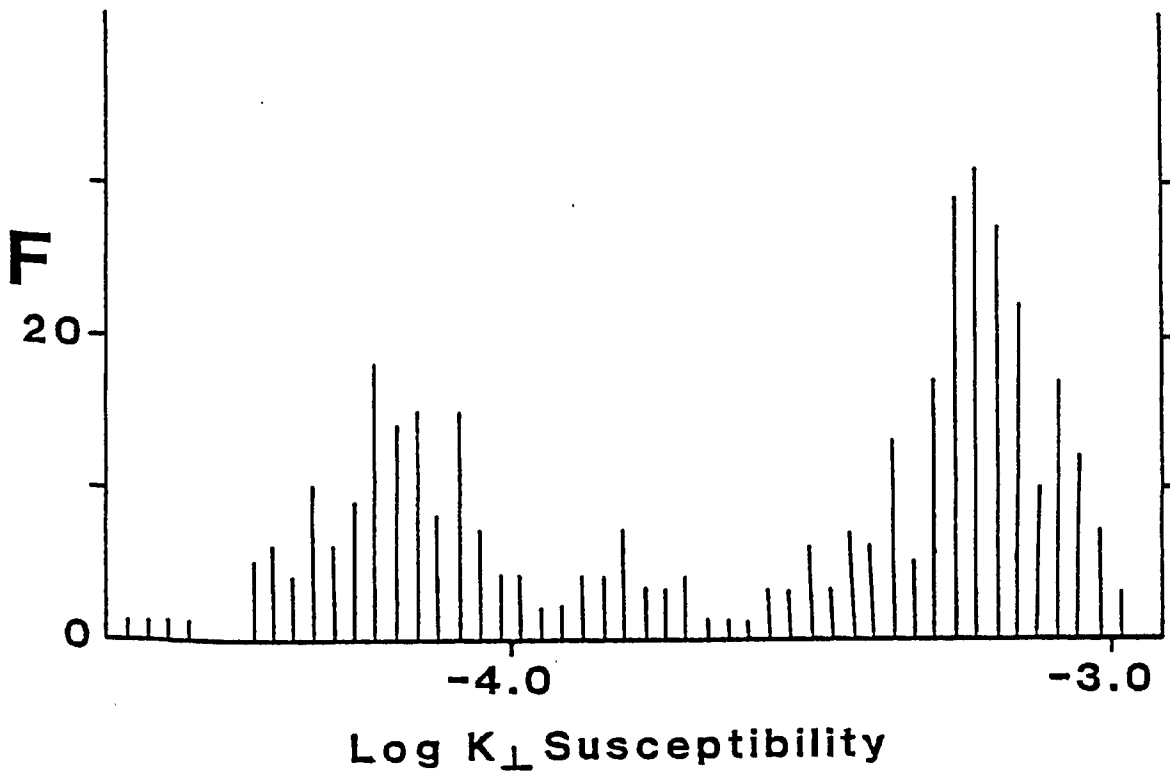


FIG. 6. Lognormal histogram of k_{\perp} susceptibility for 524 HR specimens.

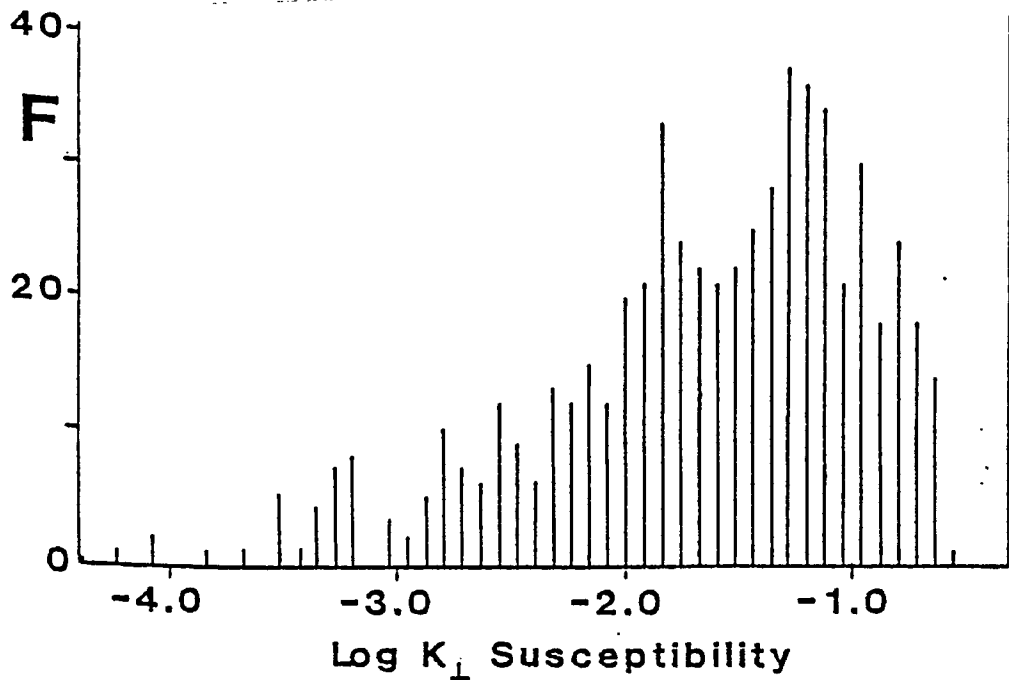


FIG. 7. Lognormal histogram of k_{\perp} susceptibility for 592 IF specimens.

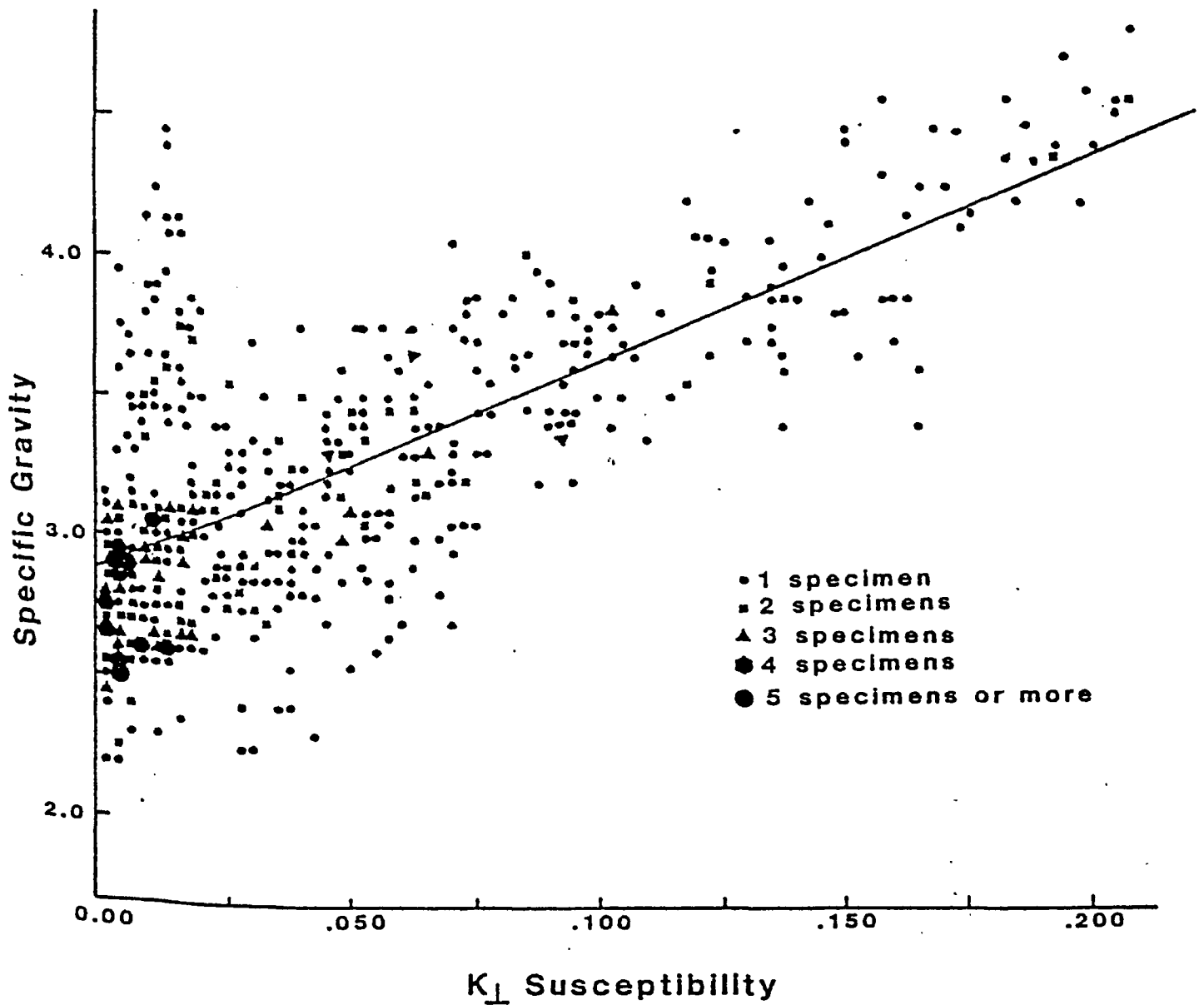


FIG. 8. Regression line of specific gravity versus k_{\perp} susceptibility for 581 IF specimens.

This is rather different from the relationships obtained at the Moose Mountain Mine (Symons, Walley and Stupavsky, 1980) and Sherman Mine (Symons and Stupavsky, 1979):

Moose Mountain : $k_{\perp IF} = 0.0912SG - 0.249$

Sherman Mine : $k_{\perp IF} = 0.0906SG - 0.245$

The regression fits for individual pits are shown on Table 4. Economic ore at the Adams Mine gives a value of 0.0645 cgs/cm^3 for k_{\perp} .

4.3 ANISOTROPY OF MAGNETIC SUSCEPTIBILITY

The expected anisotropy of susceptibility pattern for banded IF is that the minimum (k_{\min}) axial direction of the ellipsoid is perpendicular to the bedding plane and the intermediate (k_{int}) and maximum (k_{\max}) directions are parallel to the bedding plane. In this study, the specimens showed a bimodal distribution of directions with not all specimens conforming to the expected values (Figures 9a-9b). On inspection it was noticed that some specimens were too long with lengths of 0.95 cm. A total of 50 specimens were recut to 0.86cm and remeasured. Their anisotropy of susceptibility values then conformed to the expected pattern (Figure 10).

The mean magnitude ratio of k_{int}/k_{\min} is 1.47 (Figure 11) and the k_{\max}/k_{\min} ratio is 1.63 (Figure 12). The ratios were not effected by the recutting.

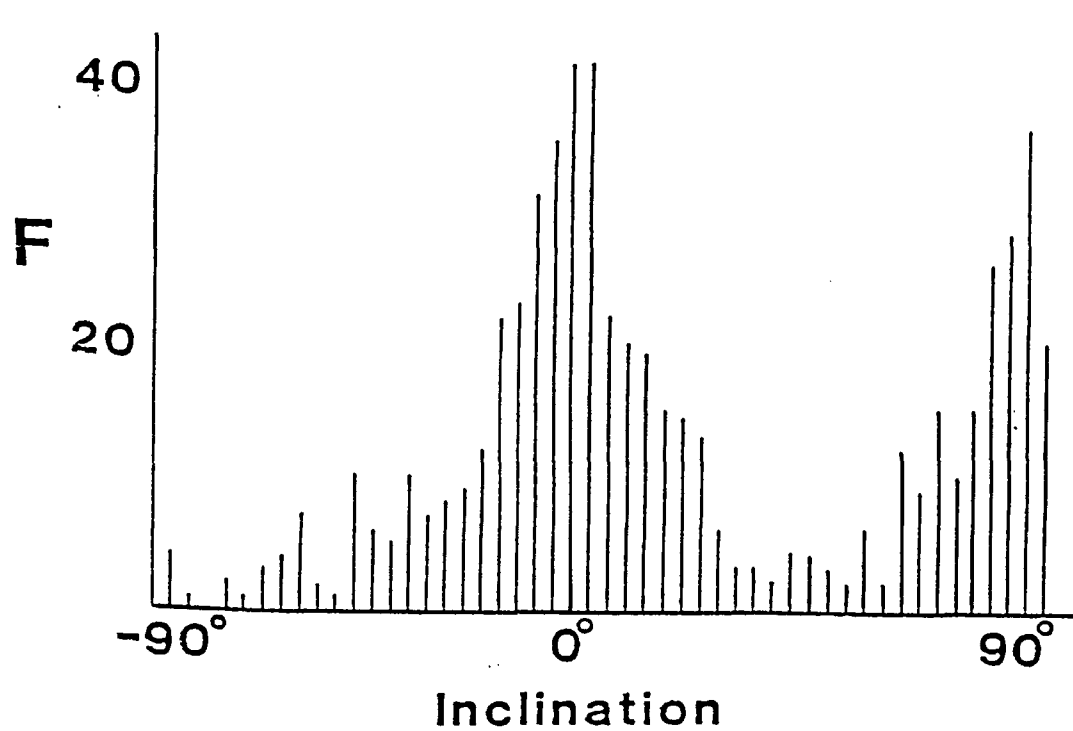
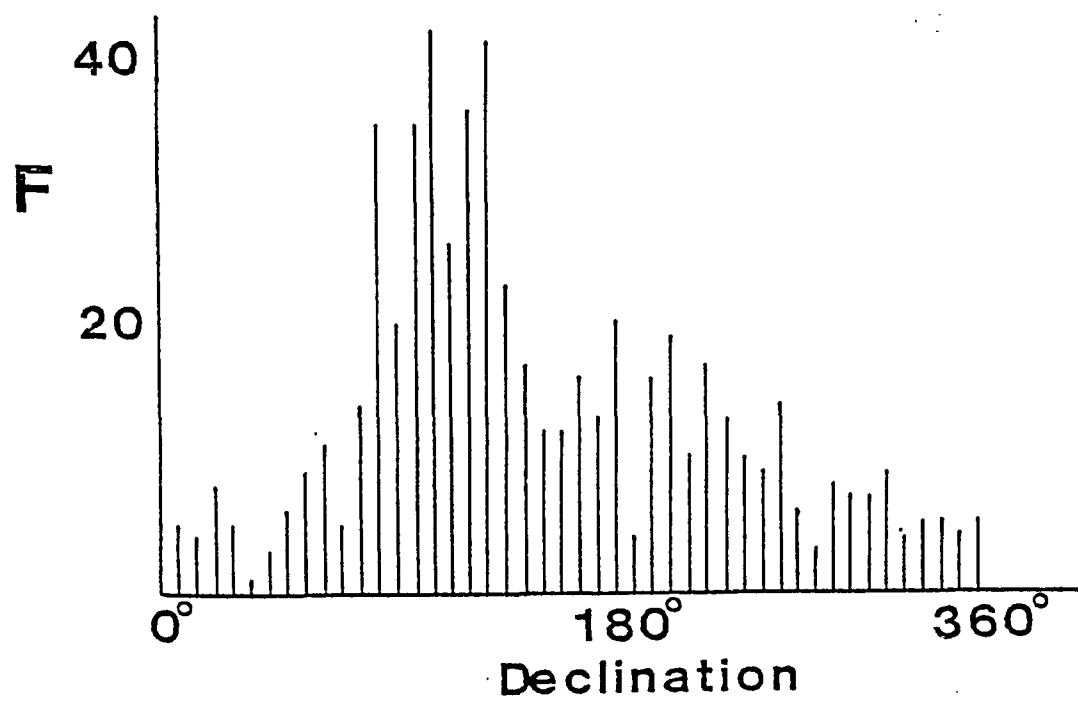


FIG. 9a. Histogram of k_{\min} (k_1) directions for 592 IF specimens.

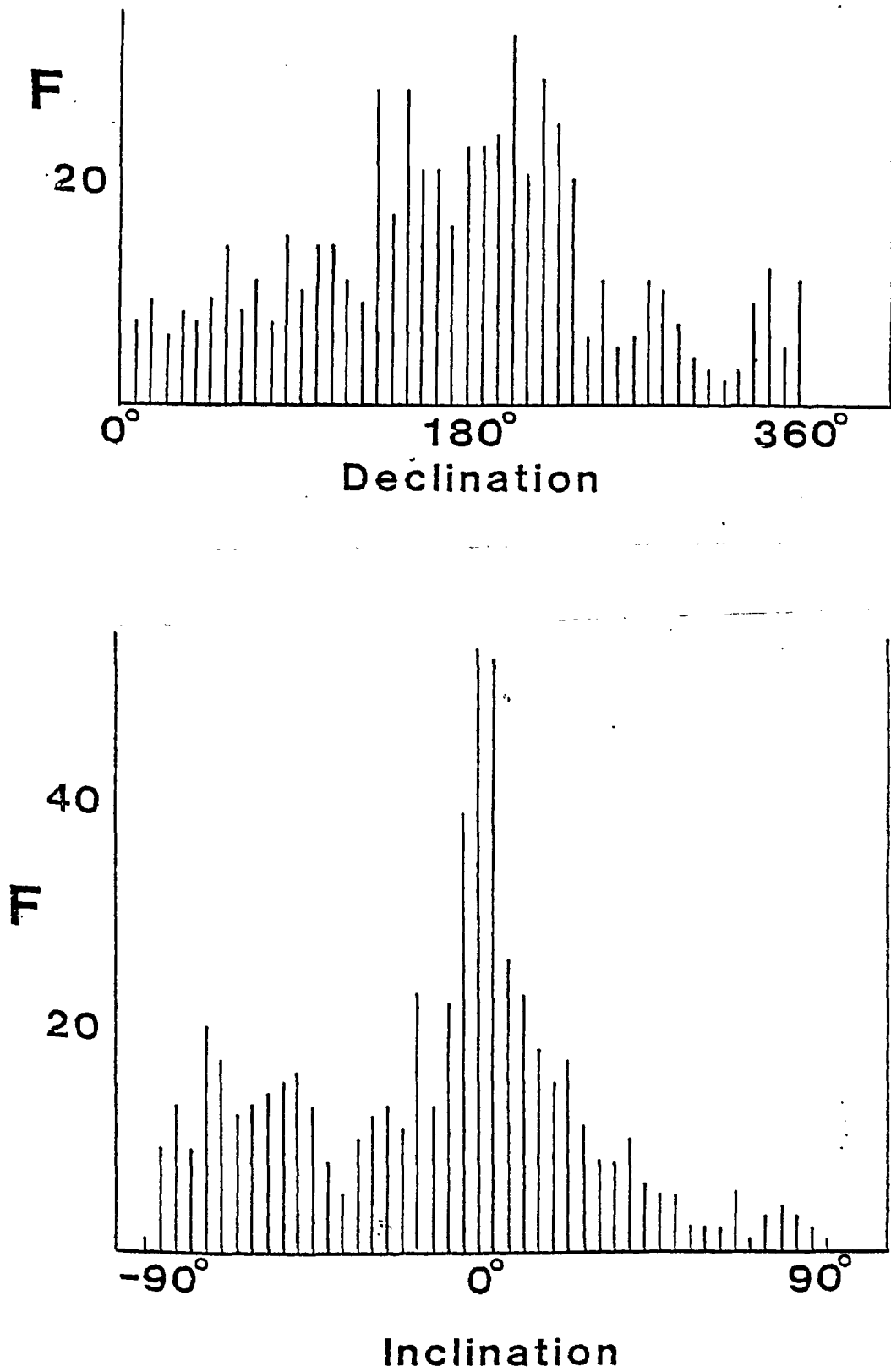


FIG. 9b. Histogram of k_{\max} directions for 592 IF specimens.

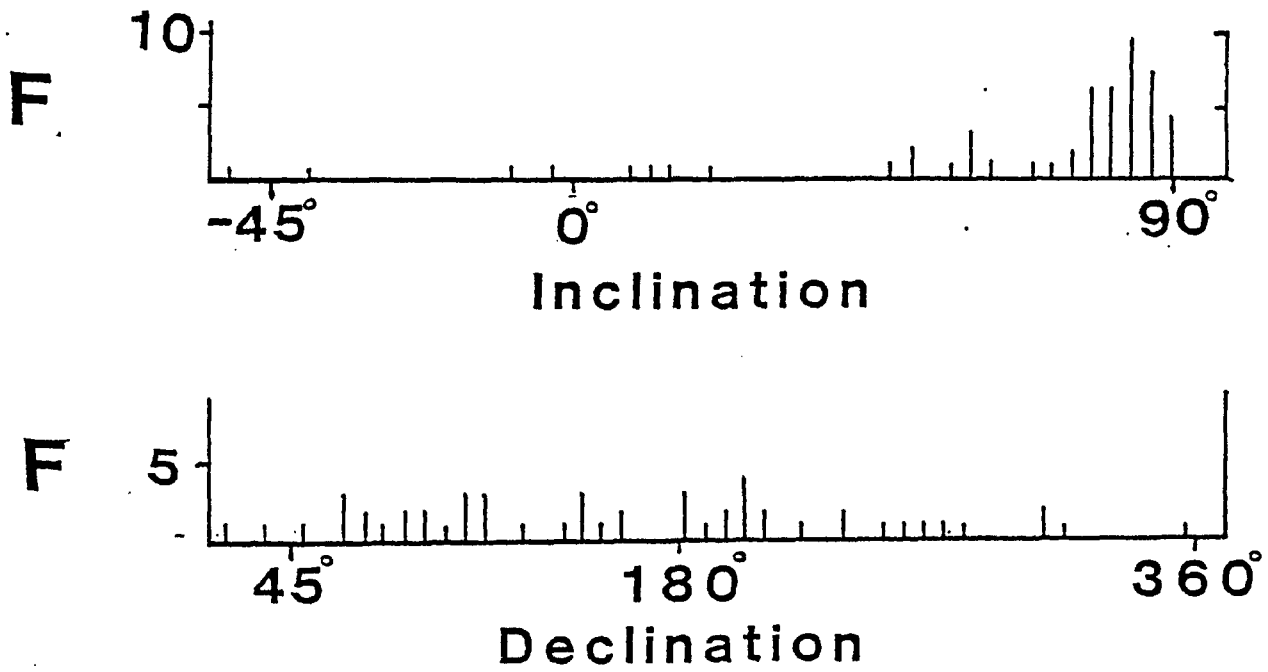


FIG. 10a. Histogram of k_{\min} (k_{\perp}) directions for 50 recut IF specimens.

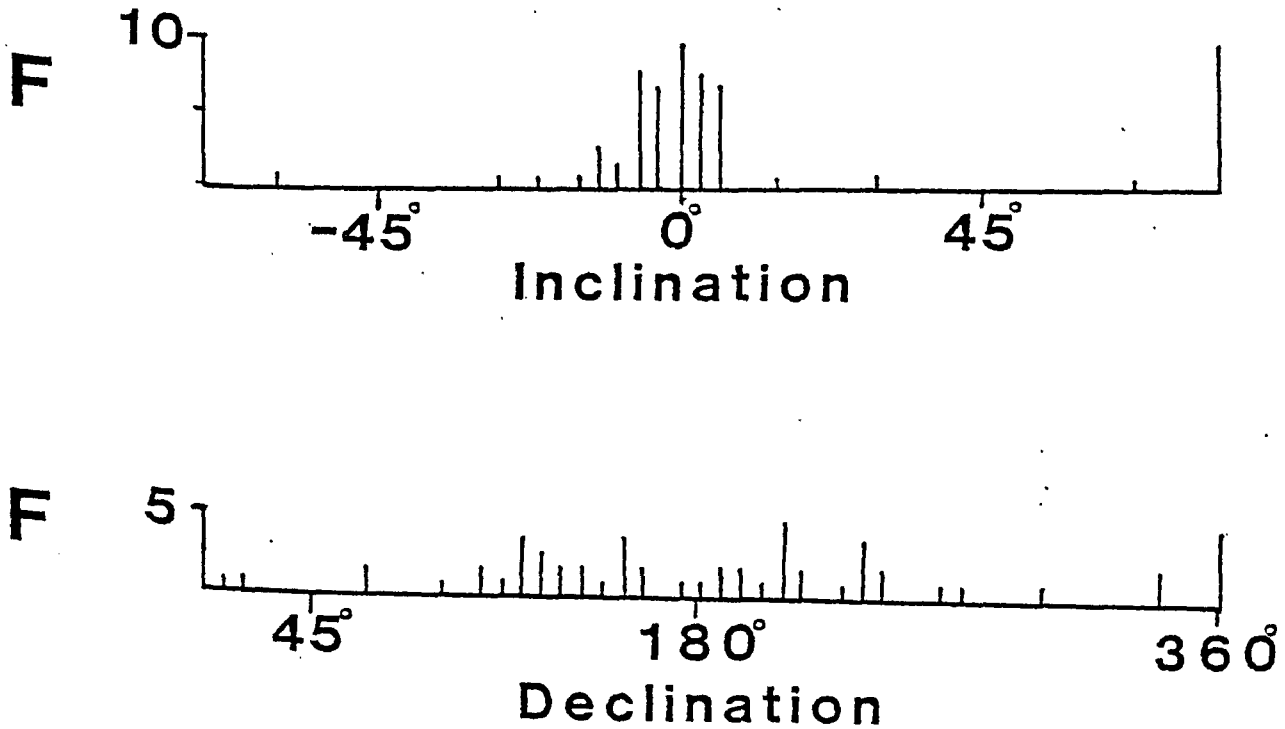


FIG. 10b. Histogram of k_{\max} directions for 50 recut IF specimens.

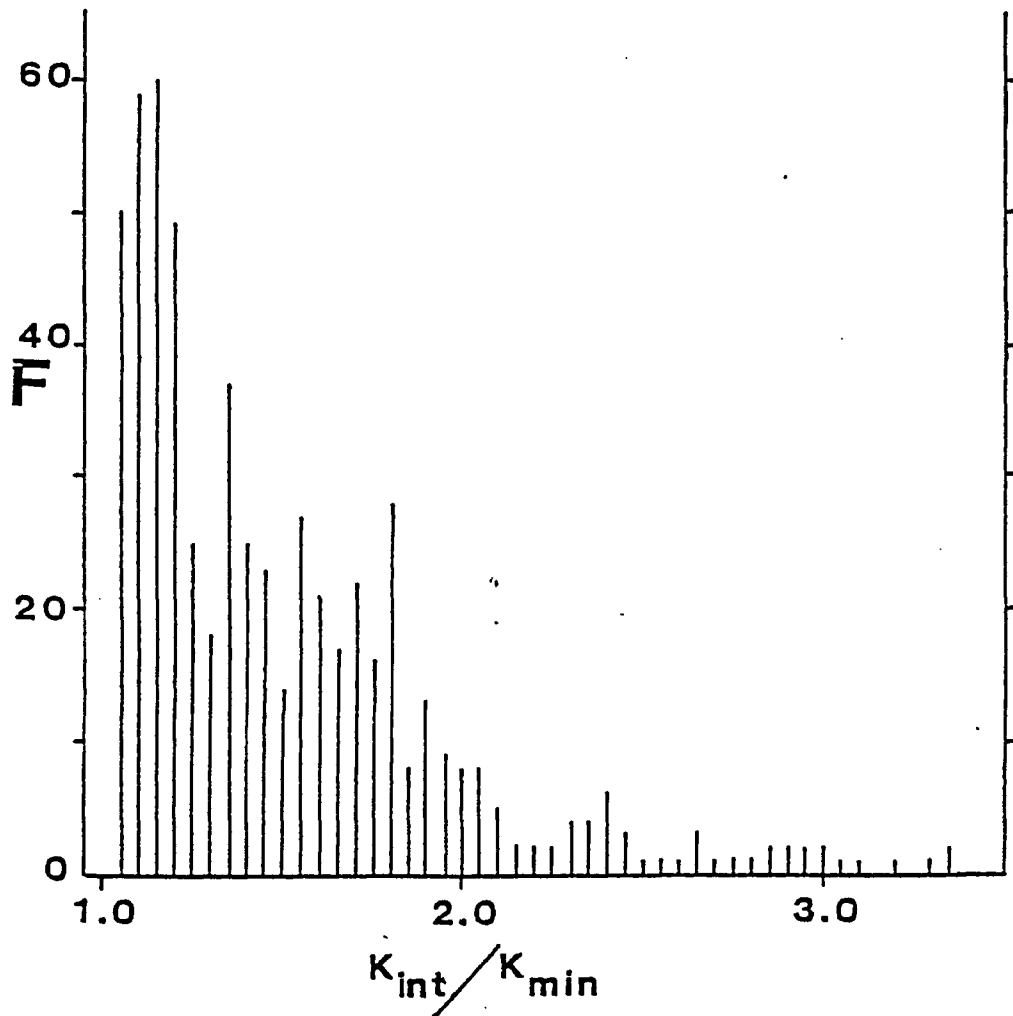


FIG. 11. Histogram of k_{int}/k_{min} for 592 IF specimens.

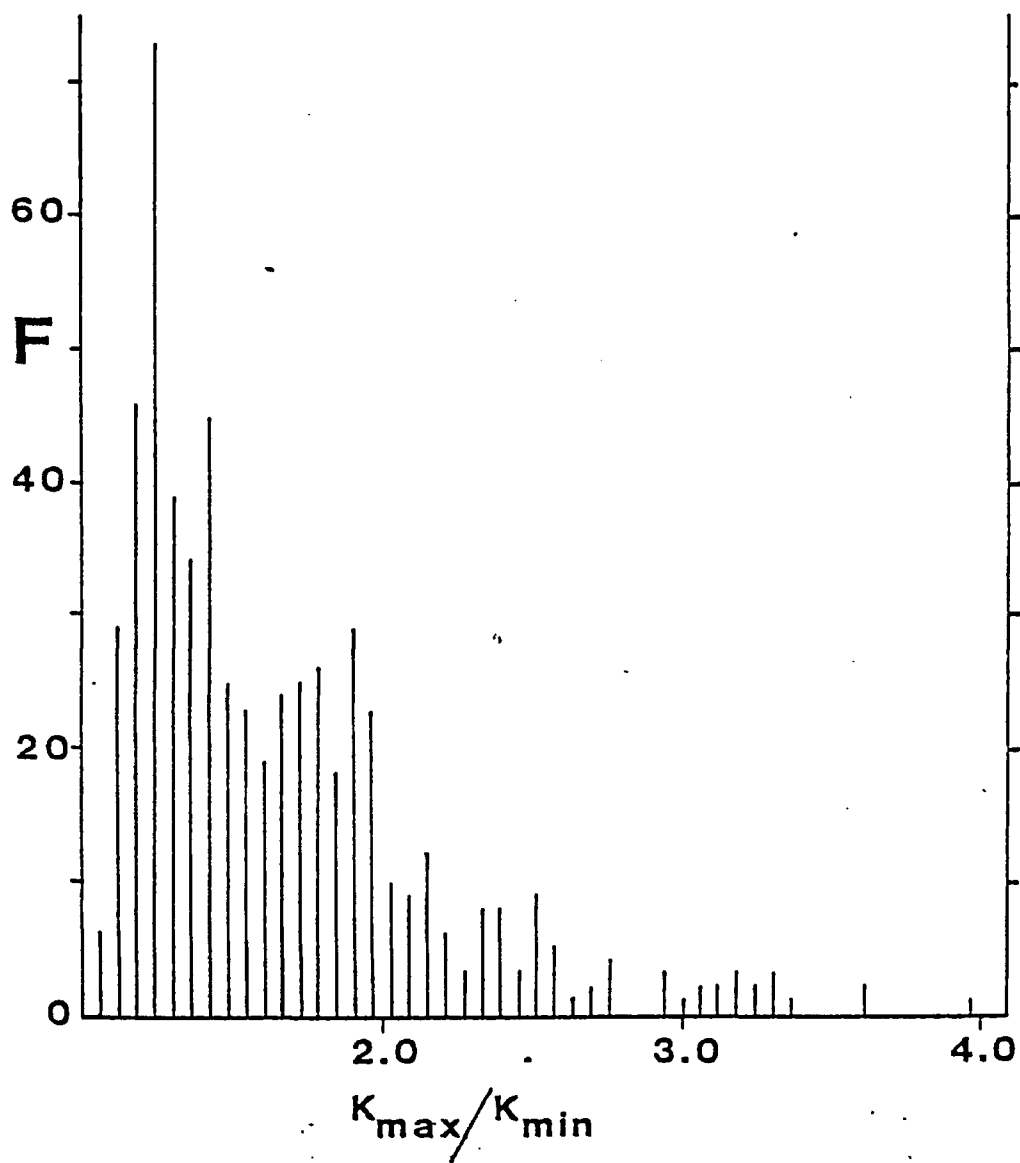


FIG. 12. Histogram of k_{\max}/k_{\min} for 592 IF specimens.

The mean bedding plane susceptibility is:

$$k_{11} = \left(\frac{k_{\max} + k_{\text{int}}}{2} \right) = 1.55 k_{\perp}$$

A total of 15 large IF specimens gave a mean magnitude ratio of $k_{\text{int}}/k_{\min} = 1.57$ and $k_{\max}/k_{\min} = 1.80$. The mean bedding plane susceptibility is:

$$k_{11} = 1.69 k_{\perp}$$

These results show that the small cores may be confined to one band of IF and hence appear more isotropic than the IF as a whole as shown with the higher value obtained in the 2.54cm specimens. A combined average of the two gives the bedding plane susceptibility of $k_{11} = 1.62k_{\perp}$ which is reasonable for a medium grade regional metamorphism. This anisotropy value is slightly higher than the $1.60 k_{\perp}$ value obtained at the Sherman Mine (Symons and Stupavsky, 1979) which suffered low greenschist grade metamorphism, and it is slightly lower than the $1.70 k_{\perp}$ value at the Moose Mountain Mine (Symons, Walley and Stupavsky, 1980) which suffered amphibolite grade regional metamorphism.

4.4 NATURAL REMANENT MAGNETIZATION

4.4.1 Host Rock NRM

4.4.1a NRM Intensity

A total of 524 HR specimens show a lognormal distribution for the NRM intensity (Jo) with a lognormal

mean of 5.970×10^{-6} emu/cm³ (Figure 13).

4.4.1b Koenigsberger Ratio

The Koenigsberger ratio (Q) of the remanent to induced magnetization also has a lognormal distribution with a lognormal mean of 0.013 (Figure 14). The mean induced magnetization of the IF is $\sim 4,300$ times greater than the mean HR NRM. Thus it is reasonable to omit the HR NRM from anomaly calculations although in a number of places its NRM contribution is important.

4.4.1c Storage Test

A storage test run on 16 HR specimens show an average NRM change of 6.75% in intensity (Figure 15a) and of 6.2° (Standard Deviation = 4.4°) in direction over a 5 week period (Figure 15b). These small changes show that the HR's NRM is stable with a small viscous component.

4.4.2 Iron Formation

4.4.2a NRM Intensity

The NRM intensities of 592 IF specimens also show a lognormal distribution (Figure 16) with a lognormal mean of 1.21×10^{-2} emu/cm³.

4.4.2b Koenigsberger Ratios

The Q ratio has a lognormal distribution with a lognormal mean of 0.67 (Figure 17). The mean NRM direction of 92.8° , 52.3° , $A_{95} = 7.4^\circ$ has a deviation angle (θ) of 42.6° from the EMF direction of

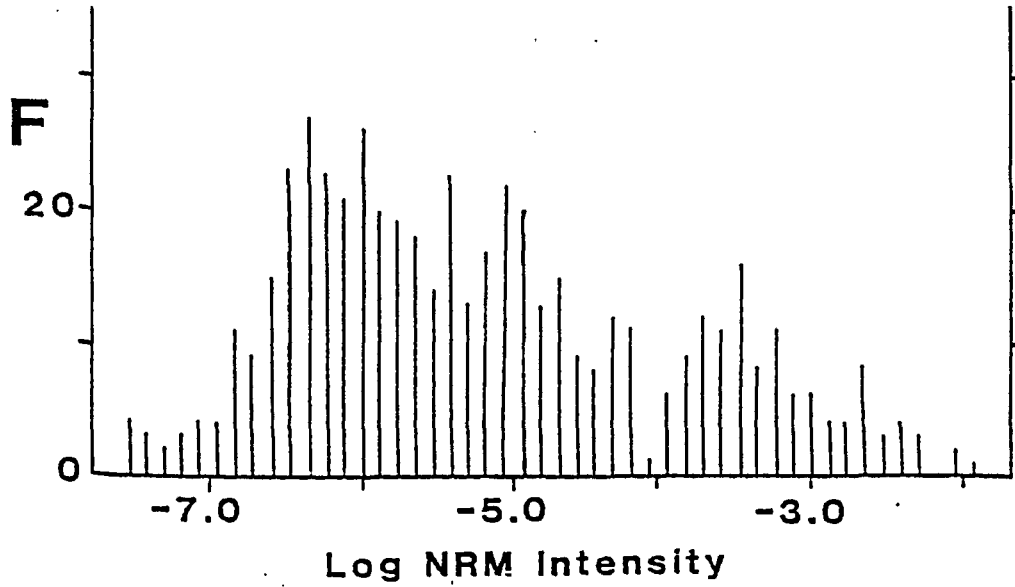


FIG. 13. Lognormal histogram of NRM intensity for 524 HR specimens.

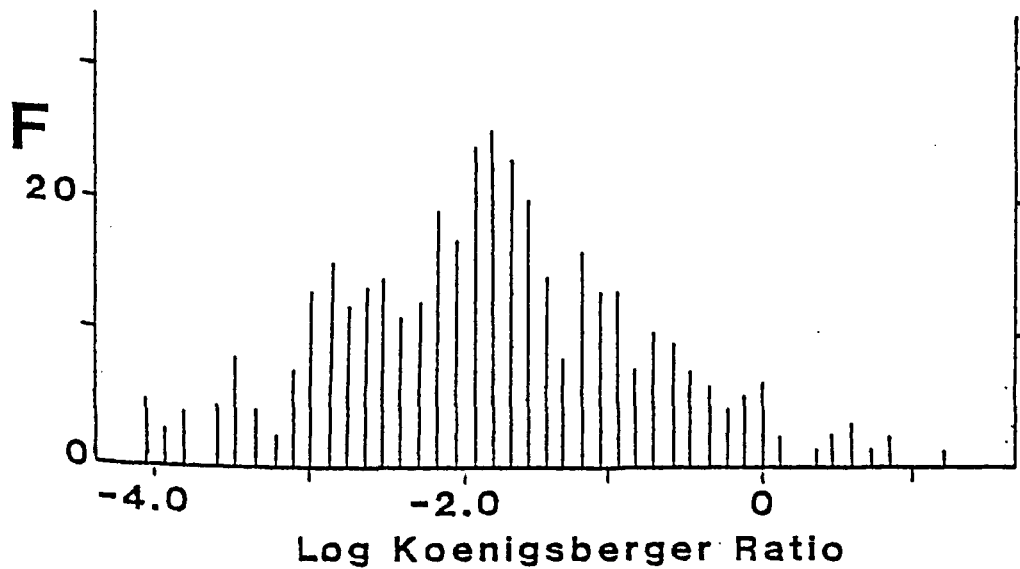


FIG. 14. Lognormal histogram of the Koenigsberger ratio (Q) for 524 HR specimens.

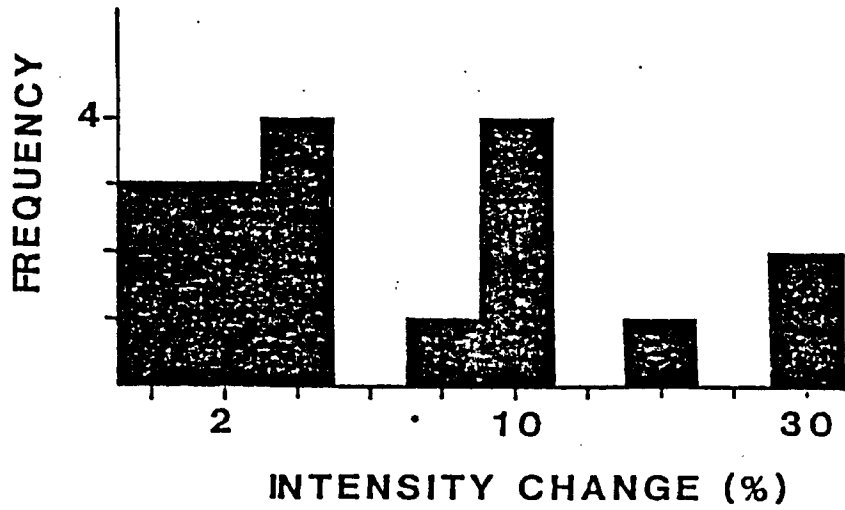


FIG. 15a. Histogram of NRM intensity change of HR specimens over five weeks.

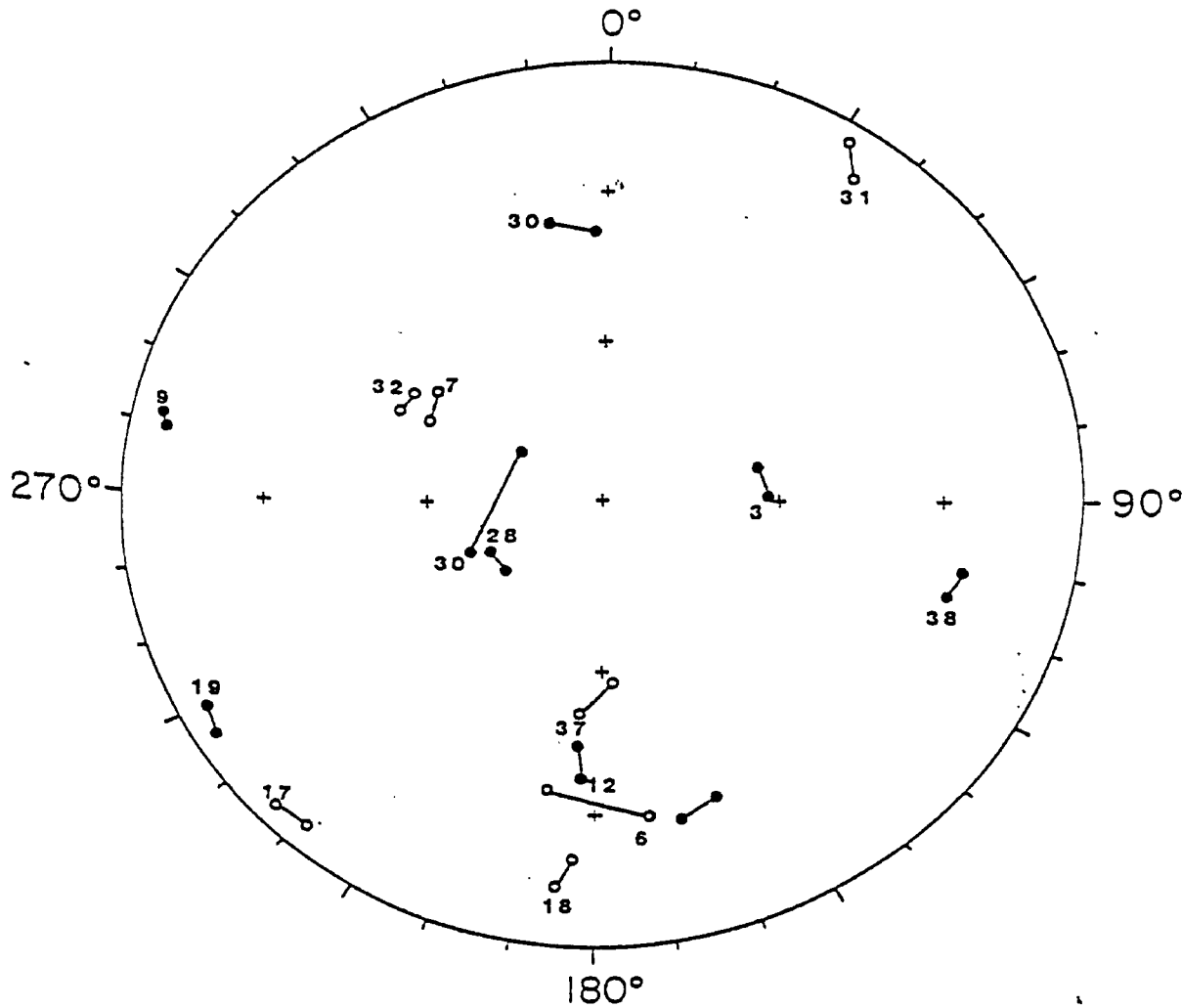


FIG. 15b. Directional changes of NRM vectors of HR specimens over five weeks.

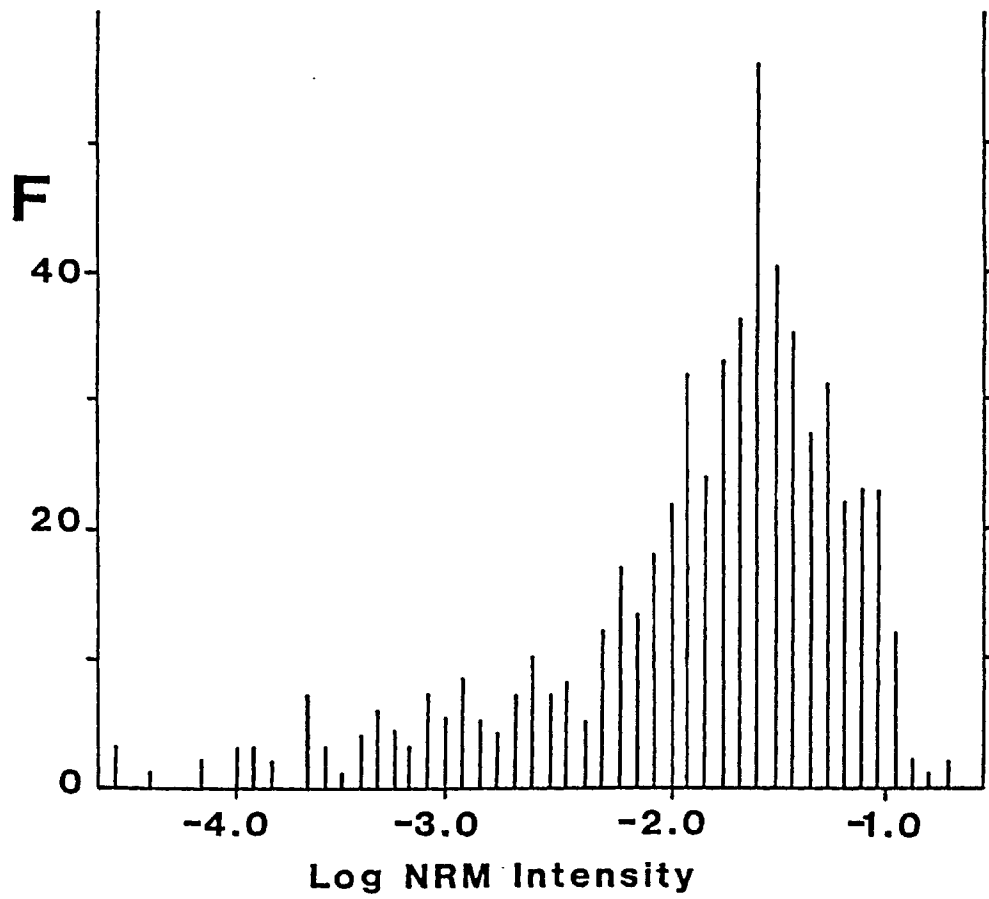


FIG. 16. Lognormal histogram of NRM intensity for 592 IF specimens.

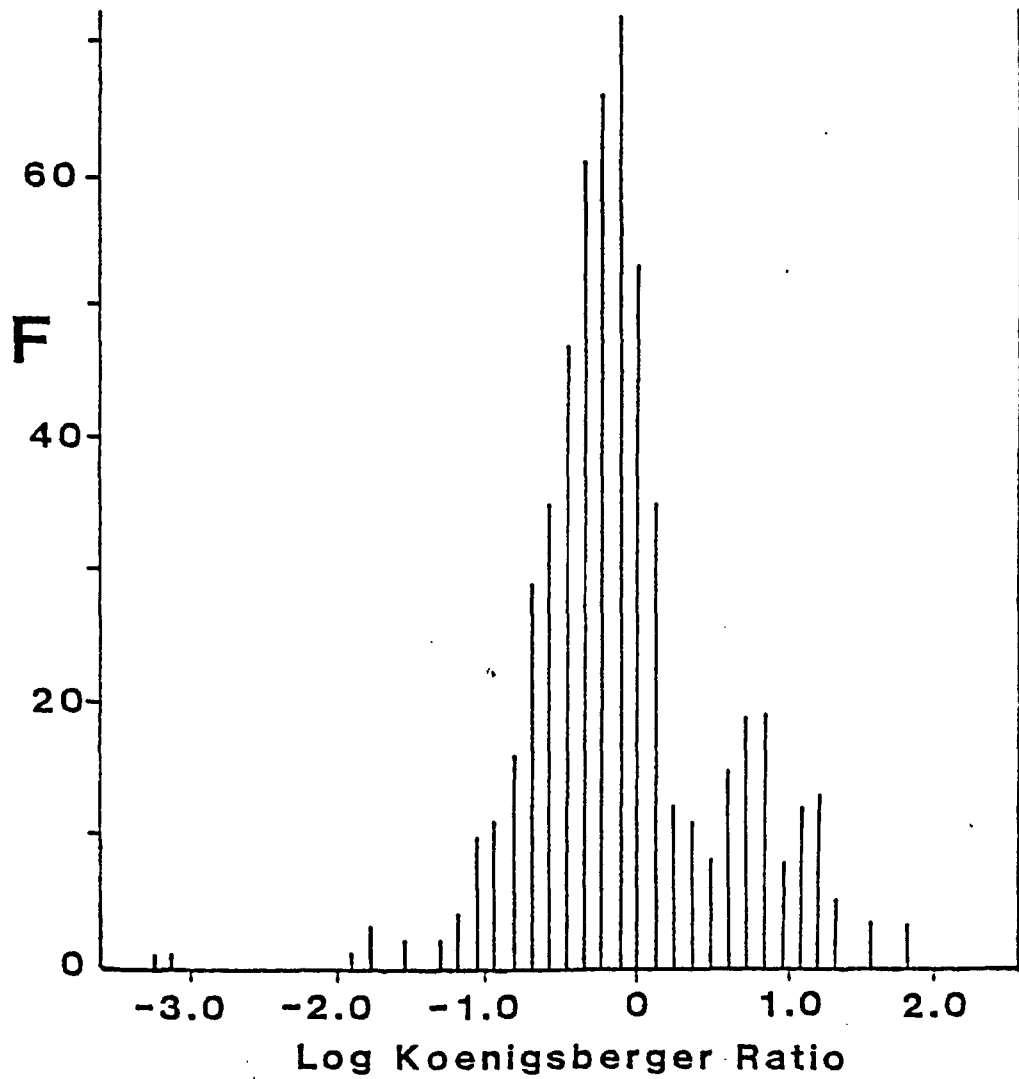


FIG. 17. Lognormal histogram of the Koenigsberger ratio (Q) for 592 IF specimens.

352°, 76°. The ratio of the vector resultant (R) to the number of specimen directions (N) gives an effective Koenigsberger ratio (Qe) of $Q_e = Q \times (R/N)$. The NRM increases the induced magnetic intensity (Ji) by $(Q_e \times \cos \theta)$ Ji to give an augmenting factor of 0.17 Ji. This value is slightly lower than the values 0.24 Ji and 0.22 Ji obtained for the Moose Mountain Mine and Sherman Mine deposits respectively.

4.4.2c NRM - k_1 Relationship.

The relationship between NRM intensity and k_1 has a correlation coefficient of 0.41 for 592 specimens (Figure 18). Results for individual pits are shown in Table 5. The NRM to k_1 relationship obtained in the Adams Mine is:

$$\text{NRM} = 0.215 k_1 + 0.016$$

This NRM intensity is lower than the values obtained at Moose Mountain Mine of $\text{NRM} = 0.439 k_1 + 0.023$ and at Sherman Mine of $\text{NRM} = 0.434 k_1 + 0.005$.

4.4.2d Storage Test

A storage test run on 18 representative IF specimens show an average NRM change of 3.6% in intensity (Figure 19a) and of $4.8^\circ \pm 3.0^\circ$ (s.d.) in direction over a 5 week period (Figure 19b). These small changes show that the IF's NRM is stable with a small viscous component.

4.4.2e Shock Test

The shock test run on 26 IF specimens show a 40%

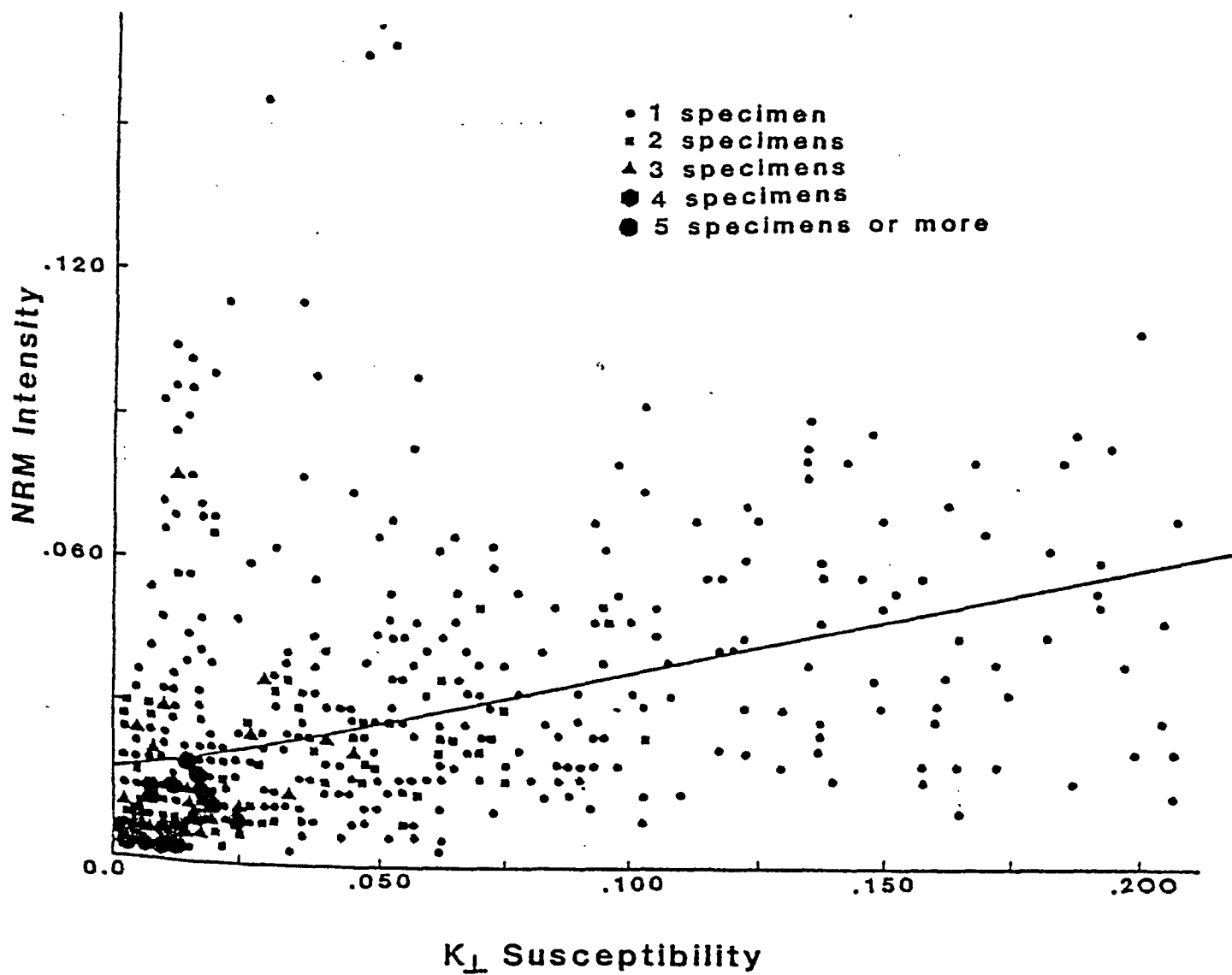


FIG. 18. Regression line of NRM intensity versus k_{\perp} susceptibility for 536 IF specimens.

TABLE 5. Summary of regression fit between k_1 and NRM

Pit	Number of Specimens N	NRM emu	Mag. susc. cgs/ccx10 ⁻²	Regression Fit: $NRM = mk_1 + c$		
				m	c	r
Peria	127	0.0101	3.74	0.3031	0.0295	0.220
North	111	0.0098	4.16	0.3181	0.0078	0.586
Central	157	0.0156	3.57	0.1097	0.0223	0.214
South	180	0.0119	6.09	0.2697	0.0114	0.616

NOTES: Regression fit calculated by BMDP6D program.
r is the correlation coefficient.

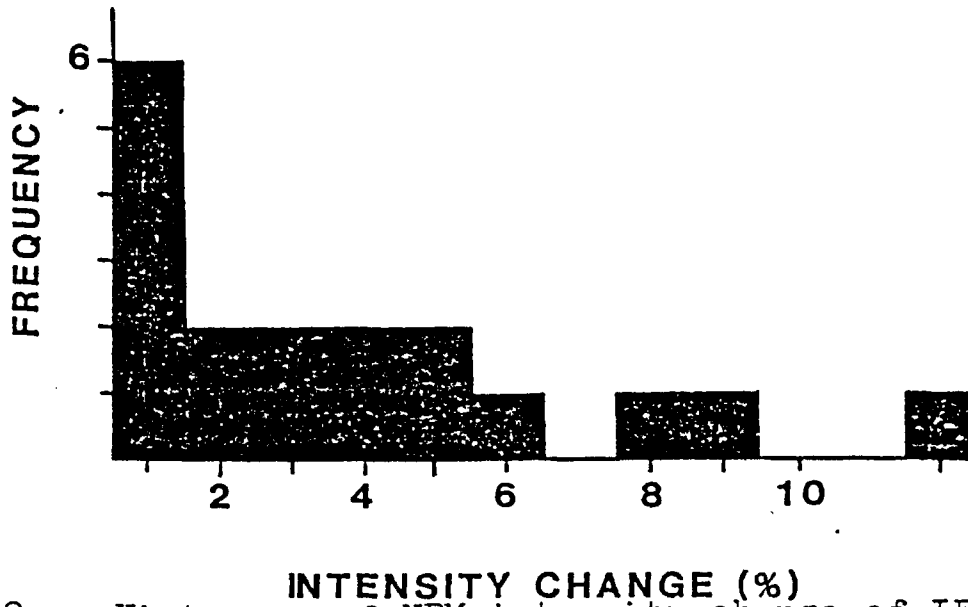


FIG. 19a. Histogram of NRM intensity change of IF specimens over four weeks.

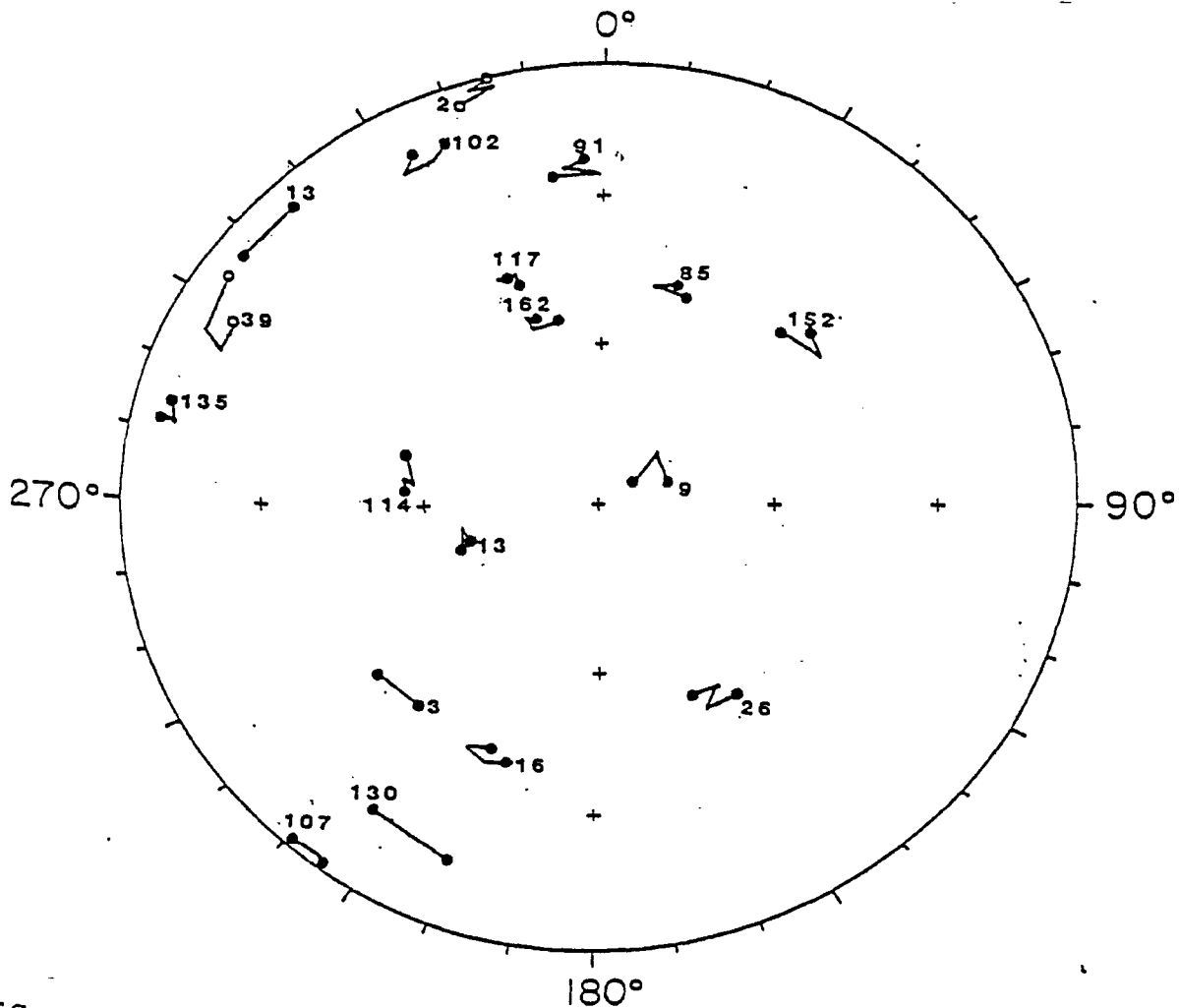


FIG. 19b. Directional changes of NRM vectors of IF specimens over four weeks.

mean reduction in NRM intensity after 40 shocks (Figure 20a) and a 20° (s.d. = 18.6) change in direction after 20 shocks (Figure 20b). These results suggest that the blasting may have affected the NRM in the IF specimens. Shapiro and Ivanov (1966) found that the resulting shock remanence can be erased by low alternating field and partial thermal demagnetization (Cisowski and Fuller, 1978).

4.5 STATISTICAL ANALYSIS

4.5.1 IF Statistical Analysis

The following conventional tiered statistical tests were performed to select reliable IF specimen directions after AF demagnetization (Table 2). The screening test consisted of using Fisher (1953) statistics to determine the degree of specimen deviation from the sample mean. If the specimen direction diverges by more than 20° from the sample mean direction then the specimen direction was rejected. Thus a homogeneous sample mean direction was formed from 2, 3, or 4 specimen directions.

A total of 43 samples gave a homogenous direction, an additional 38 samples gave a homogeneous direction after 1 specimen was rejected. An additional 4 sample groups were formed where two directions were recognized. Thus, of the original 171 samples, a total

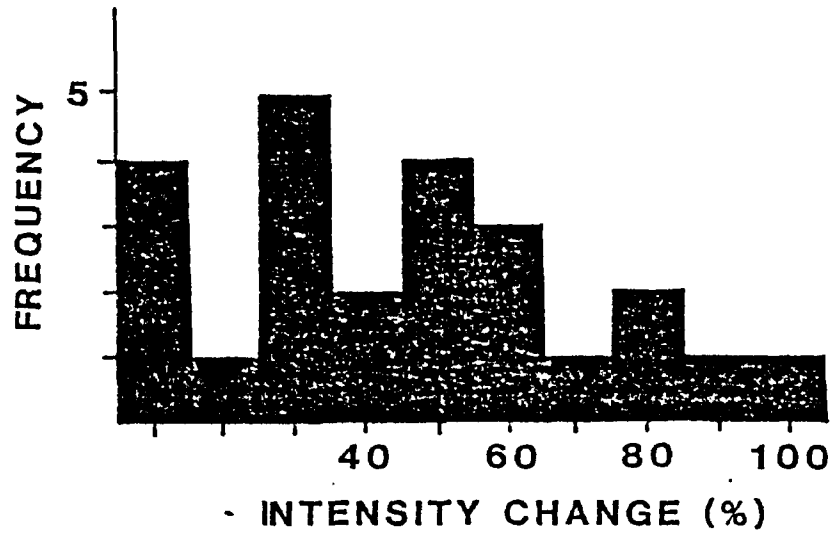


FIG. 20a. Histogram of NRM intensity change of IF specimens after induced shock.

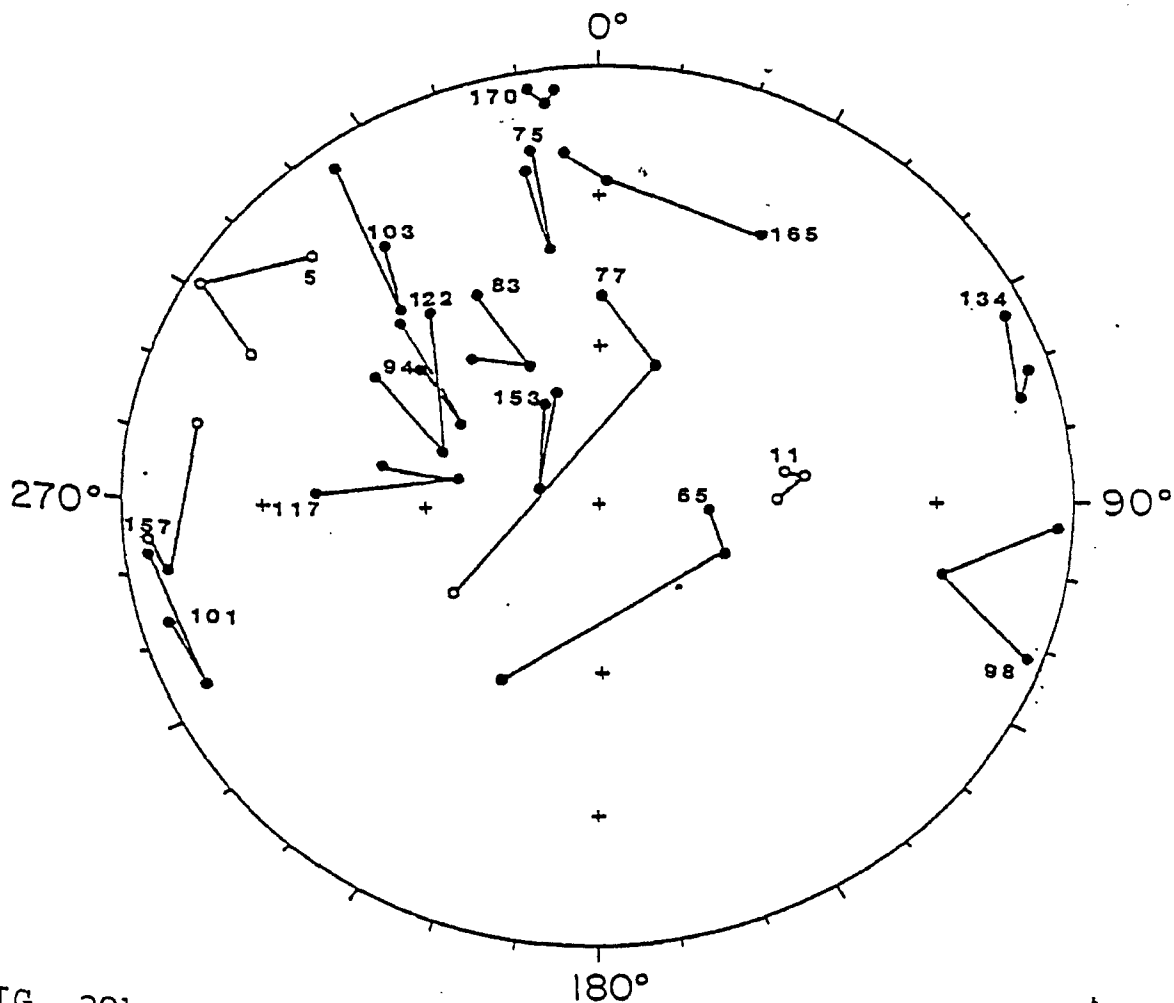


FIG. 20b. Directional changes of NRM vectors of IF specimens after induced shock.

of 85 samples yielded acceptable sample mean directions after screening tests.

4.5.2 HR Statistical Analysis

The homogeneous site mean directions for the HR were determined in a similar manner to the IF (Table 3). There are three steps by which a homogeneous site mean direction was determined; 1) core data were rejected if only one core specimen direction was available, 2) a core mean direction was accepted if the two core specimen directions diverged by $<20^\circ$, and 3) at least two core mean directions had to be acceptable to calculate a site mean direction.

A total of 231 HR cores were obtained at the 45 HR sites. A total of 51 cores were rejected because only one core specimen was obtained. In 117 of the remaining 180 cores, their directions diverged by more than 20° and thus they were rejected. An additional 5 sites were rejected because there was only one acceptable core direction. A total of 15 sites survived the screening tests.

4.6 AF DEMAGNETIZATION OF IF

4.6.1 Pilot Specimens

A total of 70 IF pilot specimens were AF step demagnetized up to 100 mT such that the nature of the IF remanence can be studied and an optimum AF cleaning field can be selected for the remainder of the samples.

On examining the pilot specimens, they showed that they could be grouped into one population. The PSI curves of representative specimens are shown in Figure 21. The curves show the removal of the unstable viscous remanence (VRM) components in the present steeply inclined EMF direction in the 0-15mT steps. The specimens showed a 20-30 deg/T directional change in the 5-15mT steps which decreased to less than 5 deg/T between 20 and 70mT steps. Above 70mT there is a slight increase in the rate of directional change because the random anhysteritic remanence (ARM) components are becoming more pronounced. The intensity decay curves (Figure 22) support this interpretation. The majority of the specimens show a rapid intensity decay up to 30-40mT as significant VRM components are removed and then there is a slight intensity decay throughout the remaining cleaning fields. Specimen 120 shows a slow intensity decay with only 65% of its intensity removed after 100mT. An additional 5 pilot specimens exhibit this behaviour which might be caused by the presence of hematite or of single domain magnetite.

The directional changes of representative pilot specimens during AF cleaning can be seen in Figure 23. The stereoplots show a movement away from a vertical direction following a counterclockwise movement. A

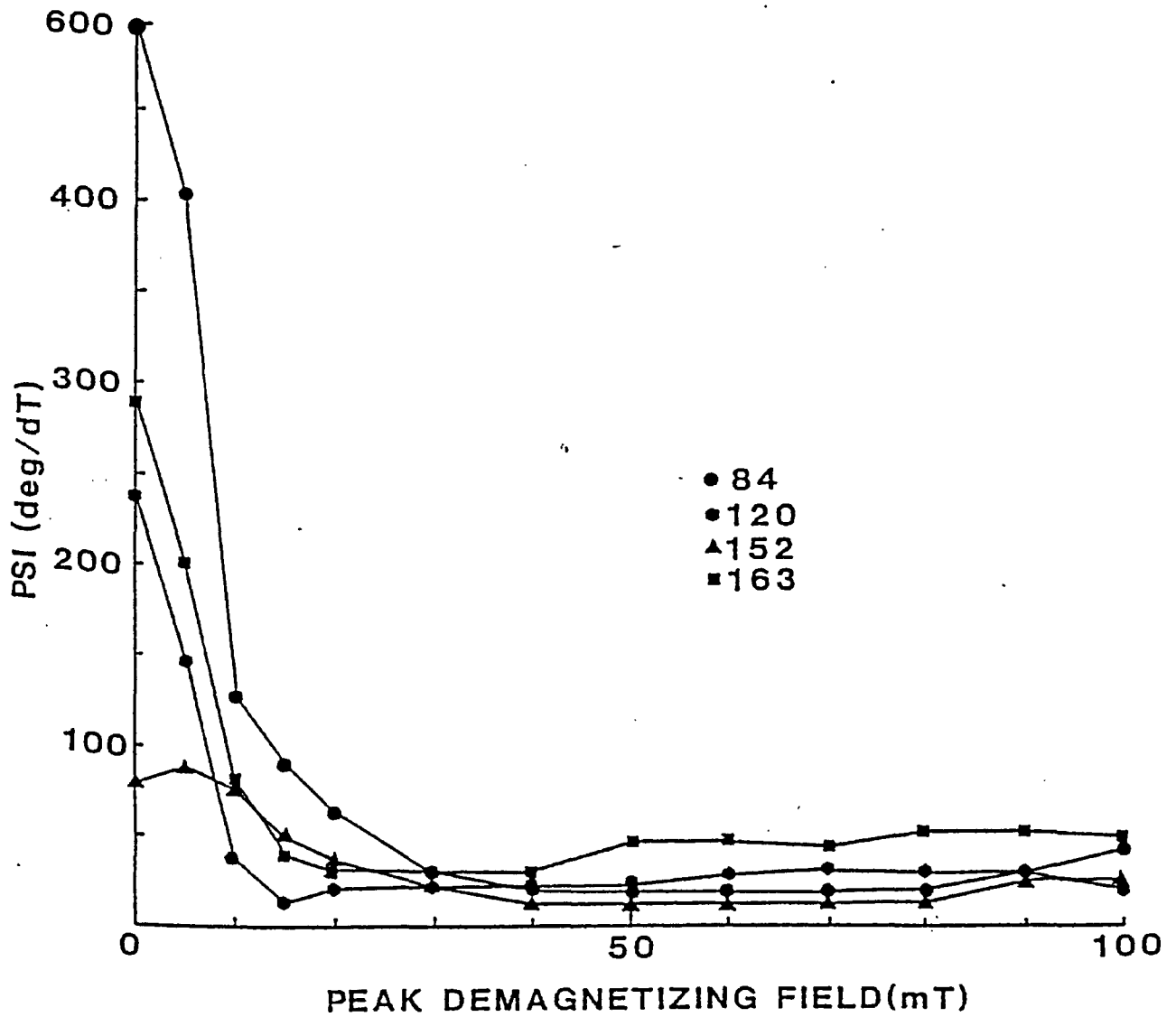


FIG. 21. IF AF demagnetization curve-Paleomagnetic stability index for directional changes

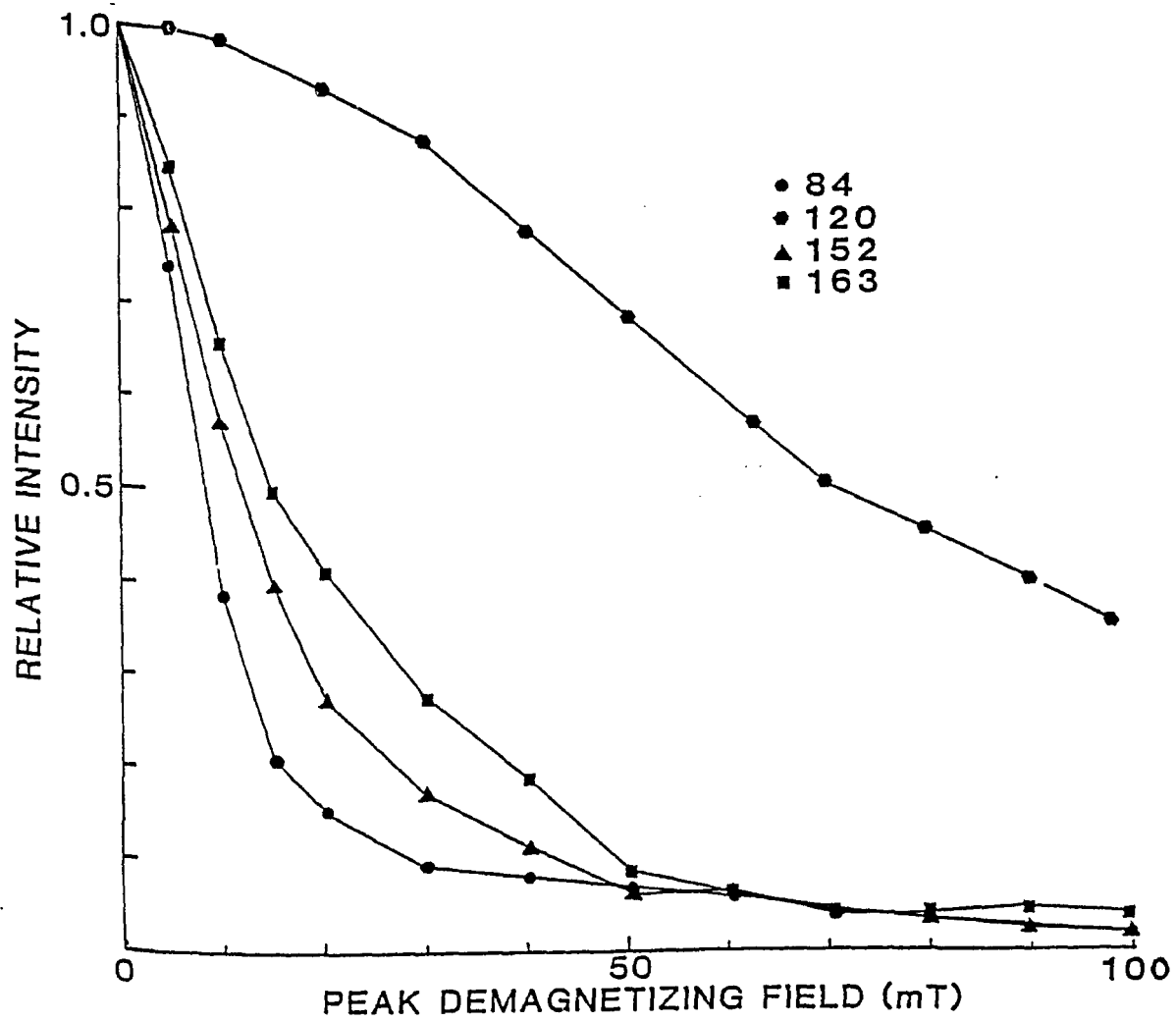


FIG. 22. IF AF demagnetization curve-relative intensity

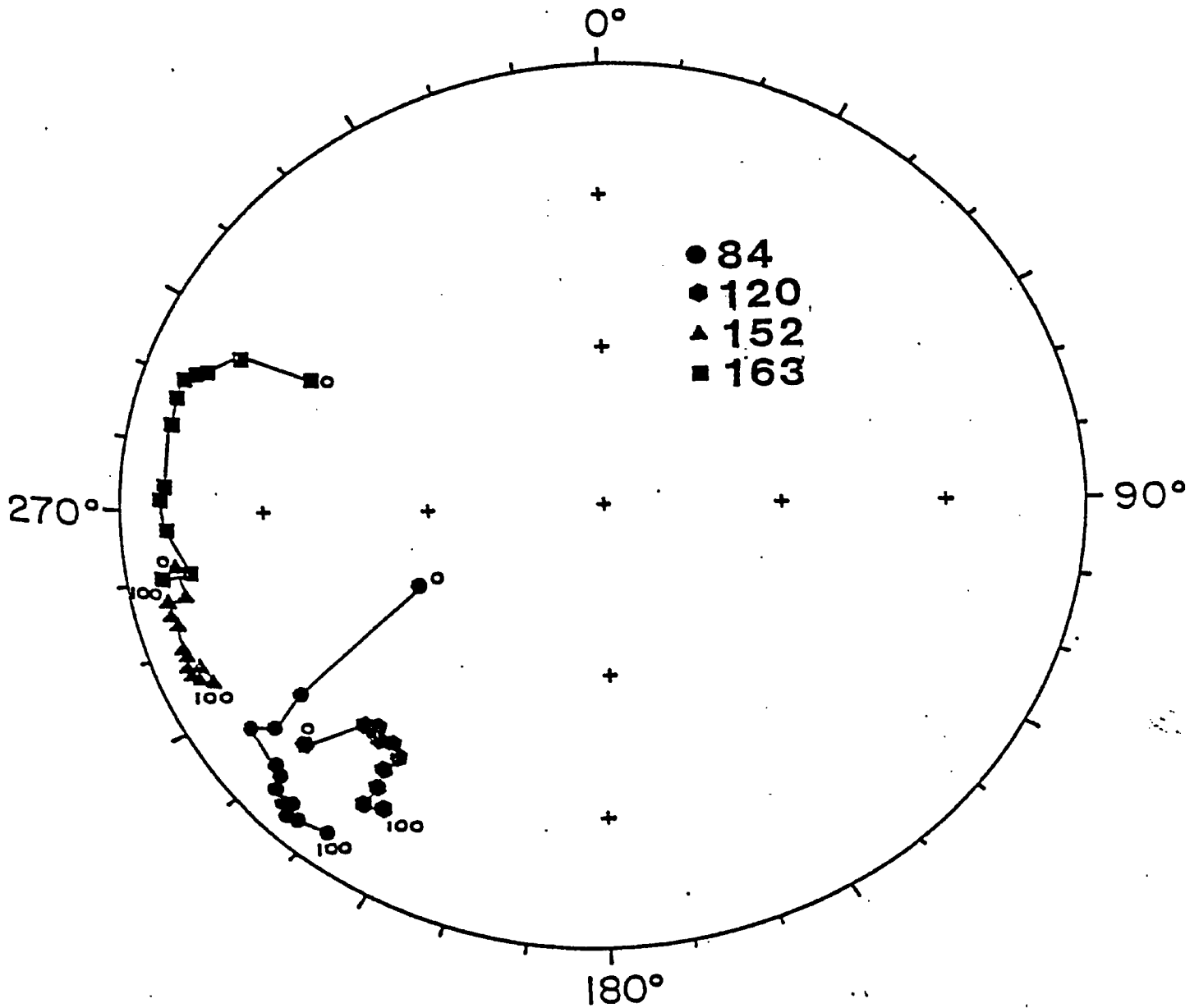


FIG. 23. Directional changes of AF demagnetization on an equal area projection for IF pilot specimens

NOTE: Change in direction on progressive AF demagnetization in fields of 0, 5, 10, 15, 20, 30, 40, 50, 60, 70, 80, 90, 100 mT, for IF pilot specimens. Solid symbols indicate up direction.

further calculation was done in which all the pilot specimens were grouped into each AF demagnetizing field and the mean direction calculated (Table 6). Even though the results are not statistically significant due to the overlapping of the radius of confidence there was a counterclockwise movement (Figure 24) with step increase in the AF field. There was also a shift towards a shallower inclination showing the removal of the VRM components. After 80mT the direction becomes random due to ARM. These results show that the optimum cleaning field selected for most samples was possibly 10mT too low. Because the AF cleaned specimens have a mean direction of 256.2° , 7.4° and these pilot specimens show continued movement towards 230° , 17° at higher cleaning fields.

The optimum cleaning fields (Figure 25) were selected on the basis of PSI minima. At the optimum cleaning field the relative intensity (J_n/J_o) has been reduced to less than 10% of its original intensity (J_o) in most specimens (Figure 26).

Least square model analysis was attempted using the IF pilot specimens, but this method was unable to isolate the characteristic remanence directions because of the erratic nature of the data.

4.6.2 Smoothing Method

The smoothing method is a single step screening

TABLE 6. Pilot specimens grouped into each AF demagnetizing field

AF Field mT	Number of Specimens N	Decl. °	Incl. +down	Intensity emu	A95 °
0	70	253.4	47.8	0.0349	24.2
5	70	250.3	48.6	0.0214	27.0
10	70	251.0	42.9	0.0146	28.4
15	70	249.2	44.0	0.0106	27.6
20	70	248.8	43.4	0.0086	27.3
30	70	246.5	45.2	0.0055	26.1
40	70	243.0	45.0	0.0038	23.0
50	70	238.5	32.3	0.0028	21.9
60	70	245.6	25.9	0.0021	18.9
70	70	231.8	24.0	0.0016	19.1
80	70	231.4	16.9	0.0013	23.2
90	70	213.3	26.6	0.0010	20.2
100	70	239.8	-1.3	0.0012	22.2

NOTE: A95 is the radius of 95% confidence (Fisher 1953) in degrees.

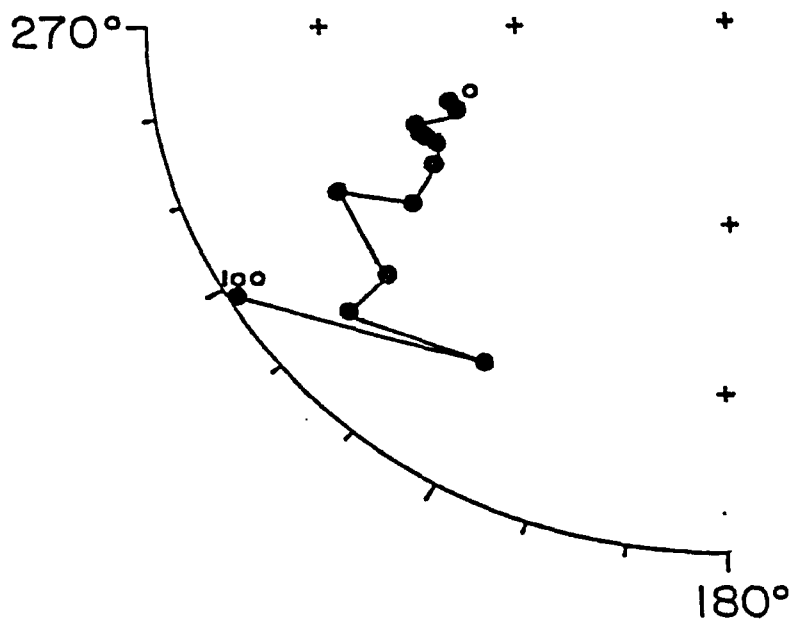


FIG. 24. Mean directional changes during AF demagnetization steps for IF pilot specimens

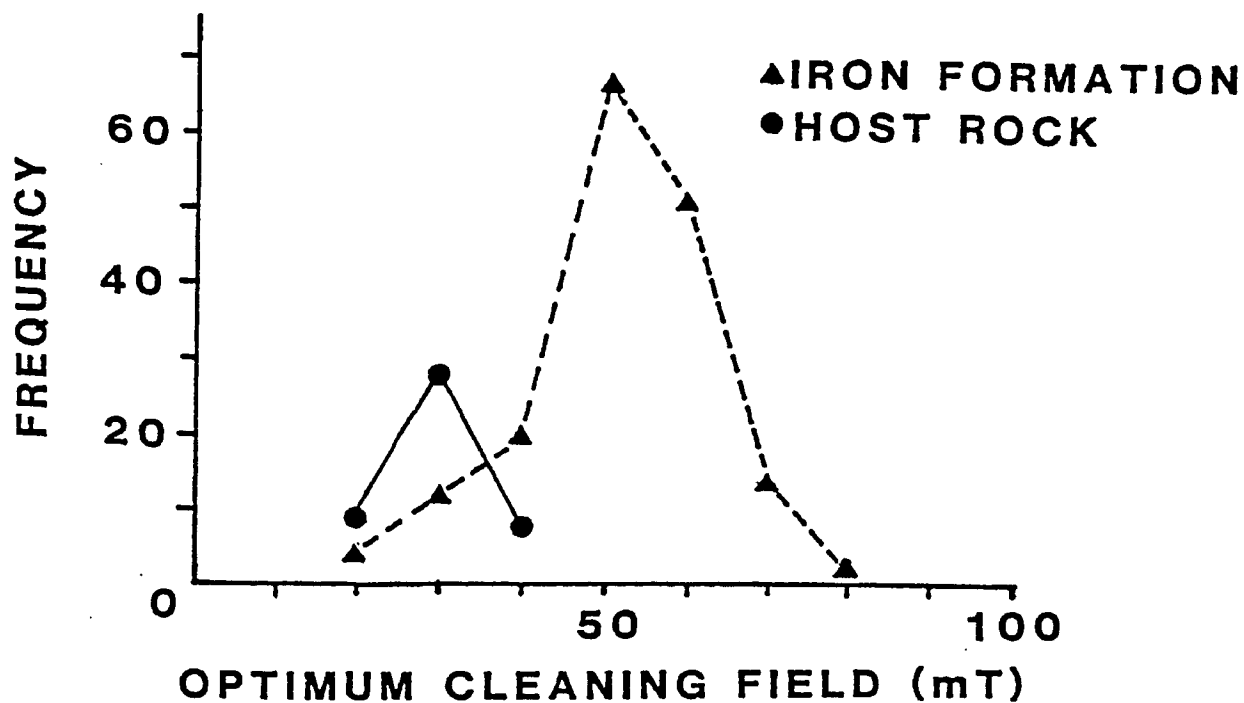


FIG. 25. Plot of optimum AF cleaning field for IF and HR specimens

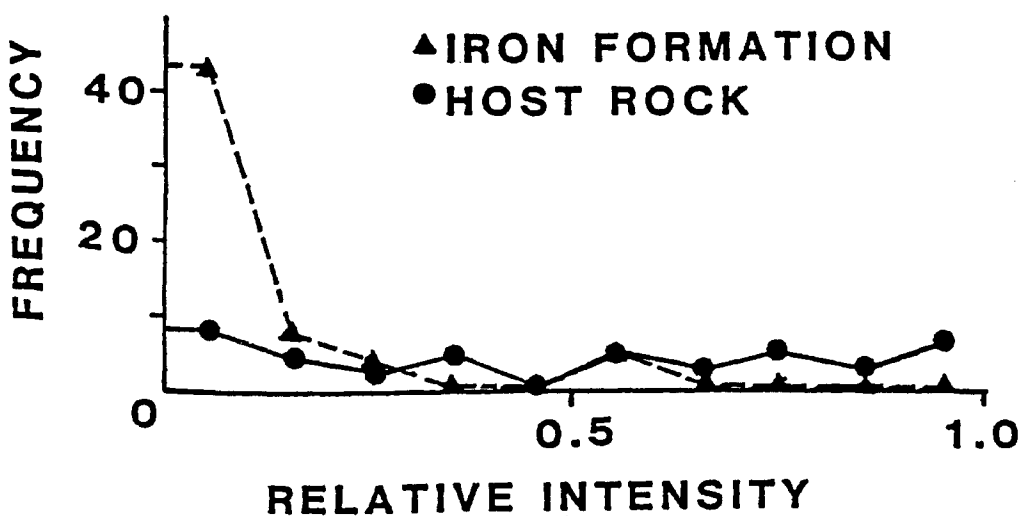


FIG. 26. Relative intensity of NRM after cleaning at optimum AF field

method at the population level. The procedure is to plot the specimen directions on a stereonet with the positive down directions on one plot and the negative up directions on another plot. The directional data can be smoothed and contoured by using a method proposed by W.B. Kamb (1959). The concentration of directions identify the various remanence components present in the rock. The difference between this method and conventional point density percentage contours is that the smoothing area (A) depends on the number of directions (N). The contour intervals are in terms of the standard deviation (σ) and expected density (E) for random sampling of N randomly directed vectors. Thus any anomaly outlined having more than $E + 2\sigma$ directions than the number expected for a random distribution of vectors will be highly significant especially if it is in one localized area of the stereonet.

The mean direction can be obtained from the anomaly maxima or by using Fisher statistics selecting directions within a given anomaly contour. The smoothing method was performed on AF cleaned IF specimens that were corrected for bedding tilt and then on AF cleaned homogeneous IF sample means. The AF IF specimens after smoothing and contouring (Figure 27) formed an anomaly. The mean declination and inclination were calculated using the specimen directions which fall

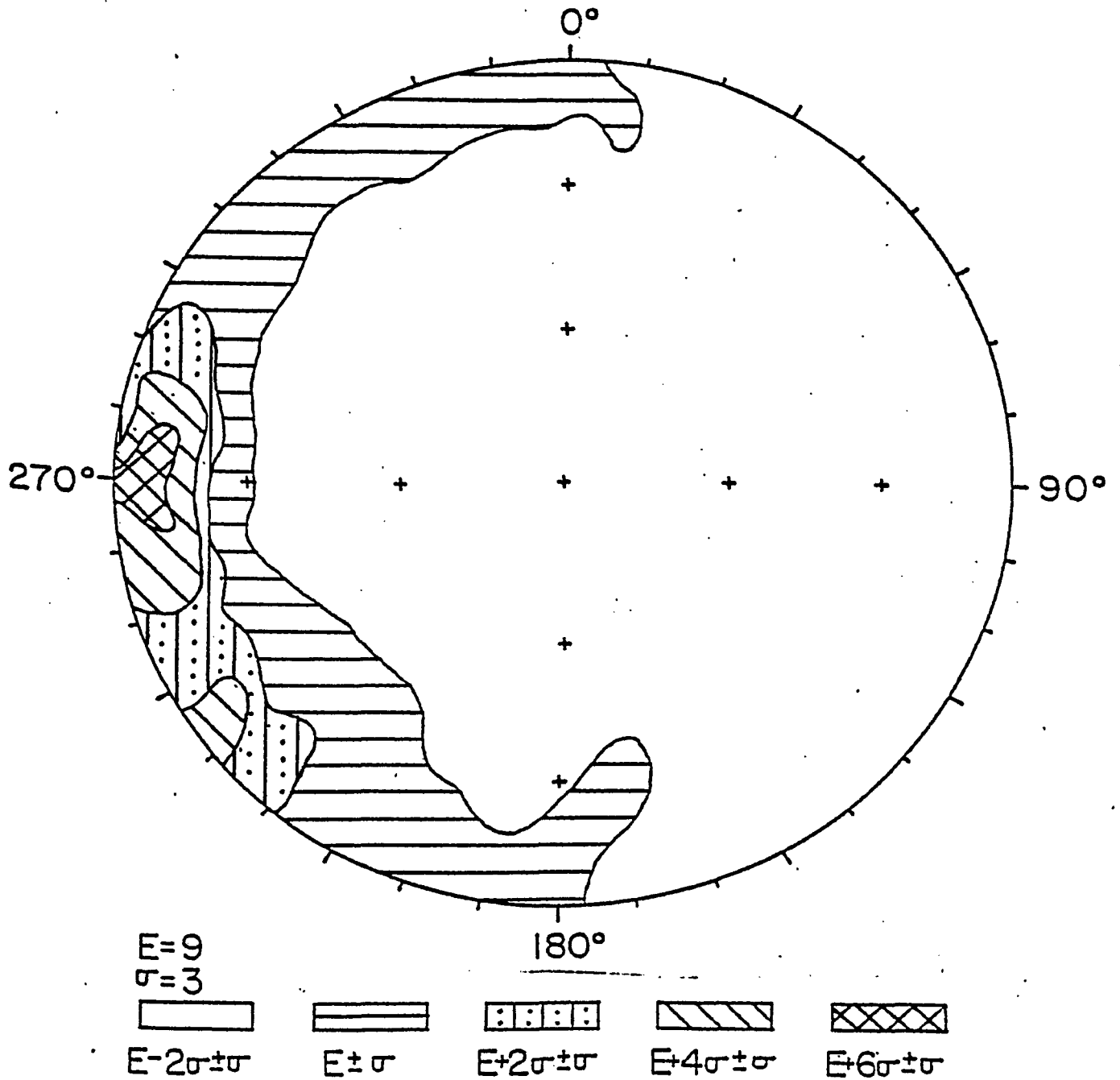


FIG. 27. Smoothing and contouring of AF cleaned IF specimens corrected for bedding tilt (down direction ; Area = 4.5cm^2)

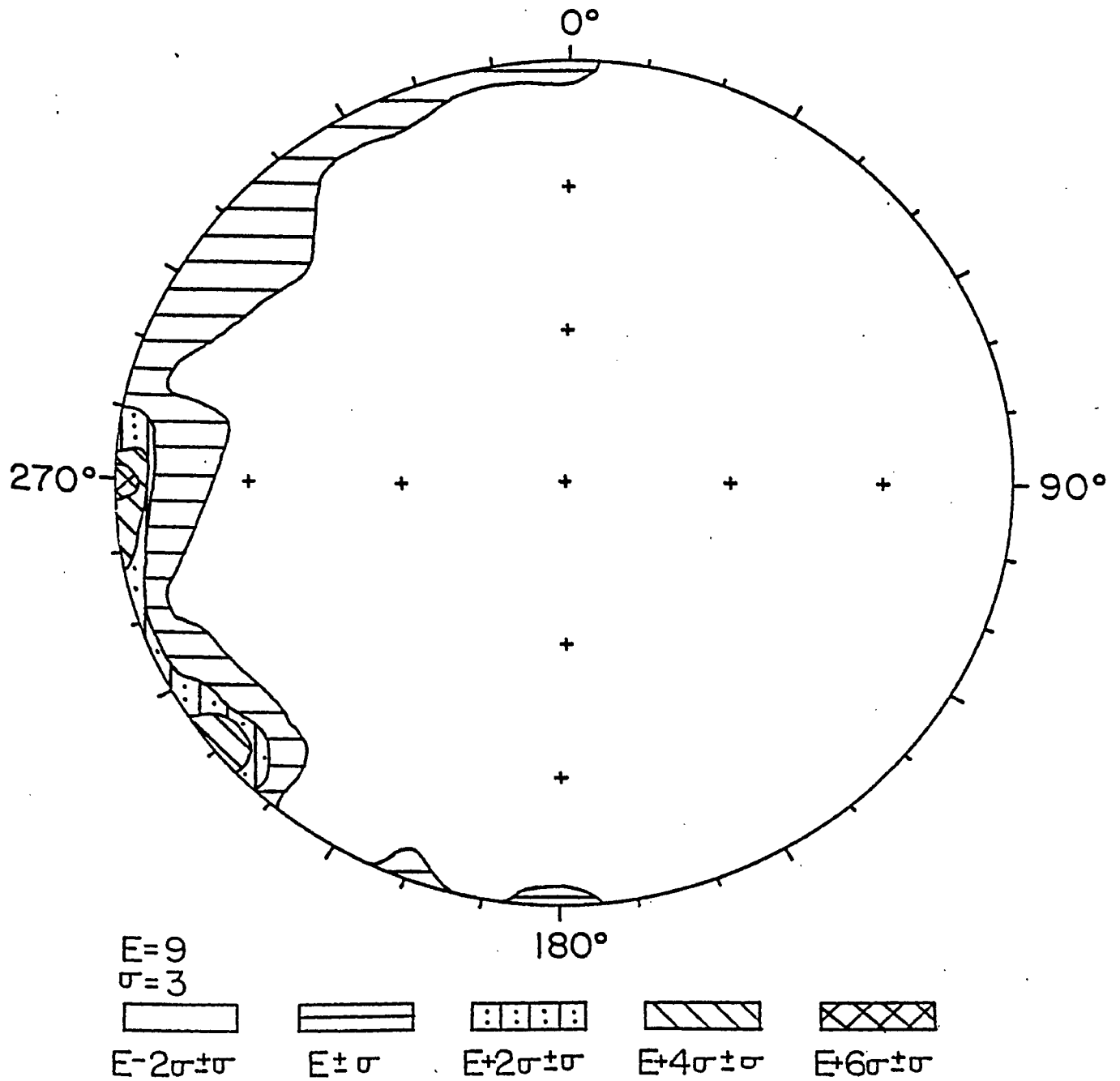


FIG. 27a. Smoothing and contouring of AF cleaned IF specimens corrected for bedding tilt (up direction; Area = 4.5cm²)

within the $E + 2\sigma$ contour. The anomaly designated component A yielded a mean direction of 256.2° , 7.4° , $A95 = 3.3^\circ$.

The AF cleaned homogeneous IF sample means (Figure 28) show a mean direction of 262.2° , 7.2° , $A95 = 6.5^\circ$ which is similar.

4.7 FOLD TEST AF CLEANING

A fold test was performed by grouping the specimens from a population within an anomaly. The specimen directions corrected for bedding tilt were compared with the uncorrected directions using the angular variance test.

The ratio of the variances in dispersion ($V = \delta_A^2 / \delta_S^2$) was calculated and compared to the corresponding theoretical statistic: $F_2(N_A - 1), 2(N_S - 1), 0.05$. If $V > F$, then the two populations have significantly different distributions and hence probably reflect different conditions of remanence acquisition or removal. A

second test of Watson (1956), computes the statistic:

$$F_c = N - 2 \left(\frac{R_1 + R_2 - R}{N - R_1 - R_2} \right)$$

where R is the length of the vector sum of the resultants of the R_1 and R_2 populations, and $N = (N_1 + N_2)$ is the total number of samples in the two populations. This is compared to the theoretical statistic: $F_{2, 2(N-2), 0.05}$. If $F_c > F$, then the two populations define signi-

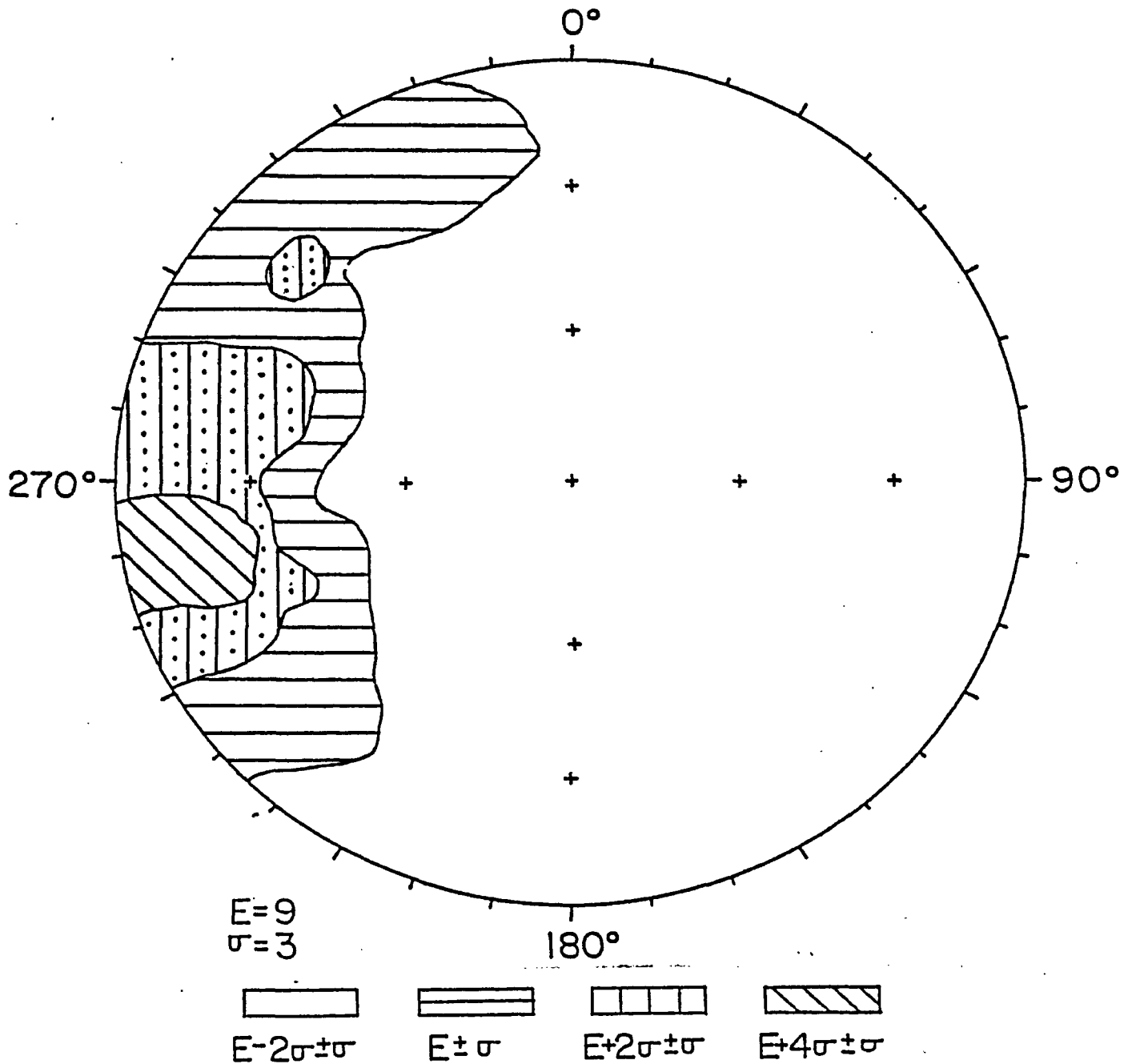


FIG. 28a. Smoothing and contouring of homogeneous AF cleaned IF samples corrected for bedding tilt (up direction; Area = 38.4cm²)

ificantly different directions, possibly as a result of folding.

All the IF specimens falling within the $E + 2\sigma$ smoothing contour of the corrected and uncorrected directions (Figure 27 and 29) were compared. The variance test indicates that there is a significant difference in the dispersion of directions because the variance ratio of 1.20 is greater than the theoretical statistic of 1.1 at the 95% confidence level. In addition, the precision parameter, k (Fisher, 1953) is greater for corrected direction population (Table 7) showing that their population is less dispersed. Therefore the remanence isolated in the IF predates the folding.

Another test was done using the homogeneous block means of the samples. The two anomalies (Figure 28 and 30) were compared using only sample directions within the $E + 2\sigma$ smoothing contour. The variance test indicates that there is a significant difference in the dispersion of directions because the variance ratio of 2.00 is greater than the theoretical statistics of 1.90 at the 95% confidence level. The precision parameter of 19.5 for the corrected direction was greater than that of 11.5 for the uncorrected (Table 7). This agrees with the first test and shows that the isolated remanence in the IF predates the folding.

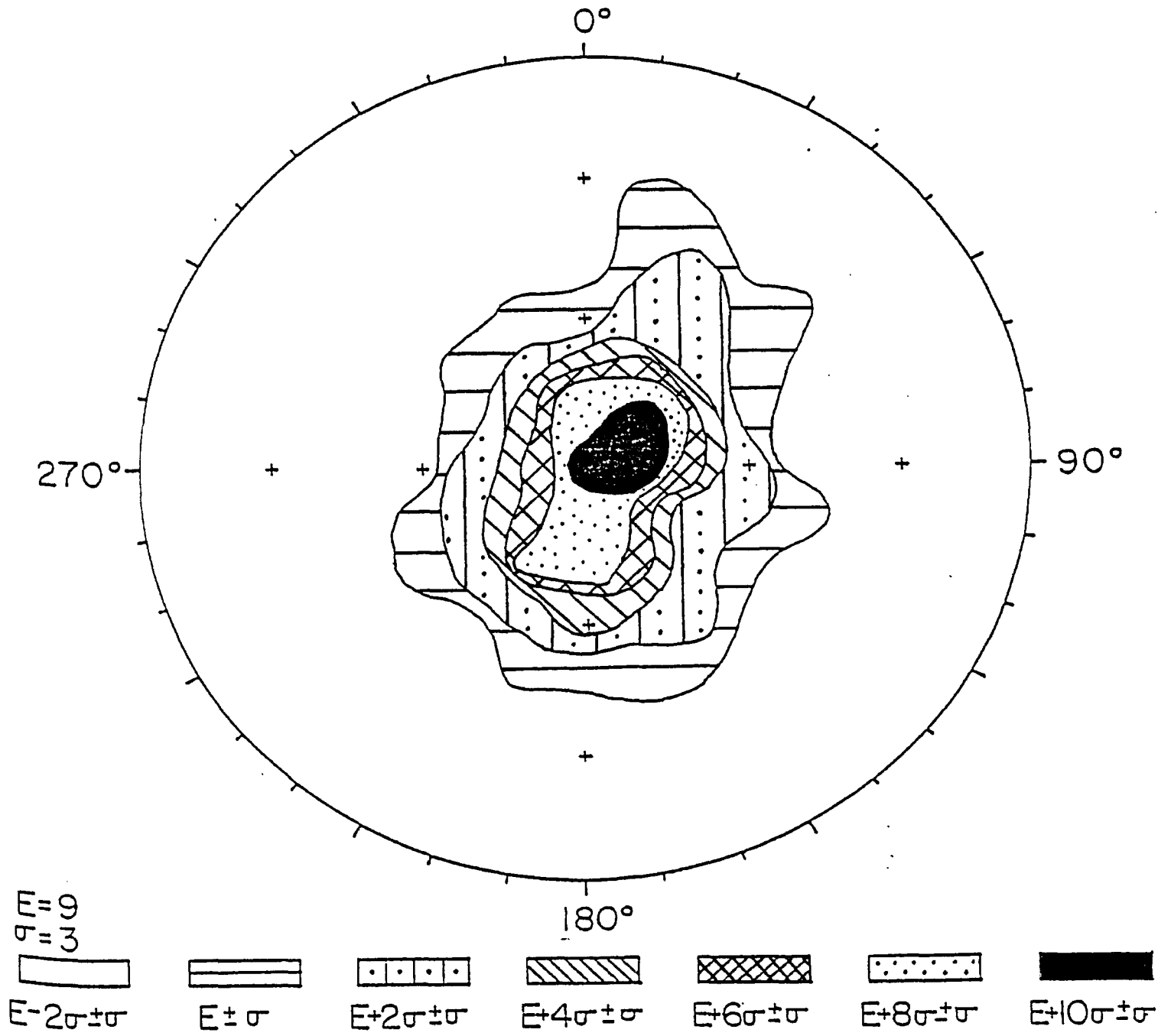


FIG. 29. Smoothing and contouring of AF cleaned IF specimens not corrected for bedding tilt (down direction ; Area = 4.6cm²)

TABLE 7. Fold Test

Groups Compared	Number of specimens	Length R	Mean Remanence Direction		k	A95 ○	V	F _{0.05}
			Decl. ○	Incl. +down				
<u>Anomaly Specimens</u>								
Corrected	151	139.75	256.21	7.41	13.33	3.27		
Uncorrected	242	218.20	98.25	85.43	11.97	2.75	1.20	1.10
<u>Homogeneous Block Means</u>								
Corrected	26	25.66	262.25	7.24	19.49	6.46		
Uncorrected	46	42.08	70.24	81.81	11.48	6.49	2.00	1.90

NOTES: R is the length of vector resultant.

k is Fisher's (1953) precision parameter.

A95 is the radius of 95% confidence (Fisher 1953).

V is the variance ratio $\sigma_{corr}^2 / \sigma_{uncorr}^2$ of the two populations.

F_{0.05} is the theoretical statistic $F_{2(N_{corr}-1), 2(N_{uncorr}-1), 0.05}$ thereby setting the test at the 95% confidence level.

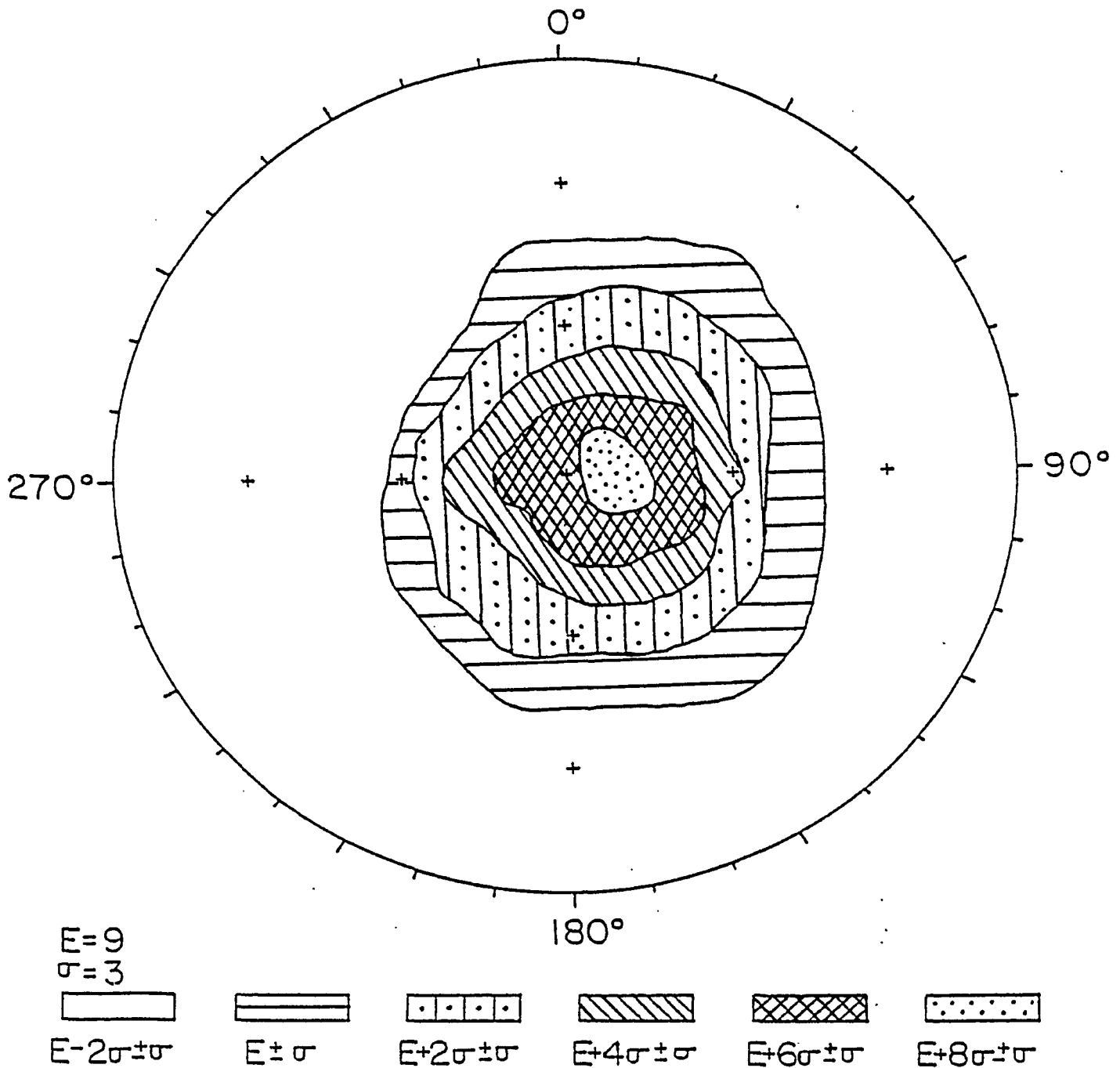


FIG. 30. Smoothing and contouring of homogeneous AF cleaned IF samples not corrected for bedding tilt (down direction ; Area = 38.4cm^2)

4.8 THERMAL CLEANING OF IRON FORMATION

4.8.1 Pilot Specimens

A total of 22 IF pilot specimens were thermally step demagnetized up to 650°C. The intensity decay curves of representative specimens (Figure 31) show an initial rapid drop in intensity up to 400°C as unstable VRM components are removed. The curves then show a blocking temperature "knee" of some grains at 475°C above which the magnetization carried by such grains is destroyed. The thermal coercivity spectrum of the stable direction is probably carried by magnetite that is blocked predominantly above 475°C. When pure, magnetite has a Curie temperature (T_c) of 585°C.

The PSI curves (Figure 32) show high PSI values which remain relatively constant up to 400°C. Above 400°C the curves record an increasing rate of directional change as the partial thermoremanent ($pTRM$) components dominate the specimen response. In Figure 33 large directional changes can be seen above 500°C as the characteristic directions are isolated.

Because of the poor isolation of a stable unit mean direction above 500°C, the remaining specimens were not thermally cleaned.

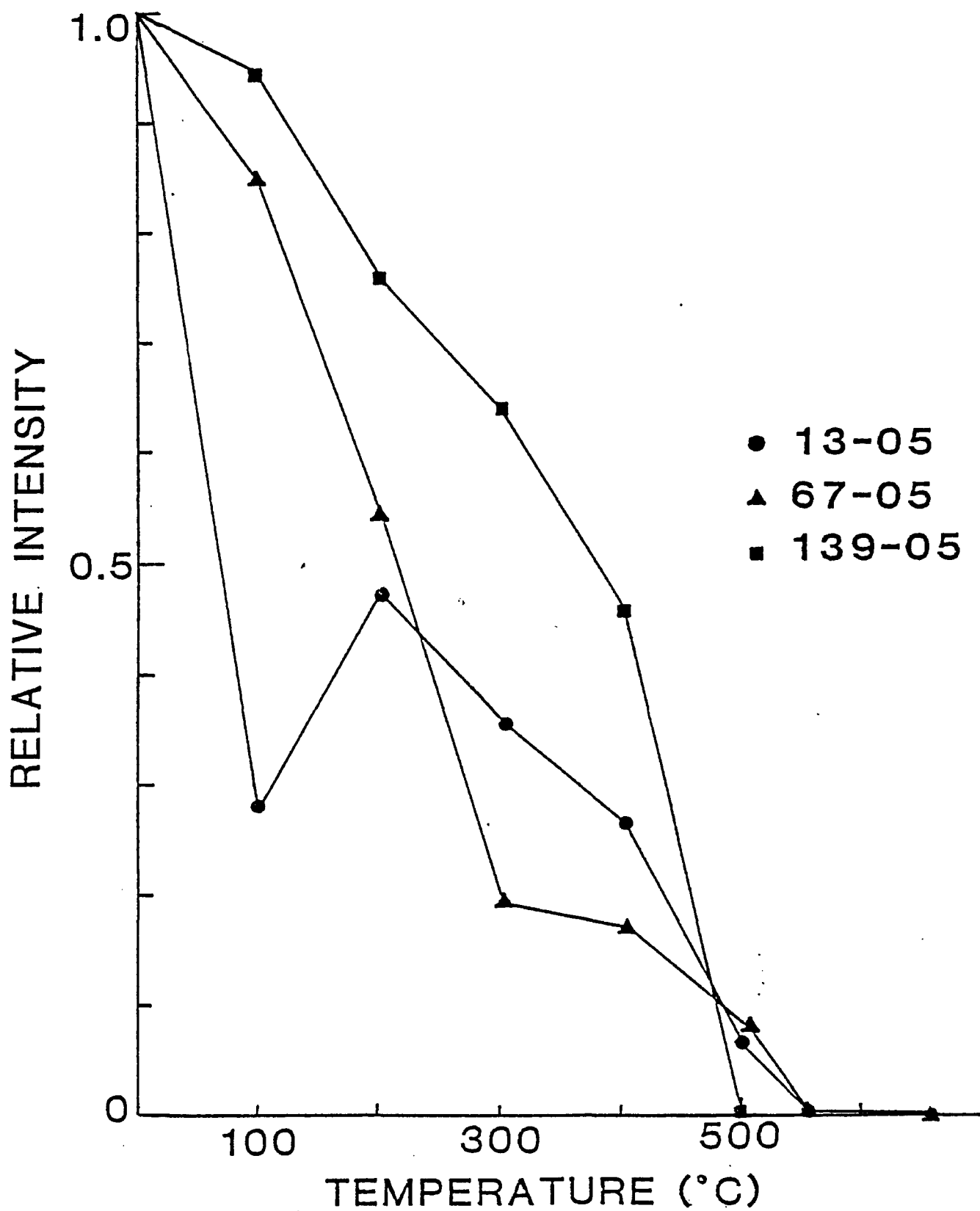


FIG. 31. IF thermal cleaning curve - relative intensity

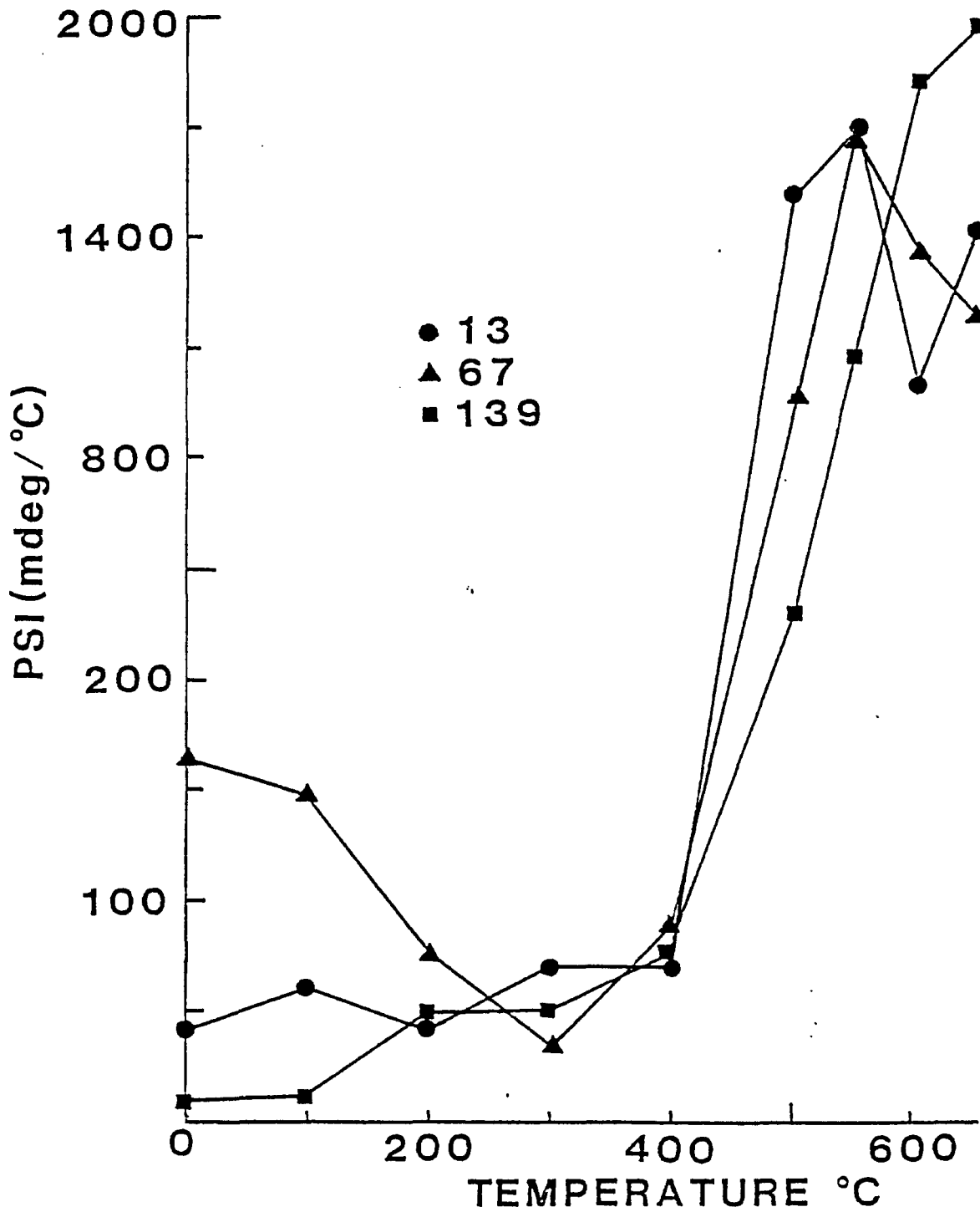


FIG. 32. IF thermal cleaning curve - paleomagnetic stability index.

4.9 CHEMICAL CLEANING OF IRON FORMATION

4.9.1 Pilot Specimens

A total of 13 out of 19 IF pilot specimens didn't disintegrate after 1641 hours in 12N HCl. Within the first 200 hours, 4 specimens disintegrated. The directional changes (Figure 34) of representative specimens show the removal of unstable steeply-inclined components, presumably carried either by relatively soluble, coarse-grained magnetite or by fine grained magnetite within magnetite bands. These are attacked faster than magnetite distributed within the cherty bands. The surviving specimens also show a counter-clockwise movement in remanence direction with duration of submergence in the 12N HCl. This counter-clockwise movement reveals the presence of a westerly-directed component of magnetization. The PSI curves (Figure 35) show large initial rates of remanence directional change within the first 100 hours as VRM is removed. Between 100-1200 hours the rate of directional change remains relatively low with the lowest PSI values for the last measurement at 1641 hours. The intensity decay curves (Figure 36) show that chemical cleaning removes up to 70% of the magnetization in most specimens. However two specimens show a gradual movement towards 240° with 99% of their magnetization removed before their directions became erratic.

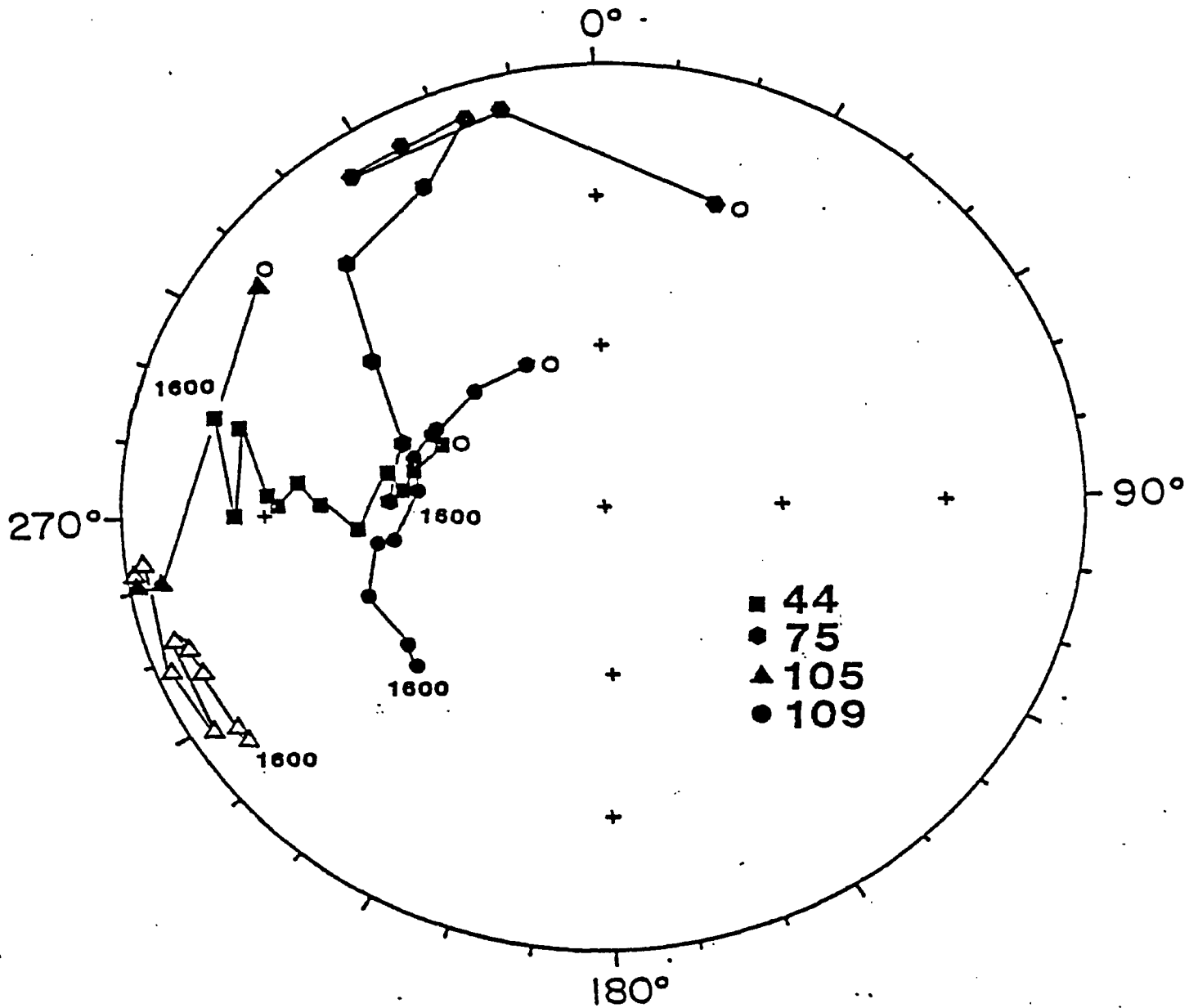


FIG. 34. Directional changes during chemical cleaning for IF specimens

NOTES: Equal area projection showing the change in direction on progressive chemical leaching at times of 0.21, 87.180, 271, 385, 525, 668, 830, 1017, 1161 and 1641 hours for IF pilot specimens. Closed symbols indicate down direction and open symbols indicate up direction.

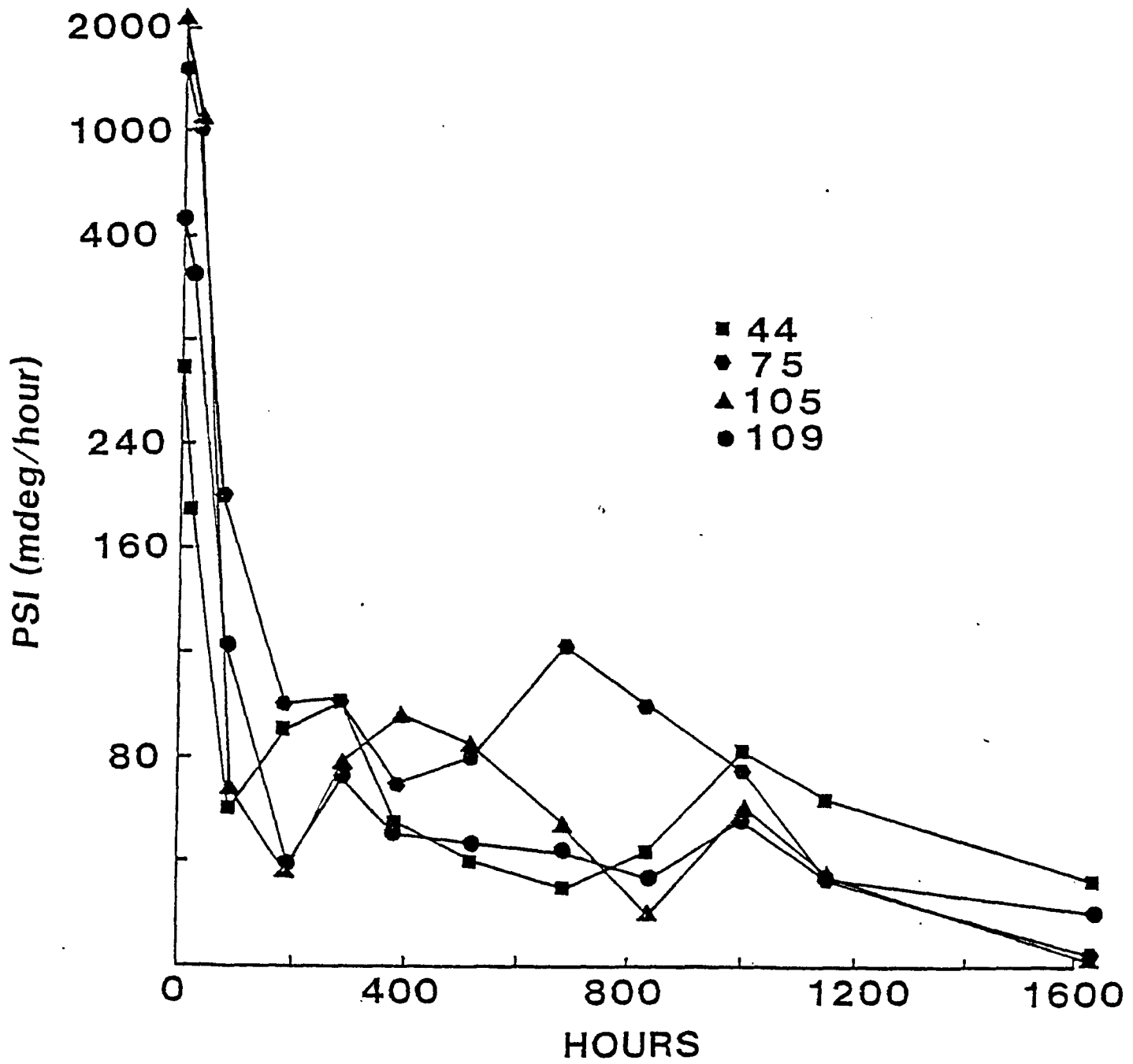


FIG. 35. IF chemical cleaning curve-paleomagnetic stability index

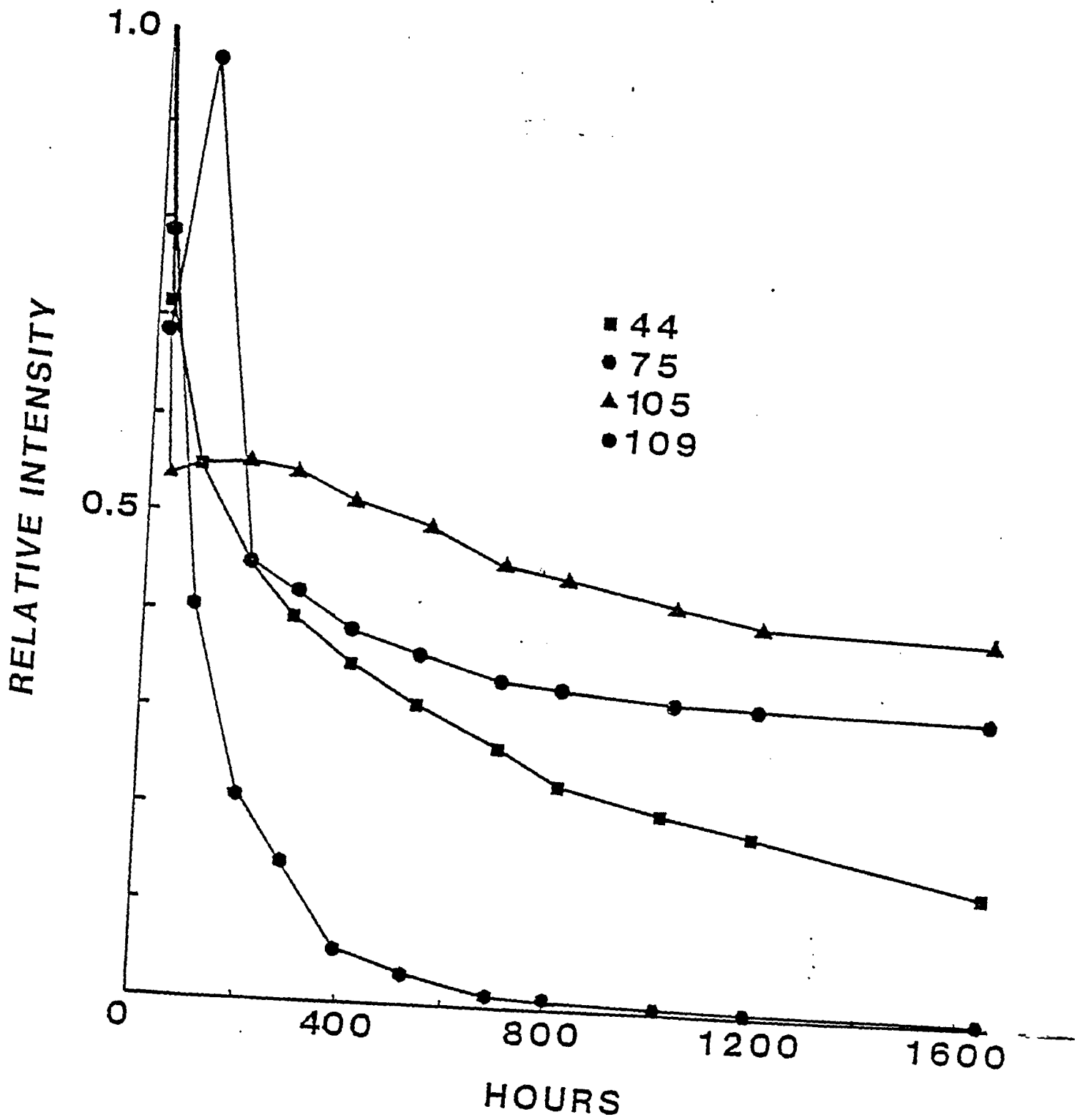


FIG. 36. IF chemical cleaning curve-relative intensity

4.9.2 Remaining Specimens

A total of 54 out of 85 chemically cleaned specimens retained coherency after 1465 hours in $12\bar{N}$ HCl. These surviving specimens showed scattered remanence directions and most specimens rather curiously showed an increase in intensity. This could be the result of the removal of an oppositely directed remanence component.

4.10 BAKED CONTACT TEST

On the intrusion of a diabase dike the host rock near the contact is heated above the Curie temperatures of its magnetic minerals and the host rock acquires the dike direction on cooling. The diabase dike located in the South pit (Figure 3) was sampled perpendicular to the dike (Figure 37). All samples collected fell within the baked contact zone assuming that a dike of $\sim 50\text{m}$ would heat a zone $\sim 30\text{m}$ of the HR intruded (Pullaiah *et al.*, 1975).

4.10.1 AF Demagnetization of Dike and Baked Contact zone

4.10.1a Pilot Specimens

One specimen from the dike and 10 from the baked contact zone were AF step demagnetized up to 100mT such that an optimum AF cleaning field could be selected for the remainder of the specimens.

The PSI curves in Figure 38 show the removal of the unstable VRM components in the present steeply inclined EMF direction in the 0-15mT steps. The specimens showed

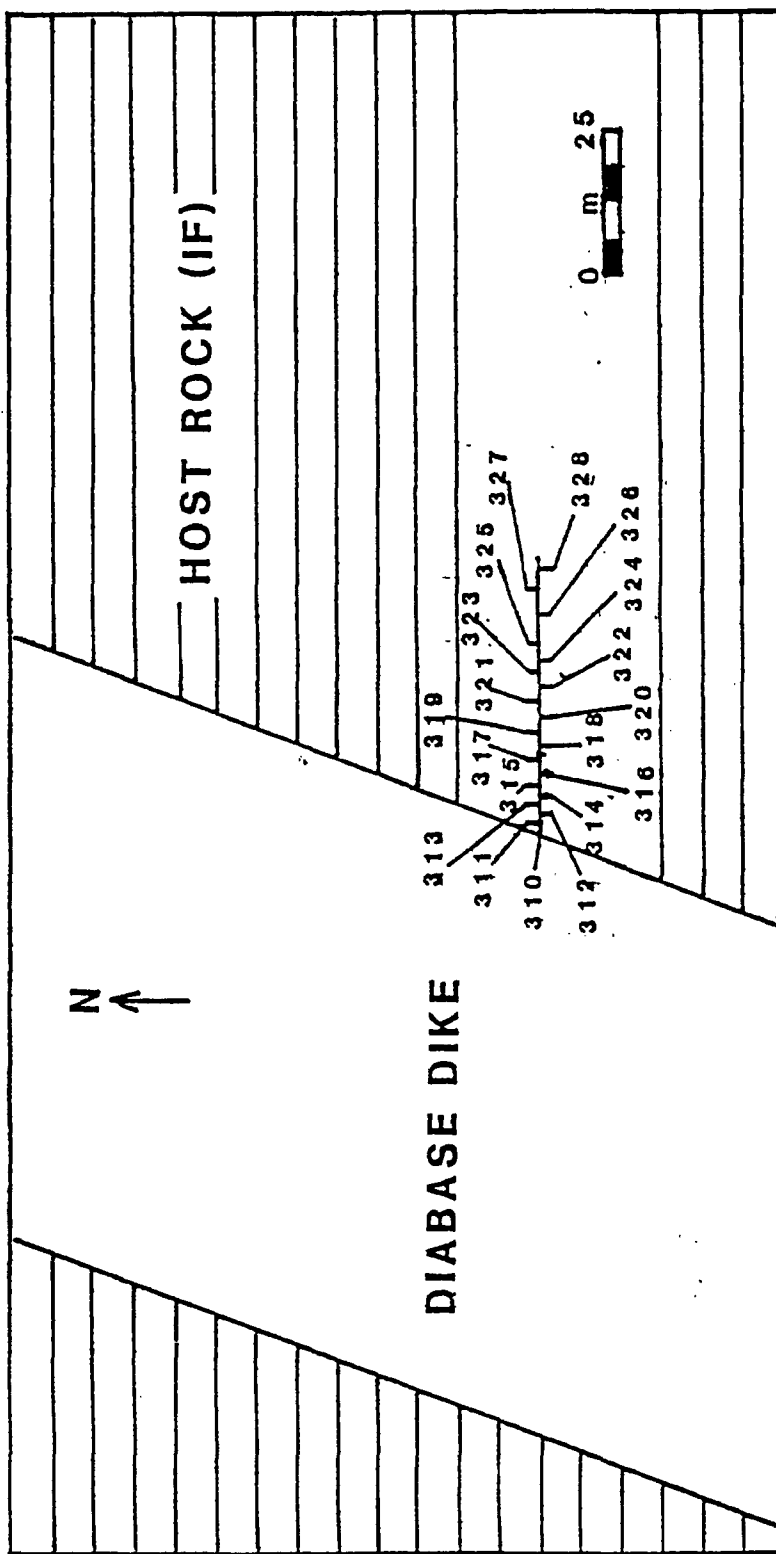


FIG. 37. Sample location for diabase dike baked contact

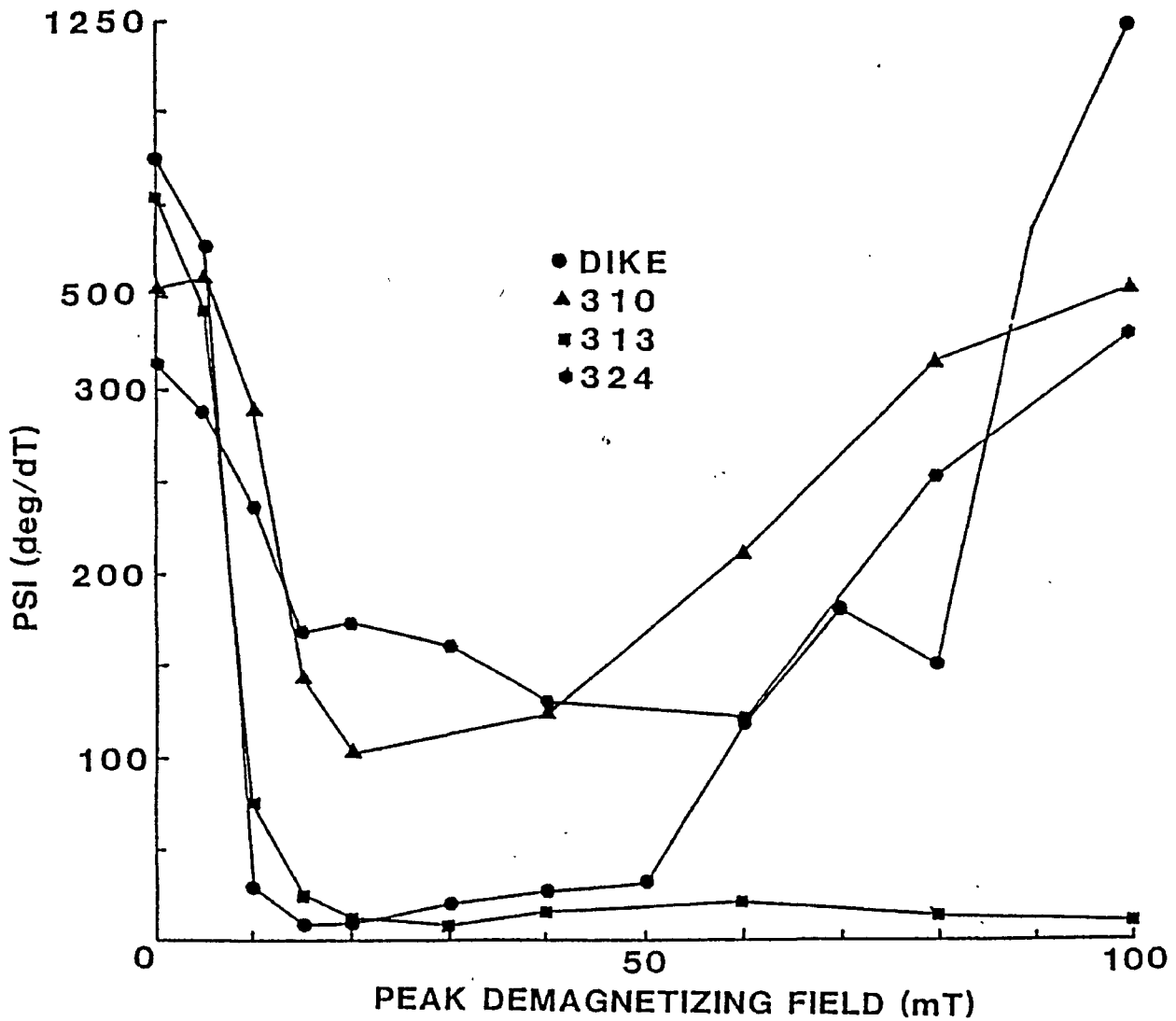


FIG. 38. Baked contact AF demagnetization curve—paleomagnetic stability index

~35 deg/T directional change in the 0-15mT steps which decreased to less than 5 deg/T between 20 and 50mT steps. Above 50mT there is an increase in the rate of directional change because the ARM components are becoming more pronounced. The intensity decay curves (Figure 39) support this interpretation. The majority of the specimens show a rapid intensity decay up to 30-40mT as significant VRM components are removed and then there is a slight intensity decay throughout the remaining cleaning fields. The vector removed components from the AF demagnetization steps were plotted on the stereonet along with the AF cleaned dike directions (Figure 40). Two anomalies were formed after smoothing and contouring of the data. One of the anomalies for the baked contact zone showed a similar remanence direction but with a steeper inclination, possibly caused by a bias of the viscous remanence component. The second anomaly may be a hybrid direction between that of the dike and the IF.

4.10.2 Thermal Cleaning of Dike and Contact zone

A total of one dike and 17 HR specimens were thermal step demagnetized up to 650°C. The intensity decay curves (Figure 41) show an initial drop in intensity up to 450°C as unstable VRM components are removed. The curves then show a blocking temperature of some grains at 475°C above which the magnetization carried by such grains is destroyed. Above 550°C the intensity drops to <3% of the NRM intensity

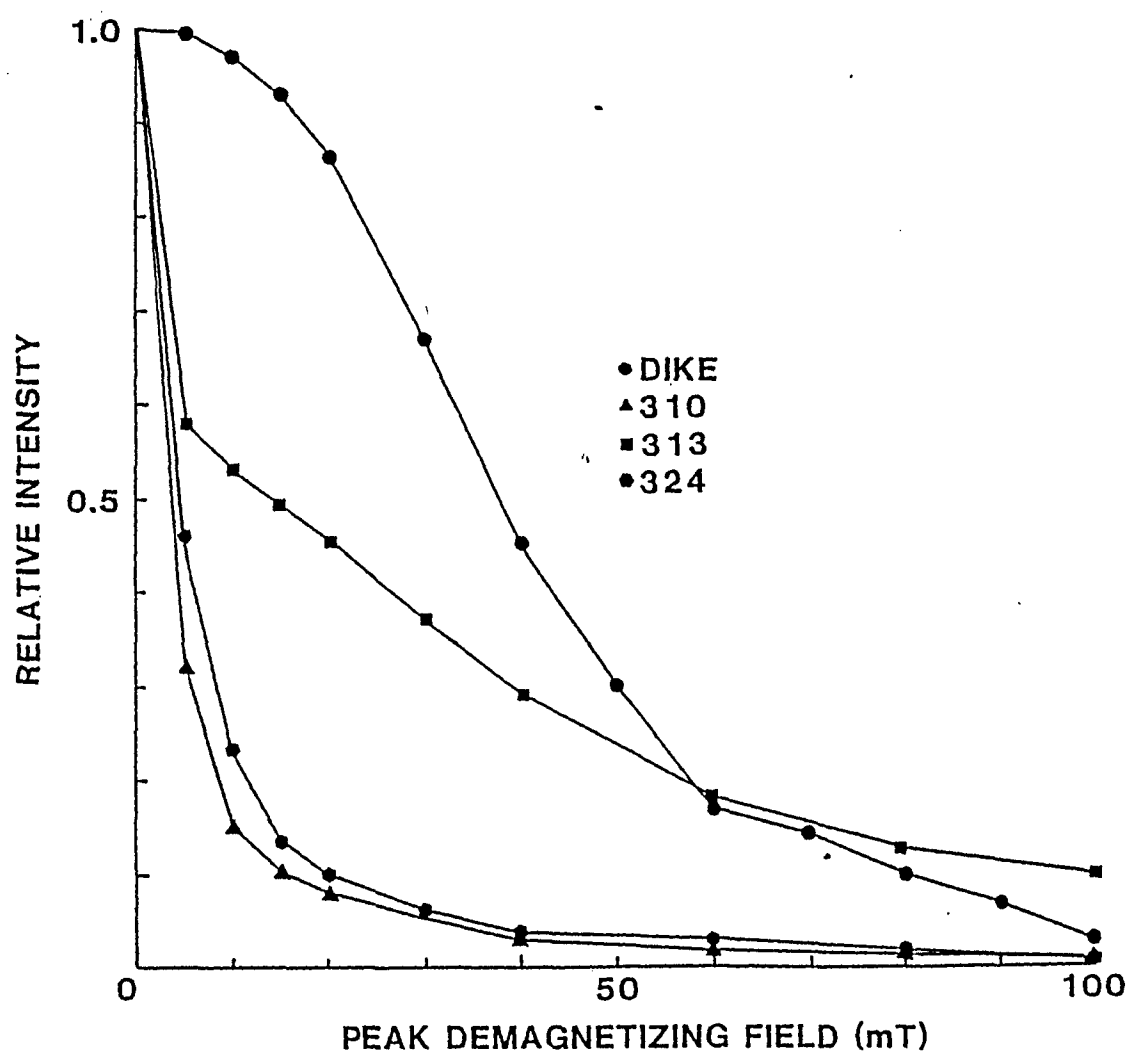


FIG. 39. Baked contact AF demagnetization curve-relative intensity

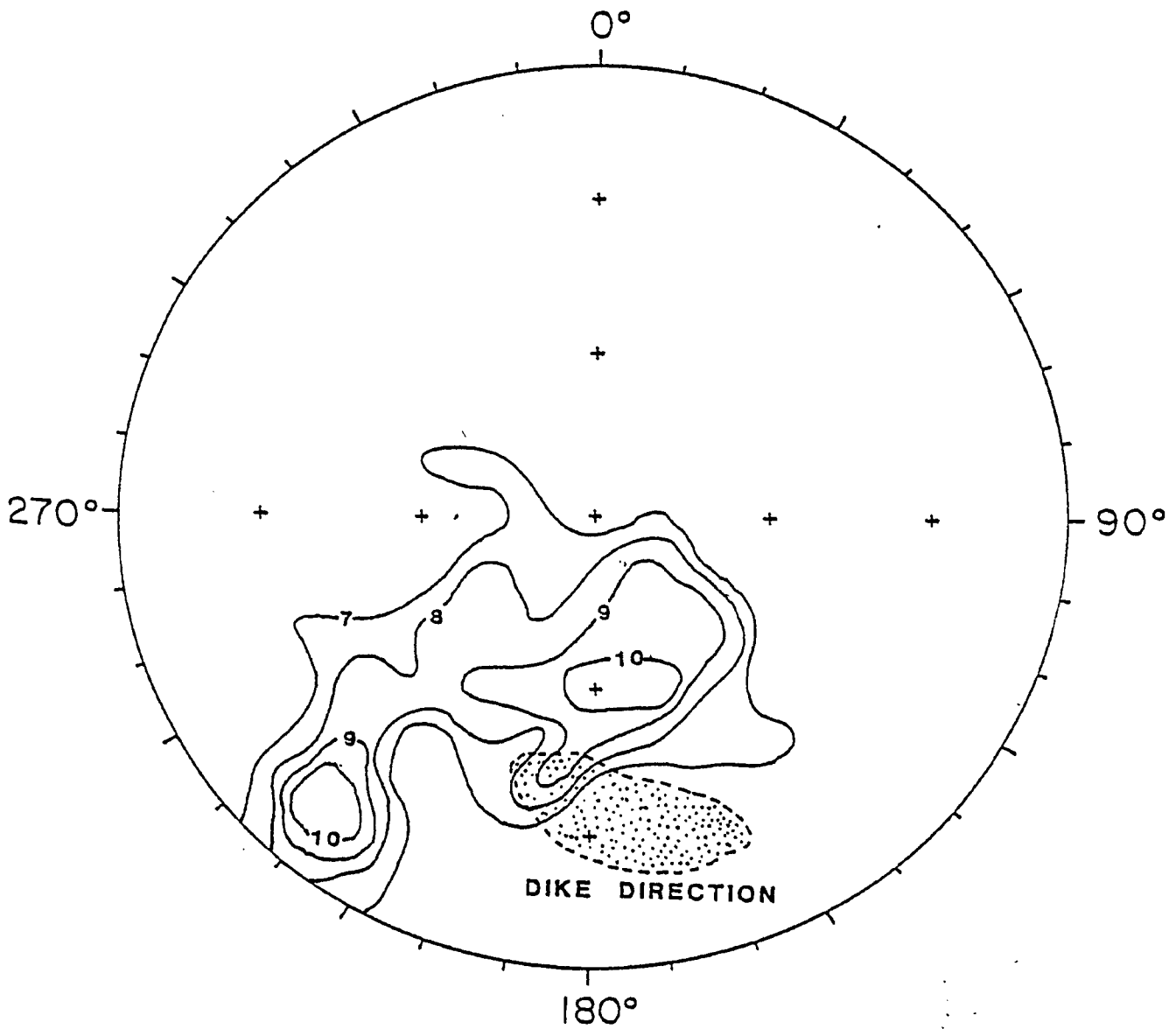


FIG. 40. Dike direction and vector removed direction for the baked contact zone.

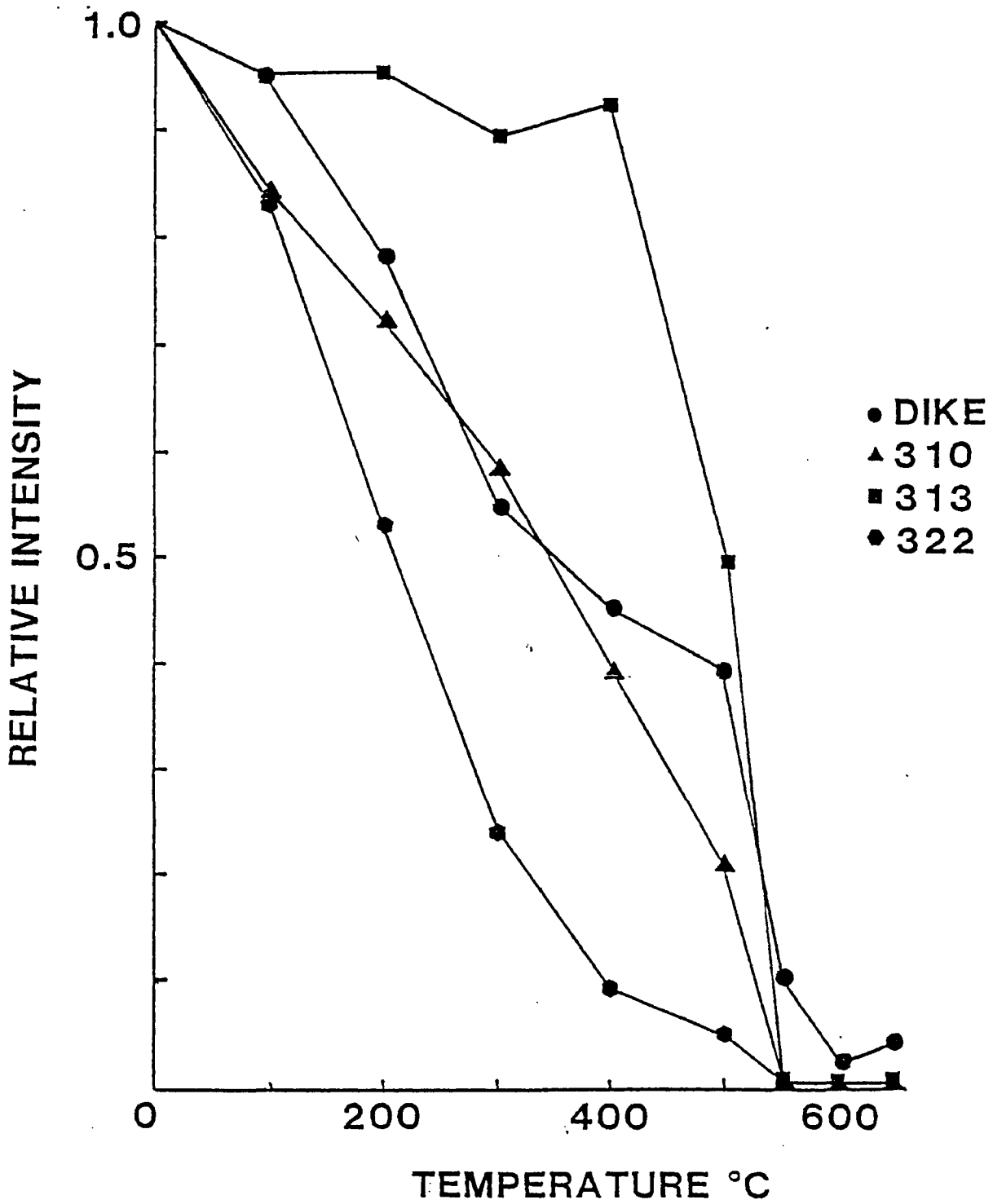


FIG. 41. Baked contact thermal cleaning curve - relative intensity

and the remanence directions scatter as the Curie temperature of magnetite is exceeded. The remanence is a secondary TRM in the magnetite acquired when the dike was emplaced.

4.11 AF DEMAGNETIZATION OF THE HOST ROCK

4.11.1 Pilot Specimens

A total of 45 HR pilot specimens, one from each site, were AF step demagnetized up to 100mT. The directional changes of representative specimens are shown in Figure 42. The PSI curves (Figure 43) show the removal of unstable VRM components in the present steeply-inclined EMF direction (353° , 76°) during the 0-15mT steps. In the 0-15mT steps the specimens show ~ 120 deg/T rate of directional change. The specimens then show ~ 30 deg/T rate of directional change between 15-30mT. Above 40mT there is a rapid increase in the rate of directional change because random ARM components are becoming more pronounced. The intensity decay curves (Figure 44) show a range of decay rates for the pilot specimens. Between 0-15mT, 33% of the specimens show a slight increase, 33% show a slow decay rate, and the remaining 33% show a rapid decay rate in remanence intensity. Most of the specimens show 70% of their NRM intensity removed by 40mT and 90% removed by 100mT.

The optimum cleaning field was selected by inspection of the PSI minima. The pilot specimens show an optimum AF cleaning field (Figure 25) of less than

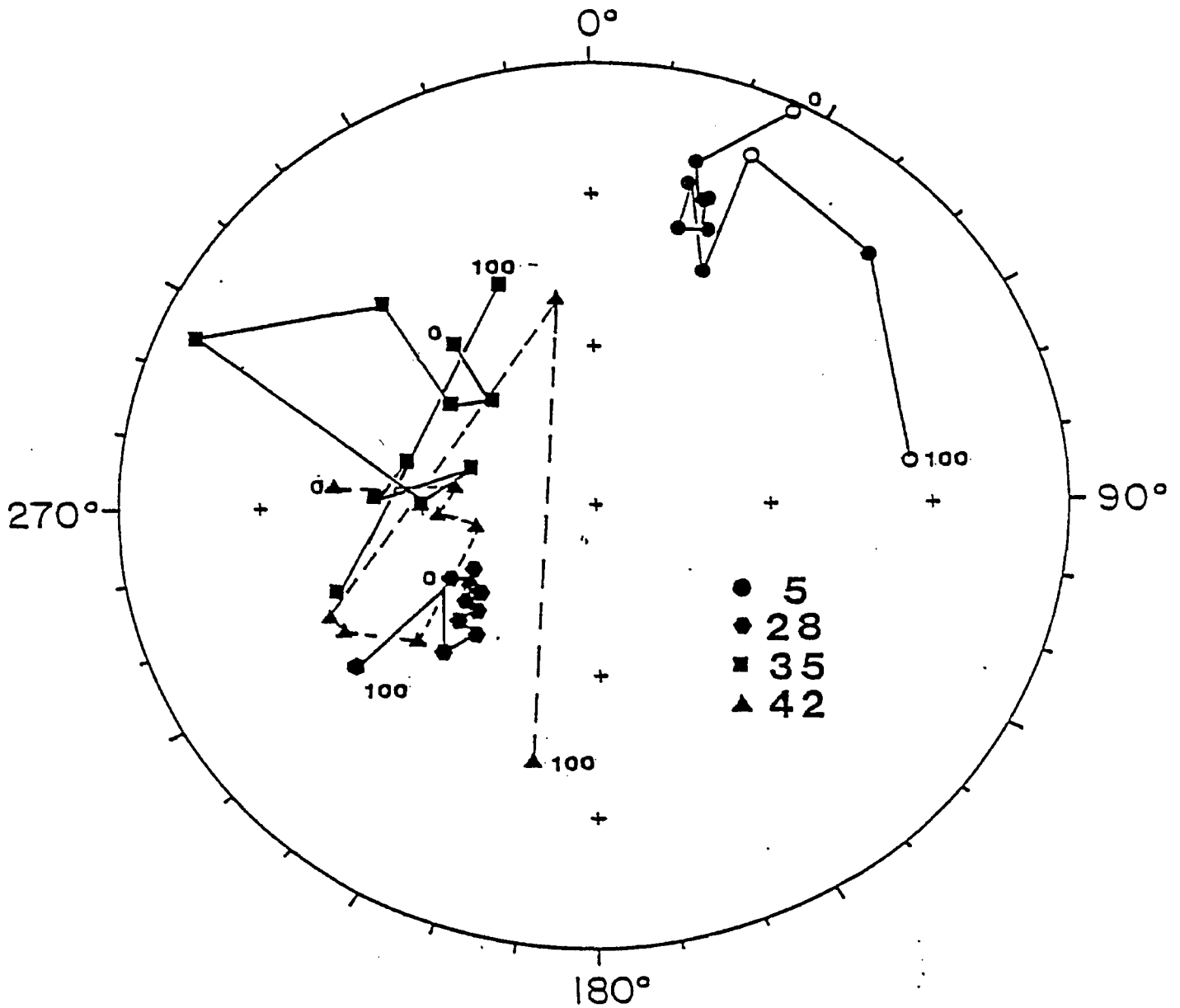


FIG. 42. Directional changes of AF demagnetization for HR pilot specimens

NOTES: Change in direction on progressive AF demagnetization in fields of 0, 5, 10, 15, 20, 30, 40, 50, 60, 70, 80, 90 and 100mT, for HR pilot specimens. Solid symbols indicate down direction and open symbols indicate up direction.

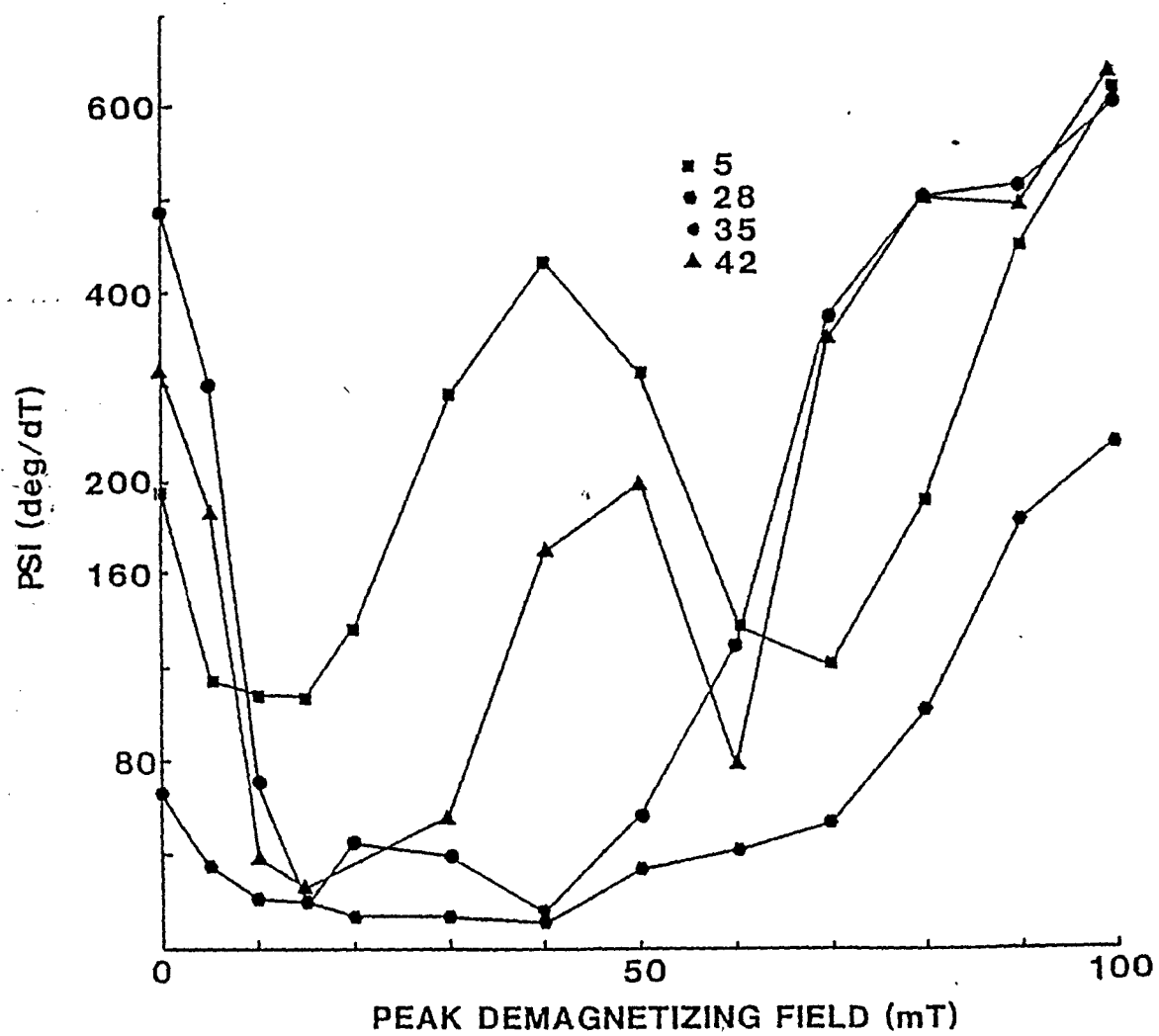


FIG. 43. HR AF demagnetization curve-paleomagnetic stability index

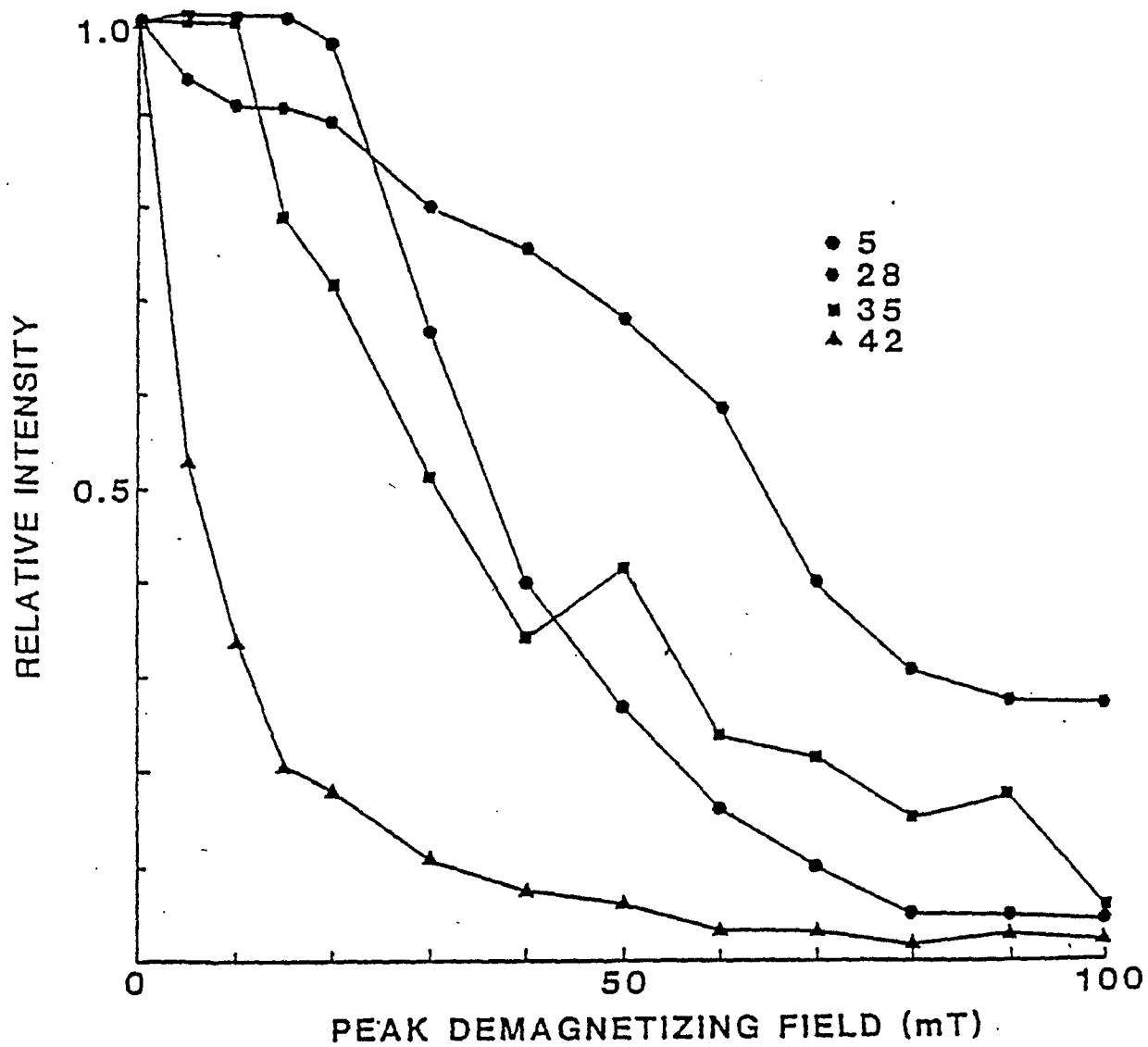


FIG. 44. HR AF demagnetization curve - relative intensity

40mT at which point the relative intensity of stable remanence (Figure 26) ranges from 10% to 90% of its original NRM intensity.

Least square model analysis was attempted using the HR pilot specimens, but this method was unable to isolate the characteristic remanence directions.

4.11.2 Smoothing Method

The smoothing method (4.7.1) is a single step screening method at the population level. The specimen remanence directions showed a better grouping when uncorrected for bedding tilt (Figure 45) than when corrected directions (Figure 46). Because the tilt-corrected directions showed a large scatter, it was not possible to perform a fold test. However the uncorrected directions showed two good anomalies. Specimen directions falling within the $E + 2\sigma$ level for each anomaly were combined to compute the mean direction. One anomaly designated component B (Table 8) yielded a mean direction of 305.0° , 79.1° , $A_{95} = 4.2^\circ$ (declination, inclination, cone of 95% confidence) and the second anomaly designated component C yielded a mean direction of 189.9° , 53.9° , $A_{95} = 3.7^\circ$ (Table 8). The A component direction is close to the original NRM direction (Figure 47) of 356.4° , 87.1° , $A_{95} = 3.3^\circ$ (Table 8). Component C was isolated by the AF cleaning process.

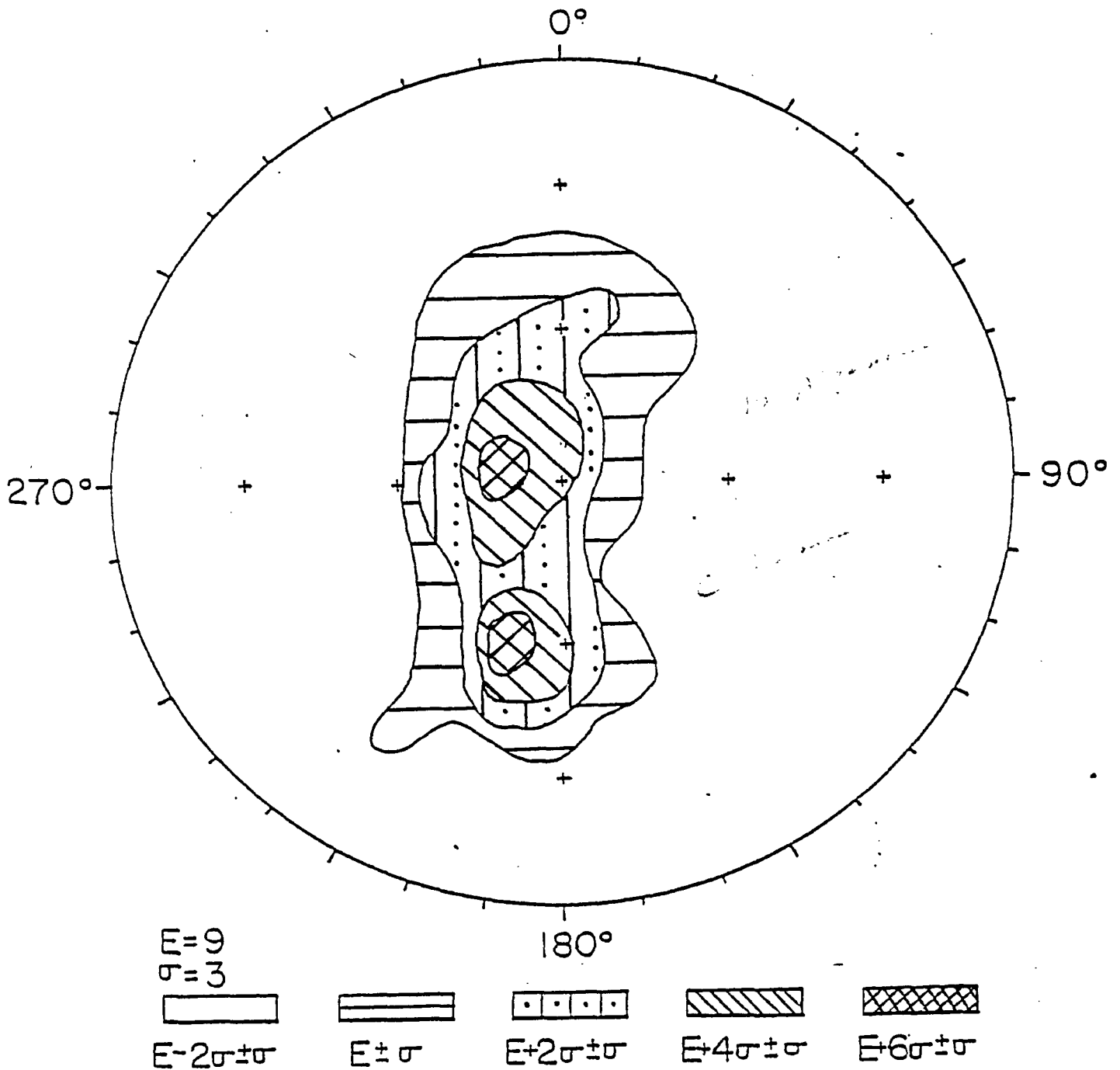


FIG. 45. Smoothing and contouring of AF cleaned HR specimens uncorrected for bedding tilt (down direction; Area = 5.3cm^2)

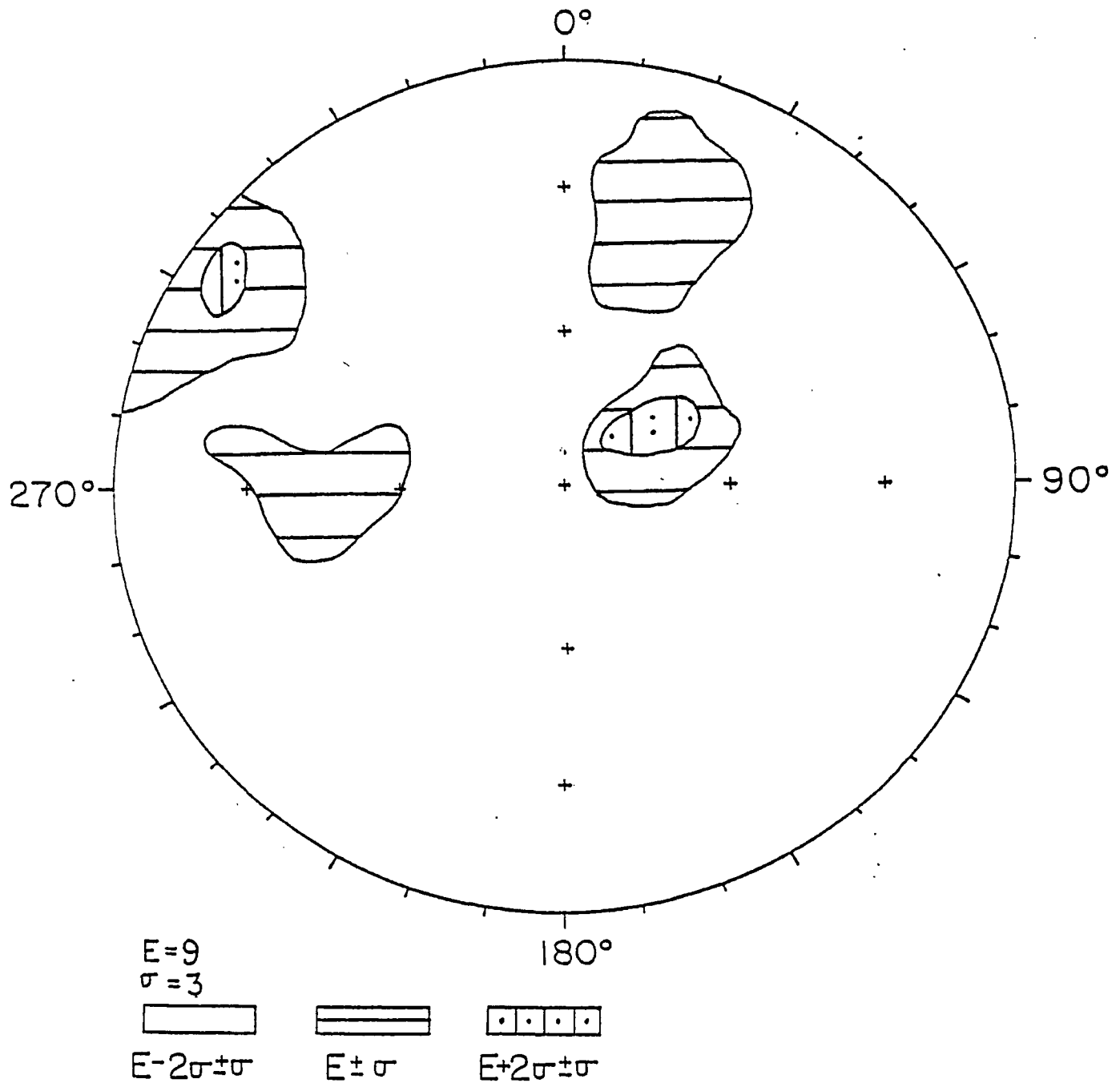


FIG. 46. Smoothing and contouring of AF cleaned HR specimens corrected for bedding tilt (down direction; Area = 5.3cm^2)

TABLE 8. Summary of host rock remanence direction

Group	Number of specimens N	Mean remanence direction				
		Length R	Decl. °	Incl. +down	K	A95 °
B component						
AF cleaned	46	44.3	305.0	79.1	25.9	4.2
NRM	110	104.6	356.4	87.1	17.3	3.3
C component	30	13.8	189.9	53.9	50.2	3.7

NOTES: R is the length of vector resultant.

K is Fisher's (1953) precision parameter.

A95 is the radius of 95% confidence (Fisher 1953) in degrees.

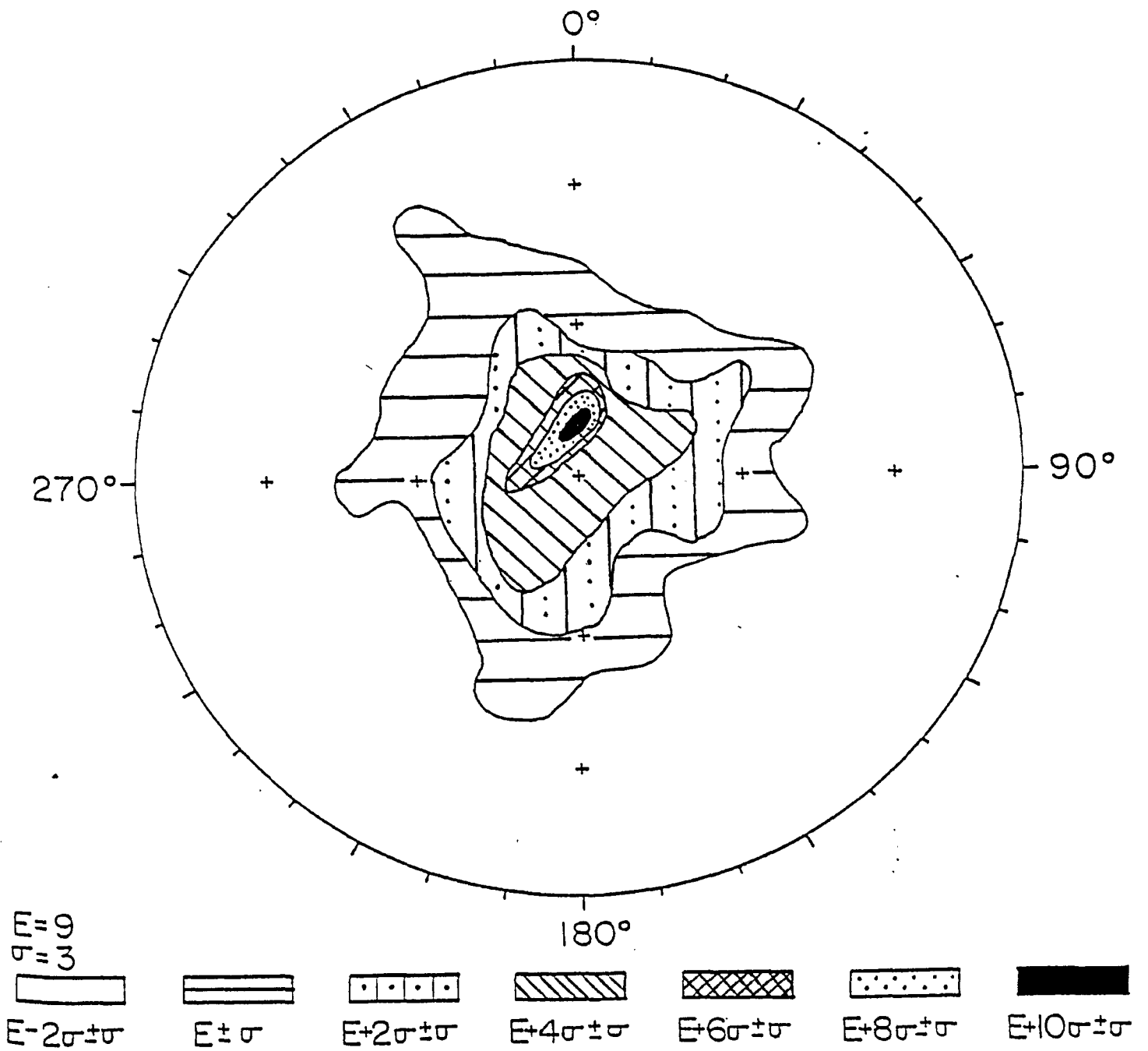


FIG. 47. Smoothing and contouring of NRM HR specimens uncorrected for bedding tilt (down direction; Area = 8.0cm²)

4.12 THERMAL CLEANING OF HOST ROCK

4.12.1 Pilot Specimens

The 24 HR pilot specimens show scattered remanence directions. A total of 3 specimens change very little in direction throughout the cleaning process. Another 14 specimens show a stable direction up to $\sim 300^{\circ}\text{C}$ and thereafter yield scattered directions. The remaining 7 specimens show scattered directions throughout the entire cleaning process. Because thermal cleaning was unable to successfully isolate any directional component, the remaining specimens were not thermally cleaned.

4.13 POLE POSITION

4.13.1 Iron Formation

As previously discussed the IF gives a stable pre-folding A remanence component. Its corrected direction gives, therefore, the pole position for the time of primary remanence acquisition upon deposition or of post depositional alternation prior to deformation during the Algoman orogeny (Table 9). Figure 48 shows this pole position superimposed on the apparent polar wandering (APW) curve for this period (Symons *et al.*, 1980). Its location gives an apparent age of ~ 2.70 Ga. This is considerably earlier than the ~ 2.5 Ga Algoman orogeny and therefore likely represents the primary remanence that IF acquired during deposition.

TABLE 9. Pole positions of the Adams Mine

Group	Number of specimens N	Mean Remanence Direction				Pole Position				
		Length R	Decl. °	Incl. +down °	K	A95 °	Long. (°W)	Lat. (°N)	d _p °	d _m °
IF A component	151	139.75	256.21	7.41	13.33	3.27	37.88	6.35	1.65	3.29
HR B component	46	44.26	304.96	79.08	25.90	4.21	111.99	56.25	7.61	8.01
HR C component	30	29.42	189.91	53.91	50.18	3.75	88.12	-7.06	3.67	5.25
Dike D component	14	13.77	175.84	32.98	58.50	5.24	75.57	-23.91	3.37	5.94

NOTES: For the pole position the longitude and latitude are in degrees west (Long. °W) and north (Lat. °N) respectively, with d_p and d_m being the semi-axes of the oval of confidence along and perpendicular^p to the^m site-pole great circle.

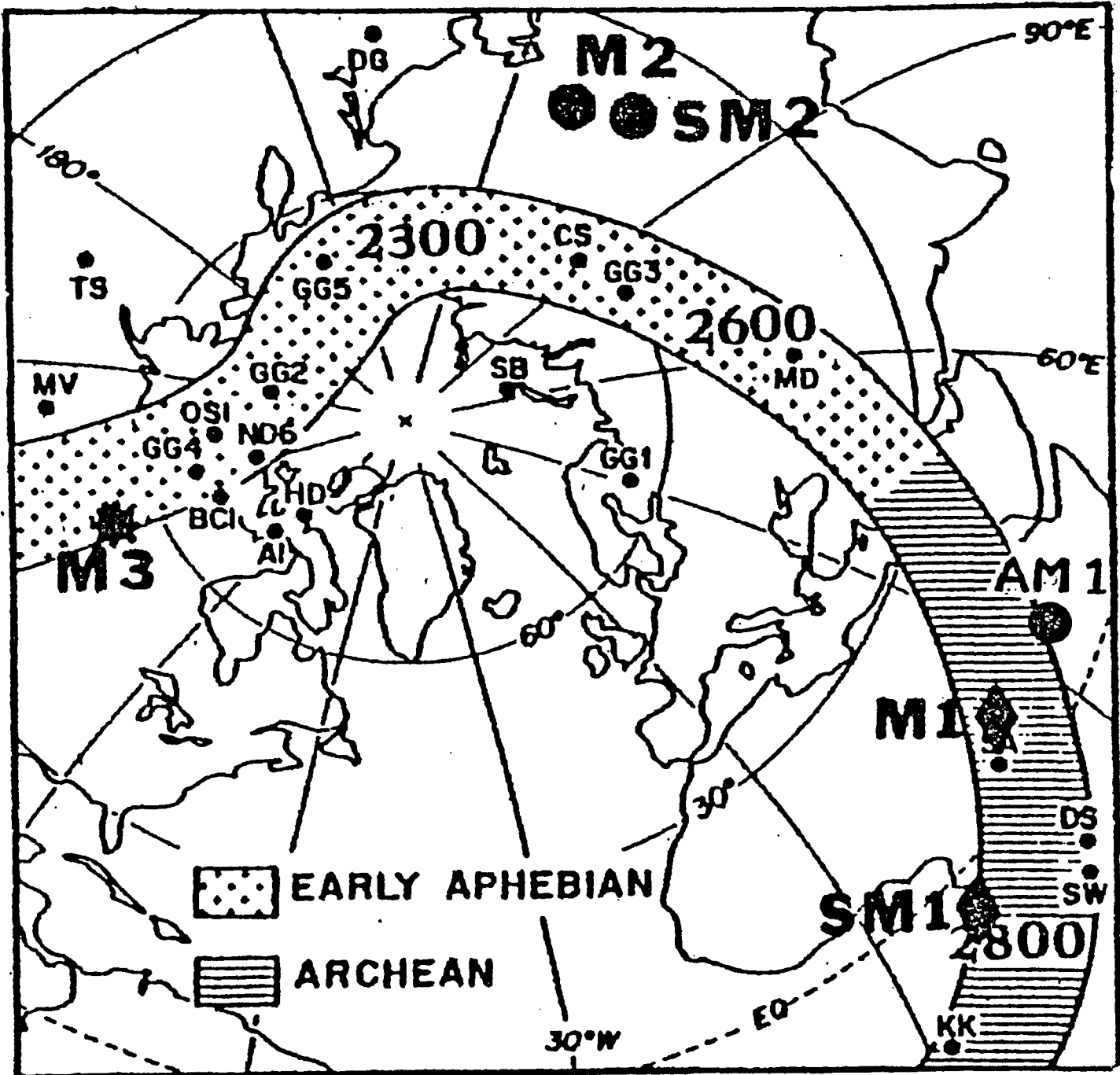


FIG. 48. Apparent polar wandering curve-iron formation

4.13.2 Host Rock

The HR shows two stable post-folding remanence directions. Therefore these directions were acquired after the Algoman orogeny. Figure 49 shows these poles superimposed on the APW path of Irving (1979). The B component pole indicates an age of ~ 2.15 Ga. This age is indistinguishable for the Rb/Sr age of 2.16 Ga that dates the intrusion of the Otto syenite stock (Bell and Blenkinsop, 1976). Furthermore Pullaiah and Irving (1975) determined a remanence direction of 330° , 71° for the Otto syenite stock which corresponds to this B component direction. Thus it seems the B component pole is a metamorphic overprint acquired when the Otto and Lebel syenite stocks were intruded.

The C component gives a pole position with an age of ~ 1.85 Ga. This post-folding metamorphic overprint is possibly associated with the emplacement of the Abitibi dike swarm, D component, which gives an age of 1.83 Ga or possibly due to the Hudsonian orogeny.

4.14 MAGNETIC MODEL

4.14.1 Infinite Depth Extent

The total intensity of the EMF at the Adams Mine is 59,760 γ (gammas) (CDM, 1965).

The magnetic anomaly produced by the South pit will be used as an example of comparison between the theoret-

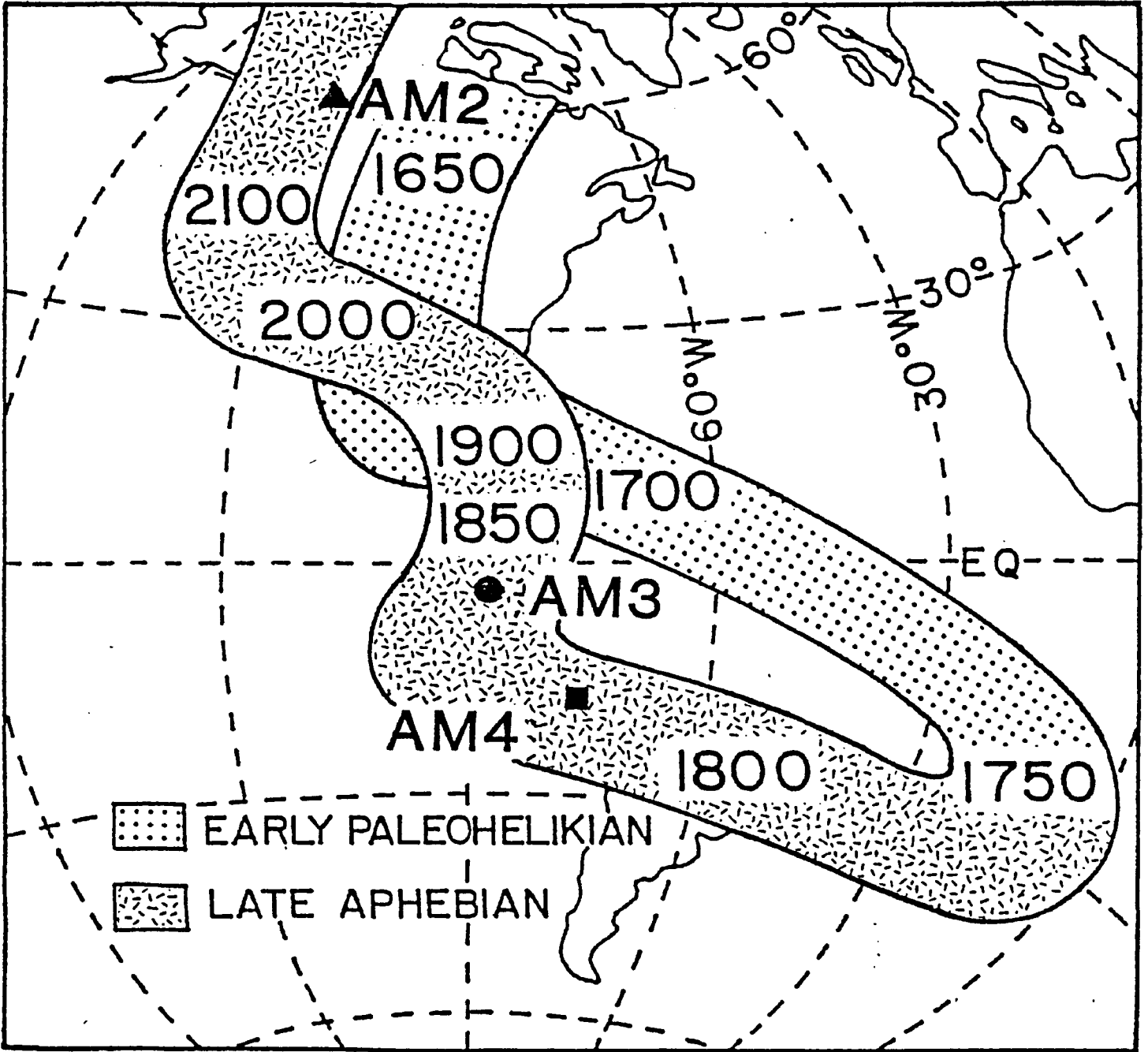


FIG. 49. Apparent polar wandering curve-host rock

ical and actual anomaly calculation. The ore zone has an average width of 165m. For the South pit, the input values are: $k_{\perp} = 0.067 \text{ cgs/cm}^3$; $k_{11}/k_{\perp} = 1.57$; the demagnetizing factor is $F = 2\pi$ (Gay, 1963); the augmenting factor is 16% for the remanence effect; and the terrain clearance is 305m for the aeromagnetic anomaly. The theoretical model anomaly was then calculated for a variety of strike directions and dip values (Figure 50 and 51).

The South pit strikes at $N93^{\circ}E$ and dips at $60^{\circ}S$ giving a computed peak anomaly of 10,000 γ . The measured peak value over the South pit is 70,250 γ (GSC, 1975). Subtraction of the background value of 59,500 γ gives a peak anomaly of 10,750 γ . Thus the calculated and measured peak values agree to within 7%. If the South pit is rotated to the horizontal, then the computed peak anomaly is reduced to $\sim 3,200 \gamma$ or 32% of its present value. This result is similar to that found in the Sherman mine study (Symons and Stupavsky, 1979) and Moose Mountain mine (Symons, Walley and Stupavsky, 1980). Because of the close similarity of the magnetic characteristics of the three deposits (Table 10a-10b), the type curves also take a similar form. Calculated and measured peak values for the other pits are shown in Table 11.

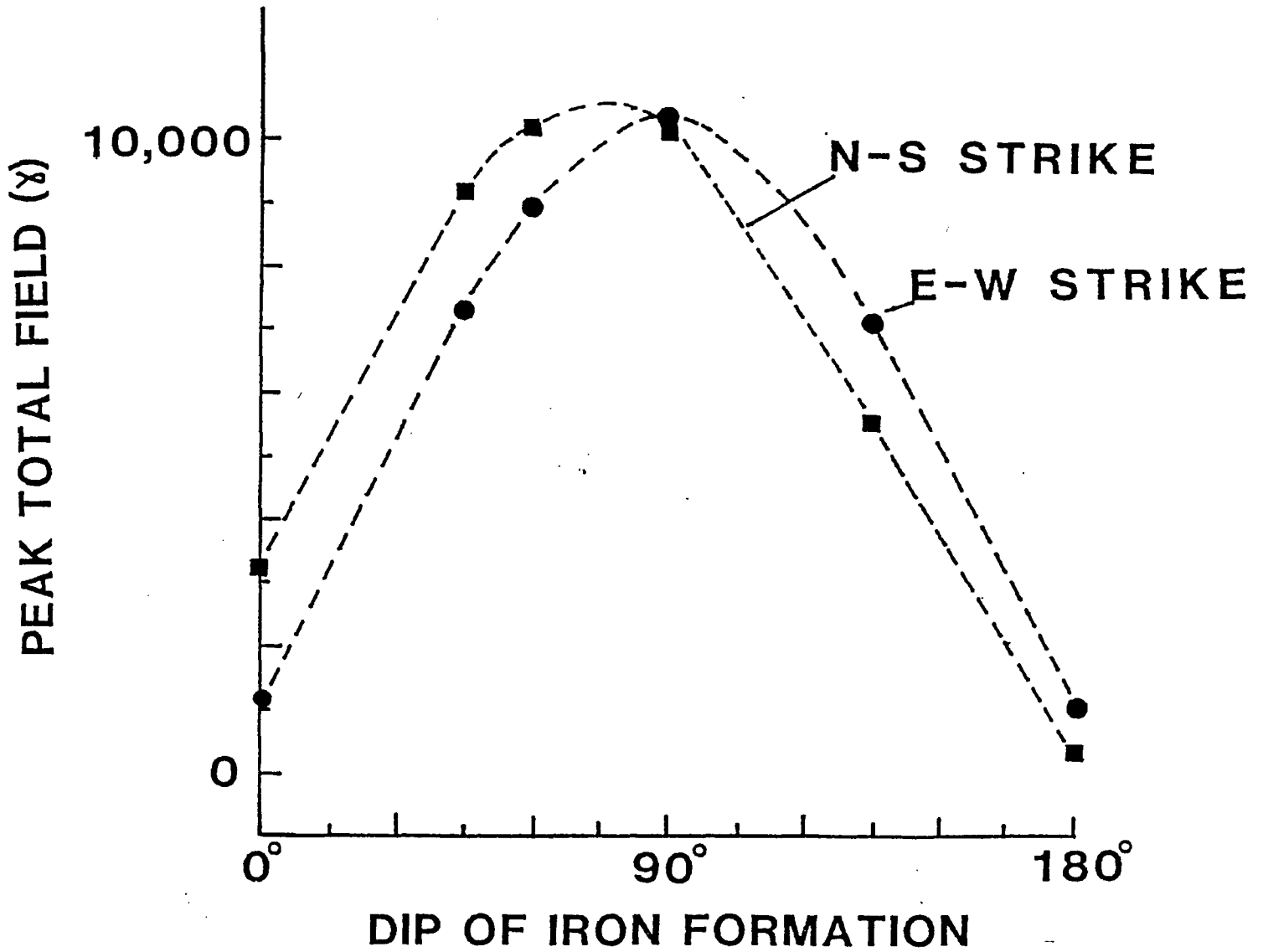


FIG. 50. Computed magnetic anomaly of IF at 305 m elevation (peak total field)

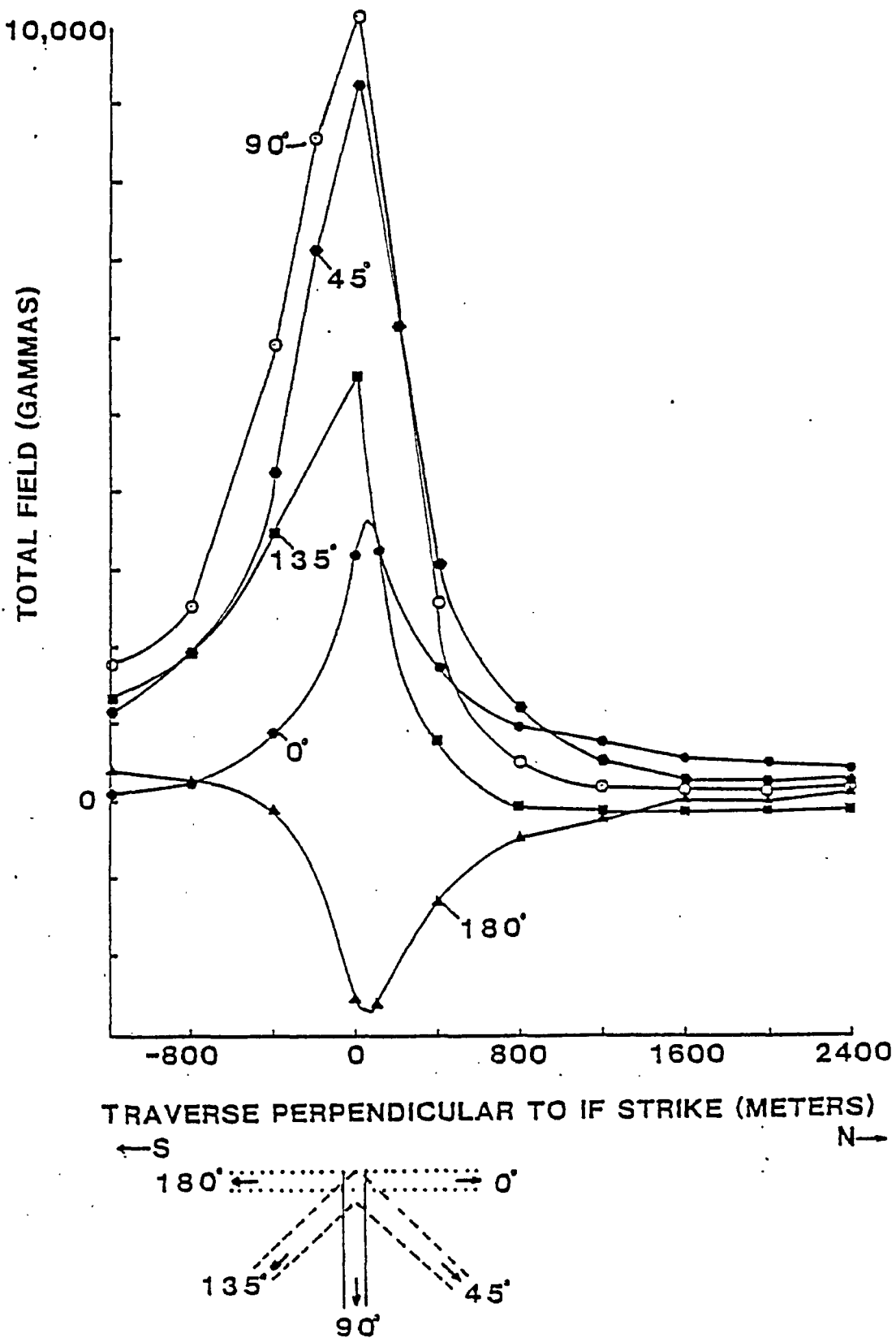


FIG. 51. Computed magnetic anomaly of IF at 305 m elevation (total field)

TABLE 10a. Summary and comparison of magnetic properties of the Sherman mine, Moose Mountain mine and Adams mine iron formation

	Sherman	Moose Mountain	Adams
1. Metamorphic grade	low greenschist	upper greenschist amphibolite	mid greenschist
2. Magnetic susceptibility 1 bedding plane, k_{\perp} (cgs/cc)	0.096	0.110	0.065
3. Anisotropy of magnetic susceptibility, k_{11}/k_{\perp}	1.60	1.75	1.62
4. NRM remanence (emu/cc)	magnetite 2.5×10^{-2} hematite 4.0×10^{-6}	4.8×10^{-2} 3.9×10^{-6}	1.21×10^{-2}
5. Koenigsberger ratio, Q	0.46	0.63	0.67
6. Effective Q, $Q_e = R/N \cos \theta$	0.22	0.24	0.17
7. AF demagnetized remanence (N and R components combined)	$(170.0^{\circ}, 0.1^{\circ}, 5.1^{\circ})$ Pr $(96.1^{\circ}, -6.6^{\circ}, 9.3^{\circ})$ Pr	$(3.7^{\circ}, 5.4^{\circ}, 8.2^{\circ})$ Pr $(80.6^{\circ}, 6.1^{\circ}, 6.4^{\circ})$ Pr $(278.4^{\circ}, 77.7^{\circ}, 16.7^{\circ})$ Pr	$(256.2^{\circ}, 7.4^{\circ}, 3.3^{\circ})$ Pr

NOTES: Remanence directions given as (Decl., Incl., A95).
 Pr. = Pre-folding at 95% confidence level. I. = Inconclusive fold-test.
 For details of the results listed, see text.

TABLE 10b Summary and comparison of magnetic properties of the host rock at the Sherman, Moose Mountain and Adams mines

	Sherman	Moose Mountain	Adams
1. Magnetic susceptibility bedding plane, k_1 (cgs/cc)	4.9×10^{-5}	5.0×10^{-5}	2.35×10^{-4}
2. NRM remanence (emu/cc)	2.94×10^{-6}	1.99×10^{-6}	5.97×10^{-6}
3. Koenigsberger ratio, Q	0.104	0.063	0.013
4. AF demagnetized remanence (N and R components combined)	($168^{\circ}, 9^{\circ}, 8^{\circ}$)Pr ($84^{\circ}, 4^{\circ}, 15^{\circ}$)I	($3^{\circ}, 5^{\circ}, 35^{\circ}$)I ($82^{\circ}, 3^{\circ}, 28^{\circ}$)I	($305^{\circ}, 79^{\circ}, 4^{\circ}$)I ($190^{\circ}, 54^{\circ}, 4^{\circ}$)I

NOTES: Remanence directions given as (Decl., Incl., A95).
 Pr. = Pre-folding at 95% confidence level. I. = Inconclusive fold-test.
 For details of the results listed, see text.

TABLE 11. Summary of aeromagnetic response of IF

Pit	Strike °	Dip °	Width m	Peak aeromagnetic response @ 305 m (γ)	
				Observed	Computed
Peria	48	80	180	8,500	8,100
North	0	90	200	11,750	10,000
Central	113	50	200	11,000	10,650
South	93	60	160	10,750	10,000

NOTES: Observed response from Map 20,137G Kirkland Lake, Ontario (GSC 1975).

CHAPTER V

CONCLUSIONS AND RECOMMENDATIONS

From the preceding discussion, a number of conclusions can be drawn:

1) The close agreement between the Adams Mine magnetic parameters and those of the Sherman and Moose Mountain mine (Table 10) suggests that the genesis of the three ore bodies was similar. The NRM intensity and anisotropy of susceptibility at Adams Mine are thought to be the result of the medium grade regional metamorphism.

2) The similarity of magnetic characteristics for the three Algoma-type banded IF suggests that the values may be representative of Algoma-type IF as a whole and may therefore be used in magnetic anomaly computation for exploration purposes.

3) For anomaly interpretation purposes the HR NRM can be omitted because the induced magnetization of the IF is $\sim 4,300$ times greater.

4) If the IF NRM directions were entirely aligned with the Earth's field, then the remanence would increase the induced anomaly by 67%. Thus the remanence intensity and direction is an important factor.

5) Computation of the magnetic anomaly curves, incorporating the effects of anisotropy, demagnetization and remanence show that if the IF were flat-lying, the peak anomaly would be reduced to 32% of its present value.

6) Variation in IF strike has little effect on the value of the peak anomaly.

7) Close agreement between observed and expected anomalies is achieved using a model of infinite depth extent.

8) The present explorational rationale of only using the most intense vertical magnetizations as targets for examination is insufficient and unjustified.

9) A more logical approach to exploration is outlined:

i) Locate potential area of interest from regional geology,

ii) Determine regional strike and dip,

iii) Using realistic values of susceptibility, anisotropy, demagnetization, remanence and depth, compute the type curves for the aeromagnetic anomaly for a number of thicknesses and depth extents,

iv) Match observed magnetic anomalies with type curves, and

v) Use detailed mapping and diamond drilling to put restraints on thickness, depth of burial and depth extent.

10) AF and chemical demagnetization of the IF results in the isolation of one stable, well defined pre-folding A remanence component at 256° ; 7° .

11) This A component is different from those isolated

at the Sherman and Moose Mountain mine IF after tectonic correction (Table 10a).

12) AF demagnetization of the HR results in the isolation of two stable, postfolding remanence components, a B component at 305° , 79° and a C component at 190° , 54° .

13) AF demagnetization of the diabase dike results in the isolation of a D component at 176° , 33° .

14) The inferred paleomagnetic pole position for the IF is 38°W , 6°N . ($d_p = 2^\circ$, $d_m = 3^\circ$). This pole is based upon smoothing and contouring method of AF demagnetization data. This pole position, superimposed on the apparent polar wander (APW) curve for this period (Symons *et al.*, 1980), gives an age of $\sim 2.85\text{Ga}$ and likely represents the primary remanence that IF acquired during deposition.

15) The inferred paleomagnetic pole position for the HR B component is 112°W , 56°N ($d_p = 8^\circ$, $d_m = 8^\circ$) and C component is 88°W , 7°S ($d_p = 4^\circ$, $d_m = 5^\circ$). This pole is based upon smoothing and contouring method of AF demagnetization data. The B component gives an age of $\sim 2.15\text{Ga}$ and is associated with the intrusion of the Otto syenite stock. The C component gives an age of 1.85Ga and is possibly associated with the intrusion of the Abitibi dike swarm or the Hudsonian orogeny.

APPENDIX I

Computer program for the calculation of the
magnetic anomaly over a thin sheet of
infinite strike and depth extent.

0001
0002
0003
0004
0005

SUBROUTINE PLUTE(X,Y,N)
DIMENSION X(N),Y(N),GL(2),VL(2),DT(2),XP(1),KC(6),A(120)

C DATA C,PLK/1H+,1H /

INTEGER C,PLK,A

DATA C,PLK / 11, 1, 1 /

DATA KC(1),I=1,62/1.E29,1.E27,1.E20,1.E27,1.E20,1.E29,1.E24,1.E21,1.E21,
DATA KC/1.E29,1.E27,1.E20,1.E27,1.E20,1.E24,1.E24,1.E23,1.E22,1.E21,1.E21,1.E2
10,1.E19,1.E18,1.E17,1.E16,1.E15,1.E14,1.E14,1.E14,1.E12,1.E11,1.E10,1.E9
2,1.E8,1.E7,1.E6,1.E5,1.E4,1.E4,1.E2,1.E1,1.E1,1.E-1,1.E-2,1.E-3,1.E-
34,1.E-5,1.E-6,1.E-7,1.E-8,1.E-9,1.E-10,1.E-11,1.E-12,1.E-13,1.E-14
4,1.E-15,1.E-16,1.E-17,1.E-18,1.E-19,1.E-20,1.E-21,1.E-22,1.E-23,1.E-
24,1.E-25,1.E-26,1.E-27,1.E-28,1.E-29,1.E-30,1.E-31,1.E-32,1.E-327

XMIN=X(1)

XMAX=X(1)

YMIN=Y(1)

YMAX=Y(1)

DO 3 I=2,N

XMAX=AMAX1(XMAX,X(I))

XMIN=AMIN1(XMIN,X(I))

YMAX=AMAX1(YMAX,Y(I))

YMIN=AMIN1(YMIN,Y(I))

3 CONTINUE

GL(1)=XMAX-XMIN

GL(2)=YMAX-YMIN

DO 10 J=1,2

DT(J)=FLOAT(J)+.0{#GL(J)}

IF(DT(J).GT.1.EJ0) GO TO 8

DO 5 I=1,62

IF(DI(J).GT.KC(I)) GO TO 6

4 CONTINUE

DT(J)=1.E-12

GO TO 10

6 CR=KC(1)

DO 7 K=2,N

IF(K.EQ.7) GO TO 7

IF(DI(J).LT.FLOAT(K)*CR) GO TO 9

7 CONTINUE

DT(J)=PC(I-1)

GO TO 10

9 WRITE(6,100)

RETURN

DI(J)=FLOAT(K)*CR

10 VL(J)=.5*(FLOAT(J-J)*50.#DT(J)-GL(J))

DATA XMIN-VL(1)

DATA YMAX+VL(2)

U=ABS(UOTX)

IF U=AMSP(U,DT(I))

002
003
004
005

014
015
016
017
018
019
020
021
022
023
024
025
026
027
028
029
030
031
032
033
034
035
036
037
038
039
040

```

0042 RINCI=PI*RINCI
0043 QJ=Q
0044 PRINT3
0045 PRINT4,RINT1,RINCI,STR,DIP,T,Z,S,RR,QQ
0046 PRINT61
0047 PRINT10,Y(1),Y(2),Y(3),Y(4),Y(5),Y(6),Y(7),Y(8)
0048 PRINT10,X(1),X(2),X(3),X(4),X(5),X(6),X(7),X(8)
0049 PRINT61
0050 PRINT10,Y(9),Y(10),Y(11),Y(12),Y(13),Y(14),Y(15),Y(16)
0051 PRINT10,X(9),X(10),X(11),X(12),X(13),X(14),X(15),X(16)
0052 PRINT61
0053 PRINT10,Y(17),Y(18),Y(19),Y(20),Y(21),Y(22),Y(23),Y(24)
0054 PRINT10,X(17),X(18),X(19),X(20),X(21),X(22),X(23),X(24)
0055 PRINT61
0056 CALL PLUFG(Y,IT,N)
0057 GO TO 9
0058 CALL EXIT
0059 STOP
0060 END

```

```

0042
0043
0044
0045
0046
0047
0048
0049
0050
0051
0052
0053
0054
0055
0056
0057
0058
0059
0060

```

7

```

0001 DIMENSION V(100),Y(100),VO(100),NAME(40)
0002 DIMENSION VII(100),YI(100),YII(100),YIII(100)
0003 FU=PI*(4*PI/3)
0004 DIMENSION X(50)
0005 FORMAT(40A2)
0006 FORMAT(100)
0007 FORMAT(F8.1,5F6.1,F10.7,2F6.1)
0008 FORMAT(110,12J#TOTAL FIELD IN GAMMA*INCLINATION#ANOMALY#STRIKE
1#DIP#AV. WIDTH(N)#DEPTH(N)#CROSS DIP MS#PARALLEL DIP MS#PARALLEL
2#
3#
4#
5#
6#
7#
8#
9#
10#
11#
12#
13#
14#
15#
16#
17#
18#
19#
20#
21#
22#
23#
24#
25#
26#
27#
28#
29#
30#
31#
32#
33#
34#
35#
36#
37#
38#
39#
40#
41#

```

```

10 FU=PI*(4*PI/3)
11 DIMENSION X(50)
12 FORMAT(40A2)
13 FORMAT(100)
14 FORMAT(F8.1,5F6.1,F10.7,2F6.1)
15 FORMAT(110,12J#TOTAL FIELD IN GAMMA*INCLINATION#ANOMALY#STRIKE
16 1#DIP#AV. WIDTH(N)#DEPTH(N)#CROSS DIP MS#PARALLEL DIP MS#PARALLEL
17 2#
18 3#
19 4#
20 5#
21 6#
22 7#
23 8#
24 9#
25 10#
26 11#
27 12#
28 13#
29 14#
30 15#
31 16#
32 17#
33 18#
34 19#
35 20#
36 21#
37 22#
38 23#
39 24#
40 25#
41 26#
42 27#
43 28#
44 29#
45 30#
46 31#
47 32#
48 33#
49 34#
50 35#
51 36#
52 37#
53 38#
54 39#
55 40#
56 41#

```

```

0009 DIMENSION V(100),Y(100),VO(100),NAME(40)
0010 DIMENSION VII(100),YI(100),YII(100),YIII(100)
0011 FU=PI*(4*PI/3)
0012 DIMENSION X(50)
0013 FORMAT(40A2)
0014 FORMAT(100)
0015 FORMAT(F8.1,5F6.1,F10.7,2F6.1)
0016 FORMAT(110,12J#TOTAL FIELD IN GAMMA*INCLINATION#ANOMALY#STRIKE
0017 1#DIP#AV. WIDTH(N)#DEPTH(N)#CROSS DIP MS#PARALLEL DIP MS#PARALLEL
0018 2#
0019 3#
0020 4#
0021 5#
0022 6#
0023 7#
0024 8#
0025 9#
0026 10#
0027 11#
0028 12#
0029 13#
0030 14#
0031 15#
0032 16#
0033 17#
0034 18#
0035 19#
0036 20#
0037 21#
0038 22#
0039 23#
0040 24#
0041 25#

```

0049
0050
0051
0052
0053
0054
0055
0056
0057
0058
0059
0060
0061
0062
0063
0064
0065
0066
0067
0068
0069
0070
0071
0072
0073
0074
0075

```

U=U-KFM
HDTX=SIGN(U,HDTX)
U=ABS(U*PY)
KEM=AMUP(U,DT(2))
U=U-KEM
TOPY=SIGN(J,TOPY)+DT(2)
DXP=10.*PI(1)
DO 17 I=1,11
XP(1)=U+XFLUAT(I-1)*DXP
WRITE(6,101)
DY2=PI*DT(2)
DO 22 JJ=1,51
I=JJ-1
DO 105 J=1,101
A(J)=K
YV=TOPY-FLUAT(I)*DT(2)
DO 18 J=1,N
IF(ABS(YN-Y(J)).GT.DY2) GO TO 14
L=I+IF(X(X(J))-HDTX)/DT(1))
A(L)=C
14 CONTINUE
IF(MOD(1,5).EQ.0) GO TO 20
WRITE(6,102) (A(J),J=1,101)
GO TO 22
20 WRITE(6,103) YN, (A(J),J=1,101)
22 CONTINUE
WRITE(6,104) (XP(1),I=1,11)
PRINT,1
PRINT,1
WRITE(6,105) XMAX,XMIN,YMAX,YMIN,DT(1),DT(2)
RETURN
100 FURMAT(1H1,10X,20HPLOT RANGE 100 LARGE)
101 FURMAT(1H1,12X,1H*,10(9X,1H*)/12X,103(1H*))
102 FURMAT(12X,1H*,101A1,1H*)
103 FURMAT(1X,19.0,1H*,101A1,2H*)
104 FURMAT(12X,10J(1H*)/4X,11(9X,1H*)/5X,11(4X,F0.0))
105 FURMAT(1X,10X,MAX=.F7.0,2X,6HX,MIN=.F7.0,2X,6HY,MAX=.F7.0,2X,7HX,INCR=.F7.0//)
11 FURMAT(101)
END

```

006
007

0115

0041
0042
0043
0044
0045
0046
0047
0048
0049
0050
0051
0052
0053
0054
0055
0056
0057
0058
0059
0060
0061
0062
0063
0064
0065
0066
0067
0068
0069
0070
0071
0072
0073
0074
0075
0076
0077
0078
0079

REFERENCES

- Bell, K., and Blenkinsop, J., 1976. A Rb-Sr whole rock isochron from the Otto stock, Ontario. *Can. J. Earth Sci.*, v. 13, p.998.
- BMDP-77., 1977. Biomedical Computer Programs P-Series, Univ. Calif. Press, Berkley, Los Angeles, London, 215p.
- C.D.M., 1965. Isoclinic, isogonic and isodynamic charts, Canada. *Can. Dep. Mines Tech. Surveys.*
- Christie, K.W., and Symons, D.T.A., 1969. Apparatus for measuring magnetic susceptibility and its anisotropy. *Geol. Surv. Can.*, Paper 69-41. 10p.
- Cisowski, and Fuller, 1978. The effect of shock on the magnetism of terrestrial rocks. *J. Geophys. Res.*, v. 83, p.3441.
- Dubuc, F., 1965. Geology of the Adams Mine. *Can. Min. Metall. Bull., Trans.*, v. 69, p.176.
- Fairbairn, H.W., Hurley, P.M., and Card, K.D., 1966. Age relations of volcanics at Kirkland Lake, Ontario with the Round Lake pluton. *Mass. Inst. Technol.*, 14th Annu. Rep., p.141.
- Fisher, R.A., 1953. Dispersion on a sphere. *Proc. Royal Soc. London, Series A*, 217, p.295-305.
- Gay, S.P., 1963. Standard curves for interpretation of magnetic anomalies over long tabular bodies. *Geophysics*, v. 28, p.161-200.
- G.S.C., 1975. Kirkland Lake, Ontario. *Geol. Surv. Can. Aeromagnetic Series Map 20, 137G*, scale 1:25,000. Survey flown July 1972.
- Hurley, P.M., and Gates, T.M., 1973. Evaluation of Rb-Sr Dating Methods Applied to the Matachewan, Abitibi, Mackenzie and Sudbury Dike Swarms in Canada. *Can. J. Earth Sci.*, v. 10, p.900.
- Irving, E., 1979. Paleopoles and paleolatitudes of North America and speculations about displaced terrains. *Can. J. Earth Sci.*, v. 16, p.669-694.
- Kamb, W.B., 1959. Ice petrofabric observations from the Blue Glacier, Washington, in Relation to theory and Experiment. *J. Geophys. Res.*, v. 64, p.1891.

- Lawton, K.D., 1957. Geology of the Boston Township and part of the Pacaud Township. Ont. Dep. Mines, v. 66, Part 5.
- Moore, E.S., and Armstrong, H.S., 1946. Iron deposits in the district of Algoma. Ont. Dep. Mines, v.55, part 4, p.3.
- Nunes, P.D., and Jensen, L.S., 1979. Geochronology of the Abitibi Metavolcanics Belt, Kirkland Lake area- Progress report. Ont. Geol. Surv., Miss. Paper 92, p.40-45.
- Pullaiiah, G., and Irving, E., 1975. Paleomagnetism of the contact aureole and late dikes of the Otto stock, Ontario, and its application to early Proterozoic apparent polar wandering. Can. J. Earth Sci., v. 12, p.1609-1618.
- Pullaiiah, G., Irving, E., Buchan, K.L., and Dunlop, D.J., 1975. Magnetization changes caused by burial and uplift. Earth and Planetary Sci. Letters, v. 28, p.133-142.
- Purdy, J.W., and York, D., 1968. Rb-Sr whole-rock and K-Ar mineral ages of rocks from the Superior Province near Kirkland Lake, northern Ontario, Canada. Can. J. Earth Sci., v. 5, p.699-705.
- Ratcliffe, J.H., 1957. The Boston Township iron range in method sand case histories in mining geophysics. Sixth Commonwealth Mining and Metallurgical Congress, p.195-210.
- Shapiro, and Ivanov, 1966. Dynamic remanence and the effect of shock on remanence on strongly magnetic rocks. Dokl. Akad. Navk. SSSR, v. 173, p.6-8.
- Strangway, D.W., 1965. Interpretation of the Magnetic Anomalies over some Precambrian Dikes. Geophysics, v. 30, p.783-796.
- Symons, D.T.A., and Stupavsky, M., 1974. A rational paleomagnetic stability index. J. Geophys. Res., v. 79, p.1718-1720.
- Symons, D.T.A., and Stupavsky, M., 1979. Magnetic Characteristics of the Iron Formation near Temagami, Ontario. Ont. Geol. Surv., Misc. Paper 87, p.133-147.

- Symons, D.T.A., Walley, D.S., and Stupavsky, M., 1980. Component magnetization of the Algoman iron formation and host rocks, Moose Mountain mine, Ontario. Ont. Geol. Surv., Misc. Paper 93, p.198-214.
- Walley, D.S., 1980. Component magnetization of the Iron Formation and the deposits at the Moose Mountain mine, Capreol, Ontario; unpublished M.Sc. Thesis, University of Windsor, 137p.
- Watson, G.S., 1956. Analysis of dispersion on a sphere. Monthly Notices Roy. Astron. Soc. London, Geophys. Suppl., No. 7, p.153-159.

VITAE AUCTORIS

Born: June 11th., 1956, in Windsor, Ontario, Canada.
Son of Mr. and Mrs. William C. Quick

Education:

Secondary School:

Kennedy Collegiate Institute, Windsor, Ontario,
Canada.

University:

University of Windsor, Windsor, Ontario, Canada.
Bachelor of Applied Science in Geological
Engineering, 1979.

B.A.Sc. Thesis: An Investigation into the Relation-
ship between Sonic Velocities and other Index
Properties of Rocks.

University of Windsor, Windsor, Ontario, Canada.

M.A.Sc. Thesis topic: Component Magnetization of
the Iron Formation and deposits at the Adams Mine,
Kirkland Lake, Ontario. 1981.